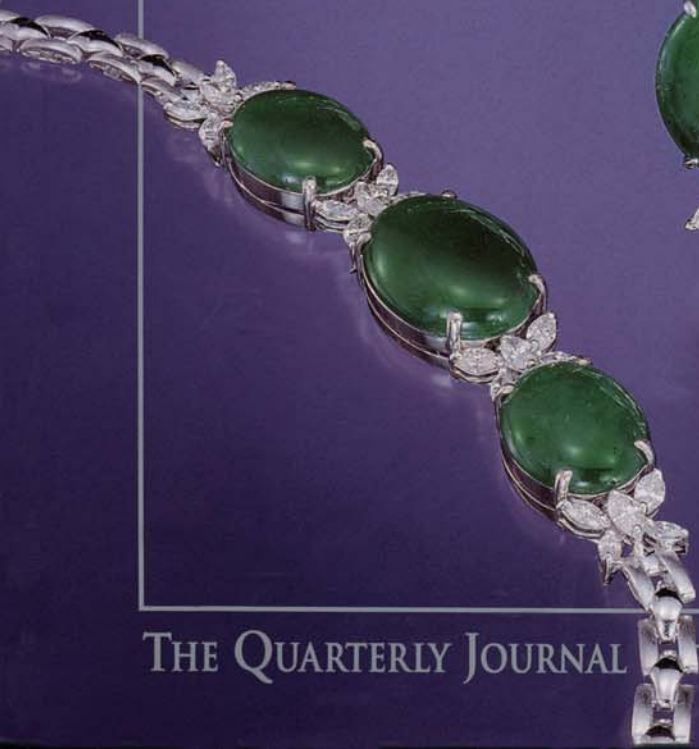


GEMS & GEMOLOGY

VOLUME XXXVI

SPRING 2000



THE QUARTERLY JOURNAL OF THE GEMOLOGICAL INSTITUTE OF AMERICA

GEMS & GEMOLOGY

SPRING 2000

VOLUME 36 NO. 1

T A B L E O F C O N T E N T S

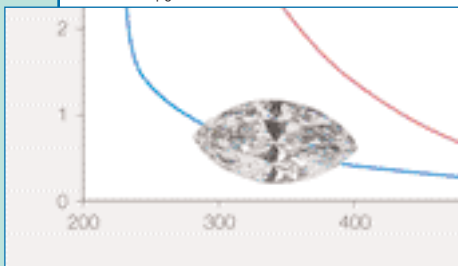


pg. 4



pg. 35

pg. 43



pg. 51



EDITORIAL

- 1 Breakthrough Technology**
William E. Boyajian

FEATURE ARTICLES

- 2 Burmese Jade: The Inscrutable Gem**
Richard W. Hughes, Olivier Galibert, George Bosshart, Fred Ward, Thet Oo, Mark Smith, Tay Thyé Sun, and George E. Harlow
- 28 Lapis Lazuli from the Coquimbo Region, Chile**
Robert R. Coenraads and Claudio Canut de Bon

NOTES AND NEW TECHNIQUES

- 42 Spectroscopic Evidence of GE POL HPHT-Treated Natural Type IIa Diamonds**
David Fisher and Raymond A. Spits
- 50 Purple to Purplish Red Chromium-Bearing Taaffeites**
Karl Schmetzer, Lore Kiefert, and Heinz-Jürgen Bernhardt

REGULAR FEATURES

- 60 Gem Trade Lab Notes**
- 66 Gem News**
- 79 The Dr. Edward J. Gübelin Most Valuable Article Award**
- 81 Gems & Gemology Challenge**
- 83 Book Reviews**
- 85 Gemological Abstracts**
- 93 Guidelines for Authors**

ABOUT THE COVER: Jadeite has long been the most prized gem in the Far East, particularly China. The primary source of top-grade material lies in the remote jungles of Burma (now Myanmar). The lead article in this issue, written by the first foreign gemologists allowed access to Myanmar's jadeite mines in over 30 years, reports on current activity at these mines and the evaluation of rough and fashioned jadeite. These pieces, set with diamonds, illustrate the special quality of Myanmar jadeite. The carving is approximately 4.9 cm high, the butterfly is 8.5 cm wide from wing tip to wing tip; the earrings are 17 mm in diameter, and the oval cabochon is about 15 mm x 11 mm. Courtesy of Ho's Jewelry, San Gabriel, California.

Photo © Harold & Erica Van Pelt—Photographers, Los Angeles, California.

Color separations for Gems & Gemology are by Pacific Color, Carlsbad, California.

Printing is by Fry Communications, Inc., Mechanicsburg, Pennsylvania.

© 2000 Gemological Institute of America

All rights reserved. ISSN 0016-626X

GEMS & GEMOLOGY

EDITORIAL STAFF

Editor-in-Chief
Richard T. Liddicoat

Publisher
William E. Boyajian

Associate Editor
John Sinkankas

Technical Editor
Carol M. Stockton

Assistant Editor
Stuart Overlin
e-mail: soverlin@gia.edu

Contributing Editor
John I. Koivula

Editor
Alice S. Keller
5345 Armada Drive
Carlsbad, CA 92008
(760) 603-4504
e-mail: akeller@gia.edu

Senior Editor
Brendan Laurs
e-mail: blaurs@gia.edu

Subscriptions
Debbie Ortiz
(800) 421-7250, ext. 7142
Fax: (760) 603-4595
e-mail: dortiz@gia.edu

Editors, Gem Trade Lab Notes
Thomas M. Moses
Ilene Reinitz
Shane F. McClure

Editors, Gem News
Mary L. Johnson, John I. Koivula,
Dino DeGhionno, and
Shane F. McClure

Editors, Book Reviews
Susan B. Johnson
Jana E. Miyahira-Smith

Editor, Gemological Abstracts
A. A. Levinson

PRODUCTION STAFF

Art Director
Karen Myers

Production Assistant
Carole Johnson

WEB SITE
<http://www.gia.edu/gandg>

EDITORIAL REVIEW BOARD

Alan T. Collins
London, United Kingdom

G. Robert Crowningshield
New York, New York

John Emmett
Brush Prairie, Washington

Emmanuel Fritsch
Nantes, France

C. W. Fryer
Santa Monica, California

Henry A. Hänni
Basel, Switzerland

C. S. Hurlbut, Jr.
Cambridge, Massachusetts

Alan Jobbins
Caterham, United Kingdom

Mary L. Johnson
Carlsbad, California

Anthony R. Kampf
Los Angeles, California

Robert E. Kane
San Diego, California

John I. Koivula
Carlsbad, California

A. A. Levinson
Calgary, Alberta, Canada

Thomas M. Moses
New York, New York

Kurt Nassau
P.O. Lebanon, New Jersey

George Rossman
Pasadena, California

Kenneth Scarratt
New York, New York

Karl Schmetzer
Petershausen, Germany

James E. Shigley
Carlsbad, California

Christopher P. Smith
Lucerne, Switzerland

SUBSCRIPTIONS

Subscriptions to addresses in the U.S. are priced as follows: **\$69.95** for one year (4 issues), **\$179.95** for three years (12 issues). Subscriptions sent elsewhere are **\$80.00** for one year, **\$210.00** for three years.

Special annual subscription rates are available for all students actively involved in a GIA program: **\$59.95** to addresses in the U.S., **\$70.00** elsewhere. Your student number must be listed at the time your subscription is entered.

Current issues may be purchased for **\$17.50** in the U.S.A., **\$22.00** elsewhere. Discounts are given for bulk orders of 10 or more of any one issue. A limited number of back issues of *G&G* are also available for purchase. Please address all inquiries regarding subscriptions and the purchase of single copies or back issues to the Subscriptions Department.

To obtain a Japanese translation of *Gems & Gemology*, contact GIA Japan, Okachimachi Cy Bldg., 5-15-14 Ueno, Taitoku, Tokyo 110, Japan. Our Canadian goods and service registration number is 126142892RT.

MANUSCRIPT SUBMISSIONS

Gems & Gemology welcomes the submission of articles on all aspects of the field. Please see the Guidelines for Authors in this issue of the journal, or contact the Senior Editor for a copy. Letters on articles published in *Gems & Gemology* and other relevant matters are also welcome.

COPYRIGHT AND REPRINT PERMISSIONS

Abstracting is permitted with credit to the source. Libraries are permitted to photocopy beyond the limits of U.S. copyright law for private use of patrons. Instructors are permitted to photocopy isolated articles for noncommercial classroom use without fee. Copying of the photographs by any means other than traditional photocopying techniques (Xerox, etc.) is prohibited without the express permission of the photographer (where listed) or author of the article in which the photo appears (where no photographer is listed). For other copying, reprint, or republication permission, please contact the Editor.

Gems & Gemology is published quarterly by the Gemological Institute of America, a nonprofit educational organization for the jewelry industry, 5345 Armada Drive, Carlsbad, CA 92008.

Postmaster: Return undeliverable copies of *Gems & Gemology* to 5345 Armada Drive, Carlsbad, CA 92008.

Any opinions expressed in signed articles are understood to be the opinions of the authors and not of the publisher.

Breakthrough Technology

On March 1, 1999, General Electric Company (GE) and Lazare Kaplan International (LKI) rocked the jewelry industry when the newly formed LKI subsidiary Pegasus Overseas Limited (POL) announced that it would market diamonds processed by GE to improve their color, brilliance, and brightness. The impact of such a claim was particularly disturbing to firms holding millions of dollars of diamond inventory. Even more troubling was the assertion that GE's process was permanent, irreversible, and unidentifiable. For years we at GIA had heard rumors of such a "whitening" process—and had even investigated such claims. But we had not yet seen definitive proof of such a treatment.

Soon after the POL announcement, GIA began a series of meetings and discussions with GE and LKI officials, which yielded a temporary, but somewhat settling result: LKI would inscribe all such diamonds with "GE POL" on their girdles and submit them to GIA for Diamond Grading Reports. The Comments section of each report would include the following: "'GE POL' is present on the girdle. Pegasus Overseas Limited (POL) states that this diamond has been processed to improve its appearance by General Electric Company (GE)." When removal of the inscriptions on some stones was detected last summer, GE and LKI sought a safer, more disclosure-friendly way to bring their diamonds to market, later determining to sell the goods directly to select retailers, rather than on the open market in Antwerp.

But why am I rehashing something that our astute *Gems & Gemology* readers already know? This issue contains a rather technical article on diamond spectroscopy that may, at first glance, go unnoticed. Yet it is of the highest importance: De Beers researchers have identified a combination of spectral features that is rarely seen in untreated type IIa diamonds—and that may prove characteristic of HPHT-treated type IIa's.

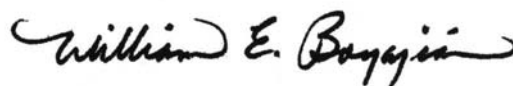
De Beers's breakthrough, part of their massive Gem Defensive Program, appears at this early stage to be pivotal. Last year, many people were in a state of panic over the possibility that the new GE process could not be detected. Truth be told, we at GIA had

many sleepless nights, too. But we publicly stated then—as we have always believed—that the level of technology used to create new synthetics and treatments would eventually also yield evidence for their identification. De Beers has produced quantifiable results that, only one year after the introduction of GE POL diamonds, represent an important step toward establishing detection criteria.

This is not, however, the end of the story. It is a solid beginning to a global effort to solve a potentially devastating problem. GIA has had close cooperation with De Beers on this issue for many months, looking at both gemological and spectral features. De Beers is also working with other research laboratories in a collaborative effort to develop the instrumentation needed to produce these high-sensitivity spectra for routine use in diamond identification and grading. They are testing more stones, both HPHT-treated and natural color, to determine if the criteria will hold for all type IIa diamonds processed in this fashion.

This is also the beginning of a new paradigm in gemology. Of course, there will continue to be more and "better" synthetics and treatments. But we are confident that, with the right resources, detection methodology will keep pace with these sophisticated materials and processes.

We applaud De Beers for their achievement and, especially, for their support of all research laboratories and of the diamond and jewelry trade at large. As research continues and further breakthroughs are made in refining identification criteria and developing instrumentation, these efforts will undoubtedly play an important role in ensuring the integrity of the diamond industry to both the trade and the consuming public.



William E. Boyajian, President
Gemological Institute of America

BURMESE JADE: THE INSCRUTABLE GEM

By Richard W. Hughes, Olivier Galibert, George Bosshart,
Fred Ward, Thet Oo, Mark Smith, Tay Thye Sun, and George E. Harlow

The jadeite mines of Upper Burma (now Myanmar) occupy a privileged place in the world of gems, as they are the principal source of top-grade material. This article, by the first foreign gemologists allowed into these important mines in over 30 years, discusses the history, location, and geology of the Myanmar jadeite deposits, and especially current mining activities in the Hpakan region. Also detailed are the cutting, grading, and trading of jadeite—in both Myanmar and China—as well as treatments. The intent is to remove some of the mystery surrounding the Orient's most valued gem.

If jade is discarded and pearls destroyed, petty thieves will disappear, there being no valuables left to steal.

— From a dictionary published during the reign of Emperor K'ang Hsi (1662–1722 AD), as quoted by Gump, 1962

Perhaps no other gemstone has the same aura of mystery as Burmese jadeite. The mines' remote jungle location, which has been off-limits to foreigners for decades, is certainly a factor. Because of the monsoon rains, this area is essentially cut off from the rest of the world for several months of the year, and guerrilla activities have plagued the region since 1949 (Lintner, 1994).

But of equal importance is that jade connoisseurship is almost strictly a Chinese phenomenon. People of the Orient have developed jade appreciation to a degree found nowhere else in the world, but this knowledge is largely locked away in non-Roman-alphabet texts that are inaccessible to most Westerners, adding further to jadeite's inscrutable reputation. The mines of Burma (now Myanmar*) are the primary working deposits for the most prized gem in the Far East (figure 1), a stone exceeded in price only by diamond.

This article will draw back the curtain on this enigmatic gem, revealing the manner in which Burmese jadeite is mined, traded, graded, cut, treated, and faked. Since the major gemological features of jade have already been extensively covered in the literature (Hobbs, 1982; Fritsch et al., 1992; Wang, 1994), emphasis here will be on these lesser-known aspects. An understanding of jadeite is not limited to the technical or exacting, but it also requires a feeling for the cultural, textural, and ephemeral qualities that make the study of jade unlike any other in the world of gemstones.

Jade has a rich history in the Orient, especially China (Box A). Historically, the term *jade* was applied to any of a number of ornamental materials that could be carved, but most importantly amphibole jade, or nephrite. The rich green material subsequently found in Myanmar proved to be composed primarily of a different mineral (a pyroxene) and



ABOUT THE AUTHORS

Mr. Hughes (rubbydick@ruby-sapphire.com) is an author, gemologist, and webmaster at Pala International, Fallbrook, California. Mr. Galibert (FGA, hons.; ING, AG) is a gemologist and Hong Kong-based dealer in colored stones and pearls. Mr. Bosshart is chief gemologist, Research and Development, at the Gübelin Gem Lab, Lucerne, Switzerland. Mr. Ward, a gemologist, writer, and photographer, owns Gem Book Publishing, Bethesda, Maryland. Dr. Thet Oo is a gemologist and Yangon-based dealer in colored stones. Mr. Smith is a gemologist and Bangkok-based dealer in colored stones. Dr. Tay is president of Evin Gems and Far Eastern Gemmological Lab of Singapore. Dr. Harlow is curator of Gems and Minerals at the American Museum of Natural History, New York City.

Please see acknowledgments at the end of the article.

Gems & Gemology, Vol. 36, No. 1, pp. 2–26
© 2000 Richard W. Hughes



Figure 1. “Windows” cut into this otherwise undistinguished boulder from the Myanmar Jade Tract reveal the presence of a rich green in the jadeite beneath the skin. Boulders such as this are the source of the fine green, orange-red, and lavender cabochons that are much sought-after in China and elsewhere. The bowl is approximately 6 cm wide \times 5 cm high. The cabochons measure approximately 15 \times 19 mm (green), 13 \times 18 mm (orange-red), and 10 \times 14 mm (lavender). Courtesy of Bill Larson and Pala International; photo © Harold & Erica Van Pelt.

was named jadeite (see Box B). In this article, *jade* encompasses both jadeite and nephrite in those instances where the general carving material is being referenced, but *jadeite* or *jadeite jade* will be used to refer to the rock that is predominantly jadeite, where appropriate.

Although jadeite deposits are found throughout the world (Guatemala, Japan, Russia, and California), Myanmar remains the primary source of top-grade material. The Hpakan jadeite region (figure 2) is one of the wildest, least-developed areas of the country. Until the authors' first trip, in 1996, no foreign gemologists had visited the mines since Edward Gübelin in 1963 (Gübelin, 1964–65, 1965a and b).

**In the local vernacular, the country has always been called Myanmar. The English name was officially changed to Myanmar in 1988. Although many people continue to refer to it as Burma, in this article, the country will be referred to by its official name Myanmar.*

One European known to have traveled in the general area was Swedish journalist Bertil Lintner, who in 1985–86 made an epic journey through rebel-held areas of northern Myanmar, including the region surrounding Hpakan (see, e.g., Lintner, 1996). But he was unable to visit the mines themselves.

On February 24, 1994, a formal cease-fire was signed between the Myanmar government and the main rebel group, the Kachin Independence Army (Lintner, 1996). In June 1996, RWH, OG, MS, and TO made a brief trip to Hpakan. To give some idea of the sensitivity of this area, months were needed to obtain permission, with final approval coming from the second-highest-ranking general in the ruling SLORC (State Law and Order Restoration Committee) military junta. RWH again visited the mines in March 1997, this time accompanied by FW and a German film crew led by Bangkok-based journalist Georg Muller. This trip included a visit to Tawmaw. In November 1997, GB and TO paid a

BOX A: JADE—HEAVEN’S STONE

More than 2,500 years ago, Gautama Buddha recognized that much of life involves pain and suffering. Consequently, few of us here on Earth have been provided with a glimpse of heaven. Instead, we mostly dwell in hell. But for the Chinese, there is a terrestrial bridge between heaven and hell—jade.

While gems such as diamond entered Chinese culture relatively recently, the history of jade (at the time, nephrite or another translucent material used for carving) stretches back thousands of years. In ancient China, nephrite jade was used for tools,



weapons, and ornaments (Hansford, 1950). Jade’s antiquity contributes an aura of eternity to this gem. Confucius praised jade as a symbol of righteousness and knowledge.

Yu (玉), the Chinese word for *jade*, is one of the oldest in the Chinese language; its pictograph is said to have originated in 2950 BC, when the transition from knotted cords to written signs supposedly occurred. The pictograph represents three pieces of jade (三), pierced and threaded with a string (丨); the dot was added to distinguish it from the pictograph for “ruler” (Goette, n.d.).

To the Chinese, jade was traditionally defined by its “virtues,” namely a compact, fine texture, tremendous toughness and high hardness, smooth and glossy luster, along with high translucency and the ability to take a high polish (Wang, 1994). But they also ascribe mystical powers to the stone. Particularly popular is the belief that jade can predict the stages of one’s life: If a jade ornament appears more brilliant and transparent, it suggests that there is good fortune ahead; if it becomes dull, bad luck is inevitable.

Jadeite (figure A-1) is a relatively recent entry to the jade family. While some traditionalists feel that it lacks the rich history of nephrite, nevertheless the “emerald” green color of Imperial jadeite is the standard by which all jades—including nephrite—are judged by most Chinese enthusiasts today.

Figure A-1. Although nephrite jade is China’s original “Stone of Heaven,” fine jadeite, as in this matched pair of semi-transparent bangles (53.4 mm in interior diameter, 9.8 mm thick), is the most sought-after of jades in the Chinese community today. Photo courtesy of and © Christie’s Hong Kong and Tino Hammid.

further visit to the Hpakan area, including a trip to Kansi and Maw Sit. Most recently, in January and February 2000, GEH visited the Nansibon jadeite deposits in the historic Hkamti area, which are located approximately 60 km northwest of Hpakan.

HISTORY

The entire pre-1950s occidental history of Myanmar’s jade mines is covered in Hughes (1999). With the exception of a brief mention in Griffith (1847), virtually the only account in English of the early history of jadeite in then-Burma is that of a Mr. Warry of the Chinese Consular Service. Hertz’s *Burma Gazetteer: Myitkyina District* (1912) quotes

at length from his 1888 report, and the historical sections of virtually all other accounts (see, e.g., Chhibber, 1934b; Keller, 1990) are based on Warry. The following also is based on Warry’s report, as quoted by Hertz (1912).

Until at least the 13th century, “jade” in China was generally *nephrite*, a tough, white-to-green amphibole rock that was a favorite of stone carvers. The most important source was south of Hotan (Khotan) in the Kunlun mountains of western China; here, nephrite was recovered from both the White Jade and Black Jade rivers (Gump, 1962). Sometime in the 13th century, according to local lore as reported by Warry (Hertz, 1912), a Yunnan

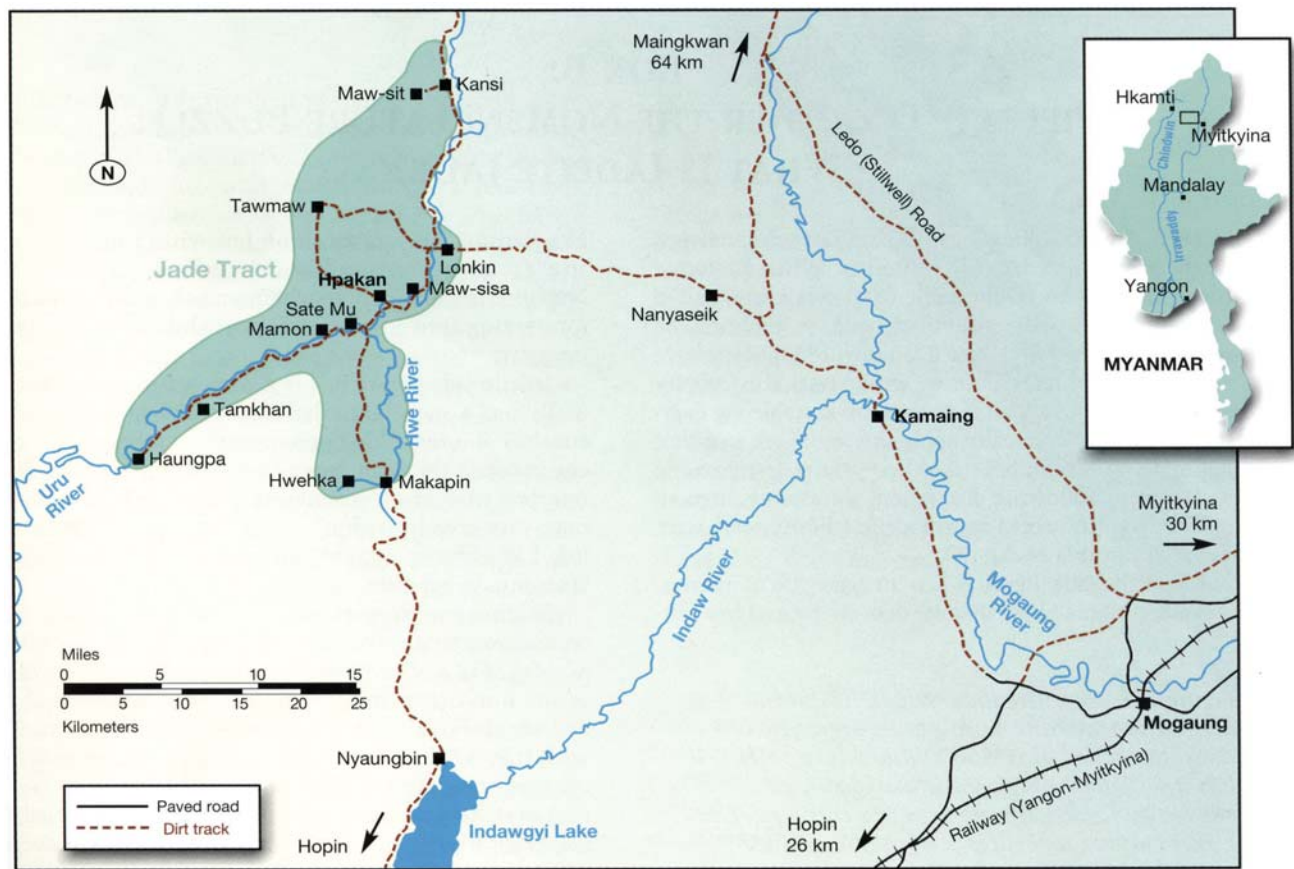


Figure 2. Hpakon is the center of the jadeite mining district (or central Jade Tract) in north-central Myanmar. There are two main routes into the Hpakon region, one from Mogaung and the other from Hopin. Adapted by R.W. Hughes and G. Bosshart from *Hind Co. Map* (1945).

trader traveling through what is now northern Myanmar picked up a boulder to balance the load on his mule. When it was broken open, the brown-skinned rock revealed a vivid, “emerald” green material with the toughness of nephrite. The Chinese were captivated by this stone.

Also according to Warry, the Yunnan government sent expeditions to find the source of this unusual material in the 13th and 14th centuries, but they were unsuccessful. Although occasional small pieces of green jadeite would appear in China over the next 500 years, their origin remained a mystery until the late 18th century.

Enter the Dragon. In 1784, Emperor Qianlong (who reigned from 1736 to 1796) extended China’s jurisdiction into northern Myanmar, where Chinese adventurers soon discovered the source of the green stone. From the late 18th century on, considerable amounts of jadeite were transported to Beijing and the workshops of China’s foremost jade carvers.

Emperor Qianlong preferred the rich hues of this “new” jade (jadeite), and soon the finest semi-transparent rich green *fei-ts’ui* (“kingfisher”) material came to be known as “Imperial jade” (Hertz, 1912).

A well-established route for jadeite from Myanmar to China existed by 1798. Although political and other circumstances forced several alterations in the original route, the “jade road”—from Hpakon through Baoshan and Kunming in Yunnan—operated until World War II.

The Rise of Hong Kong as a Trading Center. With the arrival of a communist regime in China following the Second World War, materialistic symbols such as jade fell out of favor. For the most part, the jadeite trade moved to Hong Kong, where carvers emigrated from Beijing and Shanghai.

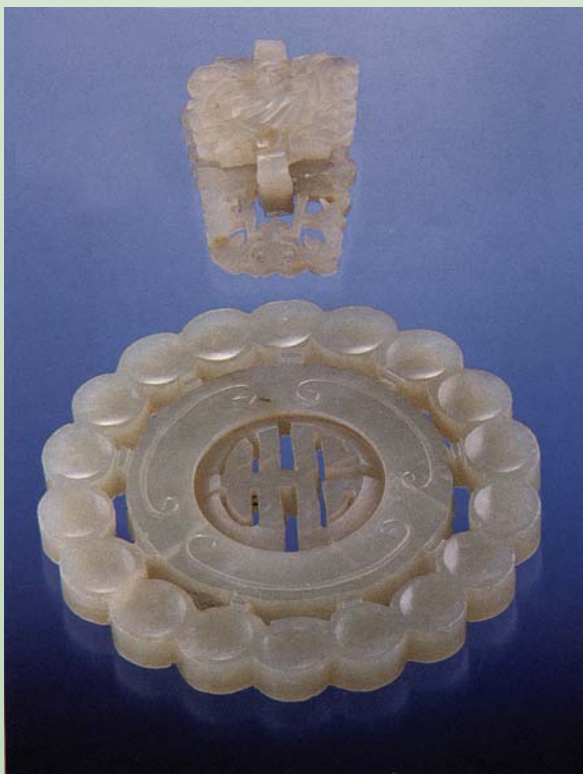
In the 1950s, jadeite dealers went directly to Hong Kong, or had their stones relayed for sale there via Yunnanese and Cantonese colleagues. Jadeite auctions were organized in hotels such as the four-story

BOX B: PIECING TOGETHER THE NOMENCLATURE PUZZLE: WHAT IS JADEITE JADE?

In 1863, French mineralogist Alexis Damour analyzed bright green jades from then-Burma. When he found these samples to be different from what was called Chinese jade (usually amphibole jade, or nephrite), he named the mineral *jadeite* (Damour, 1863). Although, as noted in the text, Chinese enthusiasts use *jade* for many ornamental materials that are suitable for carving, gemologists typically apply the term *jade* to either nephrite (an amphibole rock) or jadeite (a pyroxene rock). In the following discussion, we also distinguish jadeite jade (the rock) from jadeite (the mineral with nominal formula $\text{NaAlSi}_2\text{O}_6$).

Nephrite jade (figure B-1) is an aggregate of micron-wide amphibole fibers that are densely packed in a felt-

Figure B-1. Nephrite jade, which lies in the actinolite-tremolite series, is an aggregate of densely packed amphibole fibers. It usually has a distinctive greasy surface luster, as shown by these Chinese nephrite carvings. The larger carving measures 5.7 cm in diameter; photo by Maha Tannous.



like texture. The composition lies within the actinolite-tremolite series $[\text{Ca}_2(\text{Mg}, \text{Fe}^{2+})_5\text{Si}_8\text{O}_{22}(\text{OH})_2]$. Nephrite is supremely tough among all rocks, suitable for carving into intricate shapes while retaining its integrity.

Jadeite jade (figure B-2) is a compact rock that generally has a more granular texture than nephrite. It consists of interlocking prismatic to “feathery” pyroxene crystals that can range in length from about 10 microns to over a centimeter, with a grain size that may vary greatly within a small area. Rarely, jadeite jade has a fibrous texture, but such jadeite will still be coarser than nephrite.

Jadeitic pyroxene in jade typically is not pure: It contains varying percentages of the pyroxenes diopside ($\text{CaMgSi}_2\text{O}_6$) and/or kosmochlor ($\text{NaCrSi}_2\text{O}_6$)—as well as the iron-rich pyroxenes hedenbergite ($\text{CaFe}^{2+}\text{Si}_2\text{O}_6$) and aegirine ($\text{NaFe}^{3+}\text{Si}_2\text{O}_6$)—in solid-solution mixtures with jadeite. Nearly pure kosmochlor (formerly called ureyite; first detected in meteorites) also may be present in some dark green jades. To qualify as jadeite jade petrologically, jadeitic pyroxene should constitute over 90%–95% of the rock; otherwise, it is just a jadeite-rich rock and will probably not have the toughness of jade. The other minerals in jadeite jade from Myanmar are sodic amphibole (compositions vary between eckermannite, glaucophane, richterite, and edenite), albite, analcime, tremolite, (ilmeno-) rutile, clinocllore, banalsite, and chromite (see, e.g., Harlow and Olds, 1987; Htein and Naing, 1994 and 1995).

Jadeite (the mineral) is allochromatic; that is, it is transparent and colorless when pure. But as jade, it generally appears white due to light scattering from fractures, openings on grain boundaries, and tiny aqueous fluid inclusions. However, even white jadeite jade is commonly polymineralic, in that it is intergrown with minor albite and analcime, which introduce additional internal light scattering from the changes in refractive index across grain boundaries. A few jadeite jade colors are caused by mineral staining on grain boundaries—(1) hydrous iron oxides for red- to orange-brown, (2) an iron compound (iron-rich clay?) for some dark green streaks, and (3) graphite for some gray-to-black jadeite jades.

However, most colors of jadeite are due to substitutions of transition metal ions for the fundamental Al^{3+} and minor Mg^{2+} (from diopside content) in jadeitic pyroxene. “Imperial” green, the most highly valued jade color (which is not duplicated in nephrite), is produced by Cr^{3+} ; only a very small percentage of this

minor element is required to induce the vivid color. "Grassy" greens are the result of either Fe^{2+} or Fe^{3+} as the essential chromophore, although mixed Fe^{2+} and Fe^{3+} produces blue-green, bluish black, and blue-black jadeite; the darkest colors form in "jadeites" that have a few weight percent total iron oxide and are closer to half-jadeite/half-augite or the pyroxene called omphacite (Harlow and Sorensen, in press). Lavender jadeite is attributed to Fe^{2+} -O- Fe^{3+} intervalence charge transfer in nearly pure jadeite (Rossman, 1974; Ponahlo, 1999). The color of aggregates of jadeite and sodic amphiboles has been termed "leek" green (in contrast to the "spinach" green of nephrite).

It is not uncommon for some jadeite to be partly replaced by fibrous tremolite or actinolite (Tröger, 1967; Ou Yang, 1993) in the course of late-stage metasomatism. These polymineralic jades are polychromatic, usually white with gray-green to blackish green specks or streaks. Rarely, they appear green with fairly even color distribution. The designation of mixtures of jadeite and amphibole as "szechenyite" has been discredited (Deer et al., 1963).

Maw-sit-sit, mentioned as *hmaw sit sit* by Chhibber (1934b) and first described by Gübelin (1965a-c), is an ornamental rock that is a mottled, highly variegated intergrowth of white albite, yellowish white Mg-chlorite (clinocllore), green-black kosmochlor, chromian jadeite, and green eckermannitic amphibole (figure B-3). The latter three minerals are commonly associated with corroded black chromite $[(\text{Fe},\text{Mg})\text{Cr}_2\text{O}_4]$ crystals, from which the chromophoric Cr^{3+} ion is derived (Harlow, unpublished data; Hänni and Meyer, 1997; Harlow and Olds, 1987; Mével and Kiénast, 1986). The interstitial material (colorless, yellow, or white) within the remaining tiny crevices and cavities consists of serpentine or zeolite (thomsonite?). *Maw-sit-sit* is a "cousin" of jade, but because some samples contain compact centimeter-sized regions of chromian jadeite, a clear distinction from jadeite jade can be difficult.

Chloromelanite has been used to describe a dark green to black variety of jadeite (Tröger, 1967; Hobbs, 1982); mineralogically, it is a solid solution of roughly equal amounts of jadeite, diopside, and aegirine (Jackson, 1997). The term is used rather loosely by traders, who typically apply it to any dark green to black jade-like material. We discourage use of the term *chloromelanite* because the traditional trade usage conflicts with modern knowledge of its composition. Indeed, the name has already been discredited mineralogically, in favor of referring to the particular pyroxenes present (omphacite or aegirine-augite; Morimoto et al., 1988).

From a gemological standpoint, what does all this mean? Jadeite jade is essentially a rock with a variable

Figure B-2. "True" jadeite jade contains at least 90% jadeitic pyroxene in a rock that is typically more granular than nephrite. Note the vitreous surface luster of these translucent jadeite beads, which range from 9 to 10.5 mm in diameter. Photo courtesy of and © Christie's Hong Kong and Tino Hammid.

composition. Although some have suggested a classification scheme for jadeite based on variations in composition or structure (Ou Yang, 1993; Wang, 1994), this is impractical for gemology because of the sophisticated equipment that would be needed to distinguish the various categories.

Figure B-3. A "cousin" to jade, *maw-sit-sit* is an attractive ornamental stone that is an intergrowth mainly of albite, clinocllore, kosmochlor, chromian jadeite, and eckermannitic amphibole. These two *maw-sit-sit* cabochons weigh 9.87 ct (oval) and 8.48 ct. Courtesy of Pala International; photo © Harold & Erica Van Pelt.



Tai Tung Hotel (Benjamin S. Y. So, pers. comm., 1997). Starting in 1967, auctions were organized by the Hong Kong Jewellery and Jade Manufacturers Association (formerly Hong Kong Jade and Stone Manufacturers Association).

With the introduction of free-market reforms in China in the early 1980s, the markets and workshops of China again sought fine jade. Once more, the famous jade road was opened.

Developments in Myanmar. Like China, Myanmar also was torn by political turmoil following World War II. In 1962, the Ne Win-led military junta seized power, plunging the country into isolation. The period 1963–64 saw the jadeite mines (along with most other mines, including those of the Mogok Stone Tract) placed off-limits to foreigners. By 1969, when the government banned private exploration and mining of gems, the isolation was complete (*Mining Journal Annual Review*, 1970).

After 1962, the only official sales of jadeite in then-Burma were at the annual gem emporiums held in the capital city of Rangoon (now Yangon). But most production reached the outside world via the black market. Lower grades tended to move directly into Yunnan, while top material was brought overland to the northern Thai town of Chiang Mai, where Hong Kong buyers assembled (Benjamin S. Y. So, pers. comm., 1997).

LOCATION AND ACCESS

Kyaukseimyo (literally “Jade Land”) is located in north-central Myanmar (again, see figure 2). The major jadeite mines are roughly enclosed east and west by the Uru (Uyu) and Chindwin rivers, between the 25th and 26th parallels of latitude, within Kachin State. (Because Myanmar names are often transliterated into the Roman alphabet in different ways, the authors have included common alternative spellings in parentheses. The first spellings given throughout the text are generally those of Chhibber, 1934b.) According to current information, the northernmost mines are near Kansi (Gin Si), while the southernmost are near Haungpa (Haung Par). The westernmost mine near Lai Sai (west of Tawmaw) is situated outside the central Jade Tract.

While Mogaung was formerly an important jadeite trading center, this is no longer the case. The present center of the mining district is Hpakan (Hpakant, Phakan, Phakant), a small town about

16 km by road southeast of Tawmaw that lies along the Uru River. Tawmaw, the village adjacent to the most famous primary jadeite outcrop, lies some 120 km (75 miles) northwest of Mogaung. Other important towns in the area, also along the Uru River, include Lonkin (Lon Hkin) and Sate Mu (Seikmo, Sine Naung). The important mining town of Hwehka (Hweka) is located some 20 km due south of Hpakan, along the Hwe River (*hka* means *river*). Jadeite is also mined at Makapin (Makabin), just east of Hwehka. With the exception of Hwehka and Makapin, no jadeite mining takes place east of the Uru River.

Two major dirt roads lead into the mining district, one from Mogaung and the other (the more mountainous route) from Hopin (again, see figure 2). The authors traveled both routes—via modified trucks, cars, motorbikes, ponies, elephants, and on foot.

The area is a highly dissected upland, consisting of ranges of hills that form the Chindwin-Irrawaddy watershed (Chhibber, 1934b). Loimye Bum, an extinct volcano north of Kansi and the highest peak in the area, is 1,562 m above sea level. Tawmaw is 840 m, and Hpakan is 350 m, above sea level. The hills are covered with dense jungle. This is the area through which the Stillwell (Ledo) Road (Eldridge, 1946) was built, which was the scene of fierce fighting during World War II.

So brutal is the climate and so poor are the roads that travel is extremely difficult during the May–October monsoon season. Indeed, the November–April dry season is the only time one can be sure of reaching the mines. The authors’ first trip, in early June 1996, took three days of struggling through mud to travel the approximately 56 km from Hopin to Hpakan, with a mere 8 km traveled on the second day. The return trip on the “good” road to Mogaung took more than 15 hours. At times during the rainy season, some areas are accessible only by foot, donkey, or elephant (figure 3). But the dry season has its challenges, too. Whereas by November the roads again become accessible by motor vehicle (eight hours for the Mogaung–Hpakan trip), the brown mud is transformed into dust clouds that cloak entire valleys.

Population. The population of Myanmar’s Kachin State consists mainly of Shan, who dominate the major towns and valleys, and Kachin, who traditionally inhabit the hills (Hertz, 1912). The jade mines themselves feature a mixture of different peoples from around the country, lured by the promise of



Figure 3. Both routes into Hpakan are virtually impassable during the rainy season. They require travel through dense jungle, in dirt that rapidly turns to mud. On this June 1996 trip, even the power of two elephants could not free this vehicle. Photo © Richard W. Hughes.

riches. During our visits to the mines, we met Kachin, Shan, Chinese, Chin, Wa, Rakhine, Nepalese, and Panthay. Today, however, immigrants from China increasingly dominate the towns and trade of northern Myanmar.

Hpakan today—“Little Hong Kong.” Over the past few years, the Myanmar government has liberalized regulations concerning the gemstone sector, including the jade trade. For the first time in several decades, Myanmar citizens are allowed to trade in gems, and even to sell to foreigners (“Myanmar Gemstone Law,” September 29, 1995). Nevertheless, conducting business in Myanmar continues to be difficult, especially for noncitizens.

Since the 1994 peace agreement between the Kachin rebel groups and the government, thousands of people from across Myanmar have flocked to the Hpakan area to look for jade. Like the gold rush towns of America’s Old West, Hpakan and neighboring Sate Mu (Sine Naung) have a transient air. None of the many people we met had been at the mines for more than a decade, and most had been there less than a year. Likewise, none of the government or military officials encountered in 1996 was there nine months later.

Still, wealth lurks just below the surface, with satellite dishes sitting atop tin-roofed huts. Indeed, the locals refer to Hpakan as “little Hong Kong,” because it is said that one can get anything there, including fine cognac, expensive watches, dancing girls, and heroin. It should be noted, too, that the area has a very high incidence of AIDS.

GEOLOGY OF THE HPAKAN/TAWMAW AREA

The first Western geologist to visit the mines was Fritz Noetling, who published his report in 1893. A.W.G. Bleek followed with reports in 1907 and 1908. However, the most detailed account of the geology of the jadeite deposits is that of Harbans Lal Chhibber (1934a and b), who spent two years doing field work in the area, commencing in 1928. While substantial work has since been done by Myanmar geologists, little of this is available to Western scientists. Thus, Chhibber’s reports remain the classic references on the subject. All those who have come after him, including Soe Win (1968), based their descriptions on Chhibber’s publications.

The jadeite region, or Jade Tract, is situated in the low-altitude plateau—also referred to as the “26°N (latitude) high” (Bender, 1983)—formed by the Uru anticline (east of the Hkamti syncline), where basement rocks are exposed through the sediments of the Chindwin and Irrawaddy basins. The Jade Tract is characterized by bodies of serpentinitized peridotite (between Late Cretaceous and Eocene age) in a broken outcropping from northernmost Maw Sit, through the Tawmaw area, to Makapin, Mohnyin (80 km south of Makapin), and Mawlu (35 km farther south). The serpentinites are surrounded by crystalline schists and plutonic rocks such as granites and monzonites (Bender, 1983), which were generated by subduction of the Indian plate under the Asian continent. In contrast, the peridotite was derived from either the base of the subducted oceanic plate or the mantle underlying the Asian plate, and emplaced by thrust faulting



Figure 4. At the Ka Htan West mine, located between Lonkin and Tawmaw, large peridotite boulders can be seen at the base of this 15-m-high wall of Uru Boulder Conglomerate. Photo by George Bosshart.

(precursor of the Sagaing Fault) and uplift during the collision of the Indian subcontinent with Asia.

Jadeite formed independently of the intrusives by crystallization from hydrous fluids (derived by dewatering of the subducted Indian plate) that rose along fractures in the serpentinized peridotite at relatively high-pressure/low-temperature conditions during the Tertiary formation of the Himalayas (Bender, 1983). Fluids that form in these special conditions are saturated with respect to sodium aluminosilicates—jadeite at higher pressure, albite at lower pressure—so the passage of these fluids through serpentinites generated swarms of jadeitite, albite-nepheline, and albitite dikes. All of these dikes generally have central

jadeite zones and external chlorite and amphibolite reaction rims at the contact with the serpentinites (Thin, 1985; Harlow and Olds, 1987; Sorensen and Harlow, 1998 and 1999). Chromite in the serpentinite locally reacted with the fluid to produce bright green (i.e., “Imperial”) jadeite, usually only in late-stage veins and as clots of green in white- to lavender-white jadeite. A shift from vertical thrusting to lateral faulting on the Sagaing Fault appears to have played an important role in the uplift and exposure of jadeite-bearing serpentinite in Myanmar; similar tectonics occurred in Guatemala, Japan, and Kazakhstan (Harlow and Sorensen, in press).

Primary Deposits. The classic primary occurrence of jadeite is on the plateau at Tawmaw. This area has been worked for over a hundred years and is said by miners to have produced all color varieties of jadeite. Other primary outcrops are found in the west, northwest, and northeast portions of the Jade Tract.

In each of the primary deposits, jadeitite dikes cross-cut the serpentinized peridotite parallel to shear zones following northeasterly strikes and dips from 18° to 90°SE. Dike thicknesses are poorly reported, probably because of weathering and the irregular swelling, pinching, and faulting-off of the dikes; however Soe Win (1968) does give a width of 5–8 feet (1.5–2.5 m) for the Khaisumaw dike at Tawmaw. Some dikes contain only jadeite and albite, while others have a boundary (on one or both sides) of amphibolite-eckermannite-glaucophane (dark gray to blue-black) or actinolite (dark green). The boundary with serpentinite is marked by a soft, green border zone that consists of a mixture of the adjacent vein minerals and chlorite, with or without calcite, actinolite, talc, and cherty masses (Chhibber, 1934b; Soe Win, 1968).

A Tawmaw mine director told GB and TO that the main dike was traceable north-northwest to Hkamti and Chindwin and even to India, surfacing and diving “like a serpent,” with another branch running north to Putao. However, the recent visit to Hkamti (see pp. 14–15) and geologic constraints argue against this interpretation. Rather, the Jade Tract and Hkamti jadeite deposits appear to originate from separate, deep-seated serpentinite bodies that perhaps were derived from the same collisional process, and Putao appears to produce a different jade-like material, obviously with a different origin.

Secondary Deposits. Most jadeite is recovered from secondary deposits in the Uru Boulder Conglomerate

(figure 4), southeast of the Tawmaw-hosting serpentinite body. The conglomerate is exposed over an area 3–6.5 km in width, which is widest at Mamon. It ranges up to 300 m thick and is probably Pleistocene to sub-Recent (Chhibber, 1934b). South of Hwehka, however, jadeite boulders are found in conglomerate interlayered with blue-gray sands and coal seams that are believed to be derived from a Tertiary (Miocene?) species of tree (Bleek, 1908; Chhibber, 1934a). Typical secondary deposits are located mostly west of the Uru River, including Sate Mu, Hpakangyi (adjacent to Hpakan), and Maw-sisa.

MINING TECHNIQUES

Dike Mining. Unlike secondary deposits, where the miner has to determine which of the myriad boulders is jadeite, the dikes contain readily recognizable material. Historically, miners started a fire near the dike and then threw water on the rock to crack it. Today, at Tawmaw, often miners first must use backhoes, scrapers, and other earth-moving equipment to expose the jadeite dikes, or rudimentary digging to create shafts to reach them. Shafts observed at the time of RWH and FW's 1997 visit reached depths of approximately 10–20 m (figure 5). Once a dike is exposed, miners use dynamite and jackhammers to break the jadeite apart and away from the country rock (figure 6).

Boulder and Gravel Mining. The workings at Sate Mu and Maw-sisa are, in many respects, typical of secondary jadeite mines. The Uru Boulder Conglomerate is as much as 300 m deep in places, and alluvial mining has barely scratched the surface. It appeared from the open cuts that there is a huge

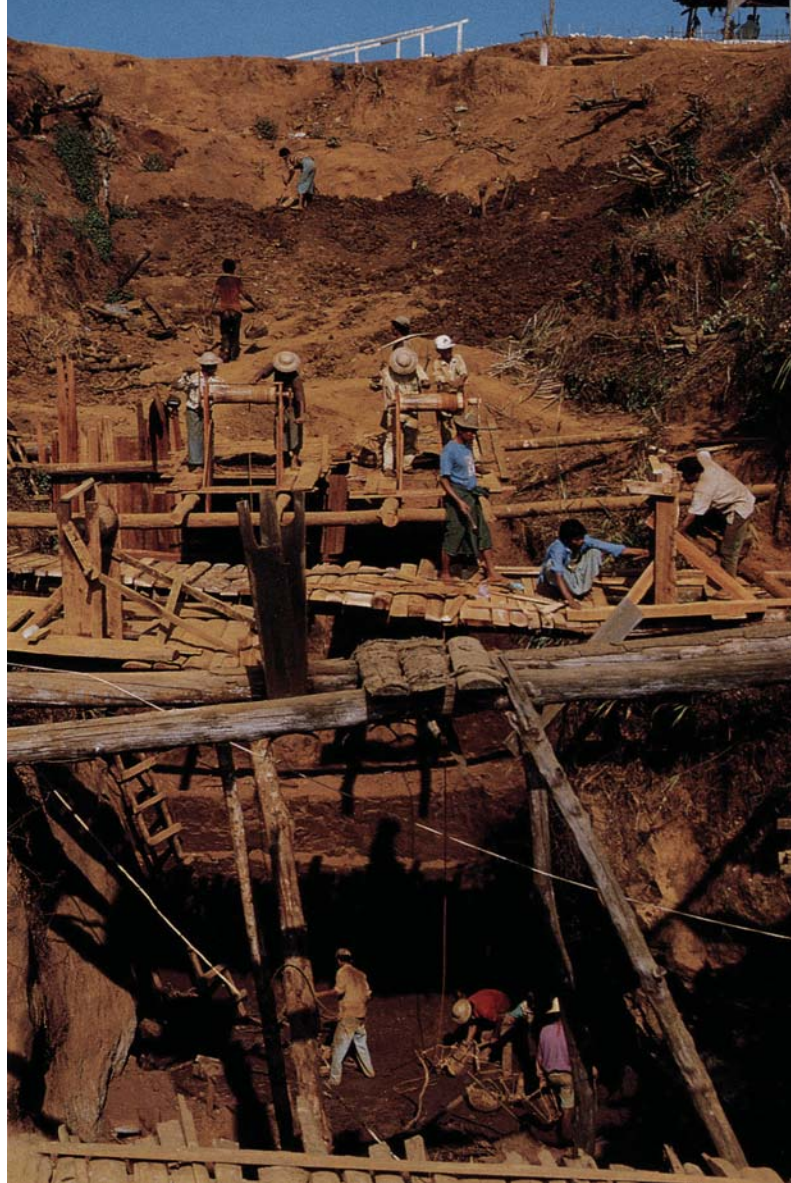


Figure 5. In some areas at Tawmaw, miners must dig deep shafts through the overburden to reach the jadeite dikes. Dirt and gravel are removed by a rudimentary winch-and-bucket system. Photo © 2000 Fred Ward.



Figure 6. Once a dike is exposed at Tawmaw, jackhammers are needed to break the jadeite apart. Photo © Richard W. Hughes.



Figure 7. Mining of the Uru conglomerate is done in step-like claims approximately 5 m wide that were originally separated by thin “walls.”
Photo by Olivier Galibert.

quantity of material remaining to be extracted. We saw people working about 18 m down into the conglomerate, stripping it away with primitive tools.

The first step in mining the conglomerate is removal of the overburden, *taung moo kyen* (literally, “head cap removal”). Since the “overburden” (per Chhibber, 1934b, a layer of alluvium of variable thickness followed by a pebble-gravel layer over the Uru Conglomerate) also may contain jadeite, workers must search this material, too. Each claim is only about 5 m wide; to keep from encroaching onto the neighbor’s area, miners leave a thin wall of conglomerate as a partition. Eventually the walls themselves weather away; nevertheless, when seen from above, the result is spectacular—several square kilometers of step-like benches, as if an ancient city were being excavated (figure 7). At Maw-sisa, diggers concentrated on mining a black conglomerate layer called *ah may jaw*, where jadeite is said to be richest.



Figure 8. Thousands of workers remove the dirt and gravel at Hpakangyi to reach the Uru conglomerate and its promise of fine jadeite. Using the most rudimentary of carrying devices—two crudely fashioned bamboo buckets—this young miner leads a trail of laborers up the steep path from the bottom of the pit to a truck that will carry the waste to the river. Photo © Richard W. Hughes.

At Hpakangyi, more than 10,000 workers excavated an area that had reached hundreds of meters deep (figure 8). Waste was piled into a waiting truck, and then emptied directly into the river that bisects Hpakan. At the dump, jade pickers scrambled over the riverbank to search for jade overlooked at the source. Along the banks of the Uru River, large mounds of boulders attest to two centuries of mining. When the water level is high, the river is worked by divers breathing via crude air pumps (figure 9).

Miners admitted that production was erratic at best. While occasionally they would find 20–30 pieces in a single day, often they would not recover any jadeite boulders for days. Most of these boulders weigh less than 1 kg, although some reach 300 kg. Only a tiny fraction of the jadeite boulders recovered contain jewelry-quality material.

Identifying Jadeite Boulders. After viewing the methods by which jade is mined, the first question any observer asks is: How do miners separate the occasional jadeite boulder from the thousands of other boulders that look so similar? Repeated questioning of various jade traders, cutters, and miners yielded the following clues.

The most important member of the mining team is the one who operates the jackhammer or hoe, for he will spot most of the jadeite boulders. When struck with a metal tool, a jadeite boulder produces a different sound (rings more) than other rocks. Such blows also may expose the “show points” (*pyat kyet* in Burmese and “pine flowers” to the Chinese; Gump, 1962)—the color of the jadeite—beneath the skin (figure 10).

Miners also look for a characteristic fibrous texture (*yumm*) in some jadeite boulders. Although jadeite jade is not normally thought of as having fibrous texture, it sometimes is found in jade that is 100% jadeitic pyroxene and in other cases may be related to partial replacement by—or admixture with—an amphibole (Htein and Naing, 1994, 1995). Also, jadeite is typically smoother than most other boulders and will not show the crystalline reflections (possibly from mica or quartz) often seen in the others. Another indicator of jadeite is a type of sheen, called *shin*. Black *shin* is said to “infect” or “damage” the stone; the miners consider it a harbinger of bad luck. According to Chhibber (1934b), *shin* is amphibolite or amphibole schist. Such an impurity would account for the lower quality of this jadeite.

Jadeite jade also has a greater “heft” (specific gravity of about 3.34) than other types of rocks in



Figure 9. At Mamon and Maw-sisa in particular, miners take advantage of the seasons when the river is high to dive for jade. While a man on land or a raft works the crude air pump (which resembles four bicycle pumps strapped together), this diver at Maw-sisa searches the river bottom for jade with the hose between his teeth (inset). Photos © Richard W. Hughes.

Figure 10. Water readily reveals the “show points” of bright green jadeite on this boulder. Photo © Richard W. Hughes.





Figure 11. At Nansibon, backhoes are used to work the serpentinite boulder conglomerate in which jadeite boulders occur in narrow horizontal concentrations. Photo by George E. Harlow.

the conglomerate. In addition, divers feel that it sticks slightly to their hands or feet under water, a property that has been used historically by the Chinese to separate both jadeite and nephrite from substitutes (“The art of feeling jade,” 1962).

Maw-Sit-Sit. The Maw Sit vein, which produces maw-sit-sit, lies about 2 km from Kansai at the northeastern end of the Jade Tract (again, see figure 2). The maw-sit-sit mine consists of a narrow, vertical trench cut that is some 9 m deep. The total length of the active mining area in November 1997 was approximately 200 m.

OTHER JADEITE LOCALITIES IN MYANMAR

According to Chhibber (1934b), other occurrences of jadeite in present-day Myanmar include Mawhun, 20 km southwest of Mohnyin, and a site on the bank of the Chindwin River, in the Hkamti area. It is possible that the latter reference is actually to the Nansibon mining region, described below, which was recently visited by one of the authors (GEH). The United Nations (1979) reported the extraction of low-quality jade from steeply dipping late-Tertiary boulder conglomerates in the Indaw-Tigyang area, which extends another 50 km south of Mawhun. Similar conglomerates were observed at Nansibon (again, see below).

Hkamti Area: Nansibon and Natmaw. On an expedition to the jade mines by a group traveling under the auspices of the American Museum of Natural History in January and February 2000, four geologists and two gemologists visited the mining area called Nansibon (Namsibum, Manhshibon). It was the first recorded visit by Western gemologists to this area. Located in the Sagaing Division, about 35 km (22 miles) southeast of the Chindwin River town of Hkamti, Nansibon is a group of joint-venture tracts that extend about 2 km along a north-south trending ridge in the middle of dense jungle (central location at N25°51'24", E95°51'30" determined by GPS measurements). The deposit is a steeply inclined (60°–90°E) serpentinite boulder conglomerate in which jadeite cobbles from a few centimeters to perhaps one meter in diameter are “concentrated” in a few narrow horizons. Mining is restricted to mechanized excavation of surface exposures of the conglomerate (figure 11), which disappears both north and south under Tertiary river sands and lake sediments of the Chindwin basin. Now largely unworked, Natmaw (Nawmaw, Nathmaw) is a smaller area roughly 30 km south of Nansibon, where miners have explored jadeite dikes in serpentinite. As the road there was impassable and time was constrained, the group could not visit these latter mines.

According to current and retired officials from the Myanmar Gems Enterprise (MGE), relative to the Jade Tract, Nansibon presently produces a large portion of the gem-quality Imperial jadeite mined in Myanmar, lesser amounts of other colors and “commercial” jadeite (used for carvings and bangles), and small amounts of “utility” jade (used for tiles, building veneers, and very large carvings; “Myanmar jade,” 1991). During the recent visit, GEH and gem-

ologist Robert Kane acquired a comprehensive suite of jadeite from Nansibon in colors including black and many shades of green, lavender, blue-green, “nearly blue,” and “carnelian orange”; these varied from translucent to semi-translucent. They saw numerous small (2–5 mm diameter) cabochons of translucent Imperial green jadeite from Natmaw.

Putao. Jadeite is also found some 320 km (200 miles) north of Myitkyina, near Putao, but the deposit was reported by Chhibber to be inaccessible and the quality of the jadeite poor. Harlow and Kane were told by U Shwe Maik, former director of jade acquisition for MGE, that the alleged jade from Putao is actually green massive hydrogrossular (now hibschite). They obtained a sample for study.

JADEITE TRADING IN MYANMAR

Contributing to the aura of mystery that surrounds jadeite is the distinctive system of jadeite commerce in Myanmar. This includes the markets for rough jadeite, the boulder “taxes,” and evaluation of the rough. The Chinese, who dominate the market for fine jadeite both within and outside of Myanmar, play an important role in this system.

Figure 12. Vendors work the morning jadeite market in Mandalay. Photo © 2000 Fred Ward.



Figure 13. In Mandalay, cutters still use a board coated with a mixture of carborundum (of various grits) and hard wax to shape cabochons (photo by Mark Smith). They then polish jadeite on bamboo lathes, often without any abrasive (inset photo © 2000 Fred Ward).

Rough Jade Markets. Most of Myanmar’s open jadeite markets are small, perhaps because the idea of free trade is still somewhat new. Nevertheless, there are markets in Hpakan, Lonkin, and Mogaung.

Myanmar’s largest jade market is in south Mandalay (figure 12), a city that is said to operate on the three “lines”—white (heroin), red (ruby), and green (jade; Cummings and Wheeler, 1996). Trading is conducted in several places along 86th Street (Kammerling et al., 1995). Here, every morning, hundreds of people can be observed haggling over jadeite. Just south of the markets, cutting workshops are also found. Despite the toughness of jadeite, many cutters in Mandalay still shape cabochons on boards that have been coated with carborundum and hard wax, and then polish the jadeite on bamboo lathes (figure 13).

Taxes. Written on each jadeite boulder we saw in the markets was a registration number and the weight of the boulder; this signified that tax had been paid on the piece. A government-appointed committee evaluates the boulders in Hpakan and then levies a tax of

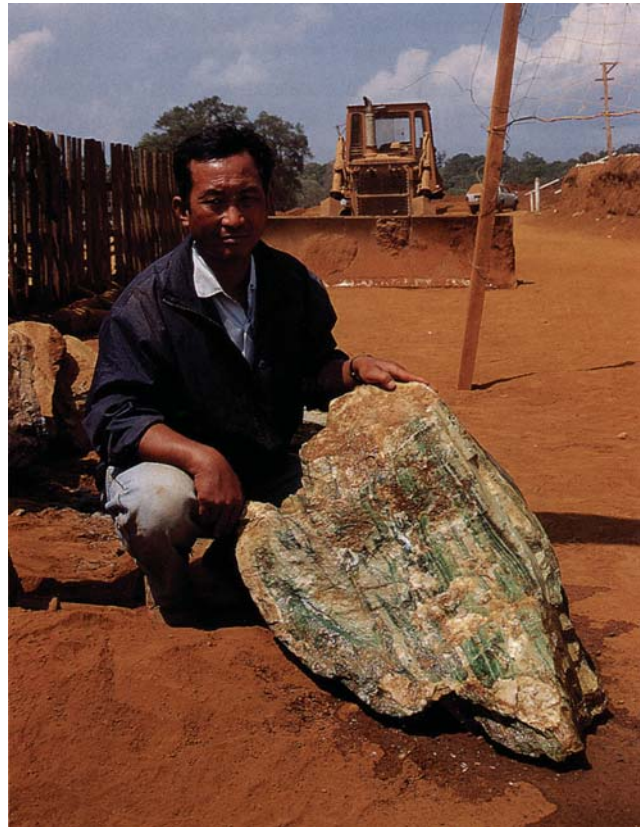
10% of the appraised value. Even though a boulder has been officially appraised, its purchase is inevitably a gamble for the trader.

Types of Jadeite Rough. Traders classify jadeite rough first according to where it was mined. *River jade*, the jadeite recovered from alluvial deposits in and along the Uru River, occurs as rounded boulders with a thin skin (figure 14, top left). In contrast, *mountain jade* (found away from the river) appears as rounded boulders with thick skins (figure 14, bottom left). The irregular chunks of jadeite quarried directly from *in situ* deposits, such as those at Tawmaw, represent a third type (figure 14, right). According to Chhibber (1934b), “it is locally believed that jadeite mined from the rivers and conglomerate is more ‘mature’ than that of Tawmaw.”

Because weathering usually removes damaged or altered areas, the best qualities are usually associated with river jade. In addition, the thin skin—and, therefore, greater likelihood of “show points”—in river jade allows a more accurate estimate of the quality and color within (figure 10). Mountain jade boulders tend to be clouded by a thick layer (termed “mist” by Chinese traders) between the skin and the inner portion of the boulder (Ho, 1996, figure 14).

The occurrence of green and lavender jadeite is independent of the deposit type, but reddish orange to brown jadeite is found only in those boulders that are recovered from an iron-rich soil. The reddish orange results from a natural iron-oxide staining of the skin of the porous jadeite, and is sometimes intensified with heat (Chhibber, 1934b).

Figure 14. Top left: This jadeite boulder shows the relatively thin skin and potentially good color that is usually associated with “river jade.” Although from the outside this appears to be a normal jadeite boulder, oxidants that entered through cracks on the surface have produced a large area of discoloration. Bottom left: Note the thick yellow “mist” around the jadeite in this boulder of “mountain jade.” Right: A key advantage to jadeite taken from *in situ* deposits is that the quality of the material is readily apparent. Photos © Richard W. Hughes.



EVALUATING ROUGH

One of the greatest challenges in the jadeite trade is the evaluation of a material that is covered by a skin that typically hides all traces of the color and clarity/diaphaneity that lies within. This skin can be white, yellow, light to dark brown, or black.

According to traders and miners with whom we spoke, they look first for any color spots or show points in those areas where the skin is thin enough to see through. Evidence of surface cracks is also important, as fractures often extend into the boulder and open a path for oxidants to discolor the interior (see figure 14, top left). Such fractures can have a strong negative impact on the value of the material.

If a show point is not available or is inadequate, the owner will sometimes polish an “eye” or *maw* (“cut” or “window”) through the skin (see figure 1). First, though, the owner will carefully examine the piece to determine the best location because, if good color shows through the window, the boulder’s value rises tremendously. Conversely, if poor color is revealed, the value drops. Such windows should be checked for artificial coatings or other tampering, which may give a false impression of the material within (see, e.g., Johnson and Koivula, 1998).

If there are no show points or windows, a common technique is to wet the surface of the boulder in the hope that the underlying color will come through (again, see figure 10). Where even a little color is suggested, traders also use small metal plates in conjunction with a penlight. They place the edge of the plate on what appears to be a promising area and then shine the penlight from the side farthest from the eye (figure 15). The plate removes the glare from the light, so any color can show through. If light penetrates the underlying jadeite, this is an indication of good transparency. But, due to jadeite’s aggregate structure, the color will have been diffused from throughout the boulder by the scattering of light. Thus, even a small area of rich color can make a piece appear attractive through the window. To see an example of this, take a jadeite cabochon that is white, but has a small green vein or spot. Shine a penlight or fiber-optic light through the cab from behind. *Voilà*, the entire cabochon appears green.

To reduce the risk of such a speculative business, much jadeite rough is simply sawn in half; this is the approach used at the government-sponsored auctions in Yangon. However, parting a boulder down the middle has the danger of cutting right through the center of a good area. A more careful



Figure 15. To get a better idea of the quality of color in this boulder, the dealer places a metal plate at the far side of a small area with potential and then uses a penlight to illuminate it. Photo © Richard W. Hughes.

method of evaluating jadeite boulders involves grinding away the skin (Lee, 1956). Alternatively, some owners gradually slice the boulder from one end (perhaps the thickness of a bangle, so that each slice can be used for bangles or cabochons) until they hit good color. They then repeat the process from the opposite end, the top, and the bottom, until the area of best color is isolated (figure 16).

Certain experienced jade traders are said to have a “golden hand” when it comes to judging jade boulders; that is, they are able to predict, by studying the outside of the boulder, what the inner color will be. Nevertheless, the jade trade seems to be a competition between sellers, who want to show the best spot of color and not disclose the remaining bad points, and buyers, who want to imagine a fine interior in a stone that shows poorly in the few *maws*.

EVALUATION OF FINISHED JADEITE

The evaluation of finished jadeite has been discussed by Healy and Yu (1983), Ng and Root (1984), and, most recently, by Christie’s (1995b), Ho (1996),

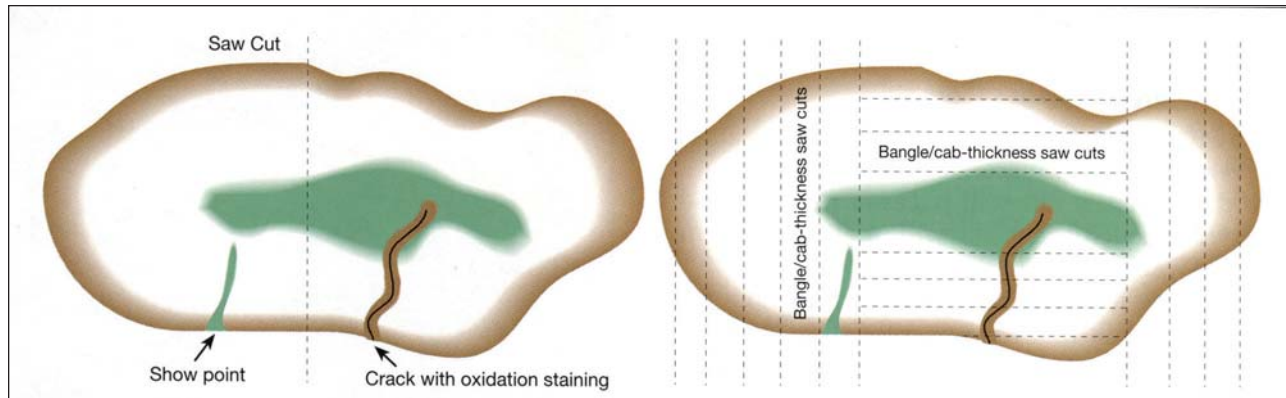


Figure 16. In sawing jadeite boulders, center saw cuts (left) run the risk of cutting through a valuable area. A better method (right) involves making shallow saw cuts from one end (perhaps the thickness of a bangle, so that each slice can be used for bangles/cabs) until one hits good color. Then the process is repeated from the opposite end, again until good color is encountered. This defines the region of top-grade material. The process is repeated until the area of best color is isolated. These cross-sections also illustrate a show point and an oxidation stain penetrating the jadeite through a crack.

and Ou Yang (1995, 1999). The basic system is summarized below in a somewhat simplified fashion. Although we use the concepts discussed in the above publications, as much as possible we have chosen language that is comparable to that used for other colored stones.

While a number of fanciful terms have been used to describe jadeite, its evaluation is similar to that of other gemstones in that it is based primarily on the “Three Cs”—color, clarity, and cut (fashioning). Unlike most colored stones, the fourth “C”—carat weight—is less important than the dimensions of the fashioned piece. However, two additional factors are also considered—the “Two Ts”—translucency (diaphaneity) and texture. In the following discussion, Chinese terms for some of the key factors are given in parentheses, with a complete list of Chinese terms for various aspects of jade given in table 1.

Color (se). This is the most important factor in the quality of fashioned jadeite. As per standard color nomenclature, jadeite’s colors are best described by breaking them down into the three color components: hue (position on the color wheel), saturation (intensity), and tone (lightness or darkness). Color distribution must also be taken into account. The necklace in figure 17 is an excellent example of top-quality hue, saturation, tone, and color distribution.

- Hue (*zheng*): Top-quality jadeite is pure green. While its hue position is usually slightly more yellow than that of fine emerald and it never quite reaches the same intensity of color, the ideal for jadeite is a fine “emerald” green. No brown or gray

TABLE 1. Chinese jade nomenclature^a.

Chinese name	Meaning
<i>Yu</i>	Chinese word for jade
<i>Ruan yu</i>	Nephrite
<i>Ying yu</i>	“Hard jade” or jadeite
<i>Fei-ts’ui (feicui)</i>	“Kingfisher” jadeite
<i>Lao keng</i>	“Old mine” jadeite—fine texture
<i>Jiu keng</i>	“Relatively old mine” jadeite—medium texture
<i>Xin keng</i>	“New mine” jadeite—coarse texture
<i>Ying</i>	Jadeite type with the highest luster and transparency
<i>Guan yin zhong</i>	Semi-translucent, even, pale green jadeite
<i>Hong wu dong</i>	Lesser quality than <i>guan yin zhong</i> , with a pale red mixed with the green
<i>Jin si zhong</i>	“Golden thread” jadeite: A vivid green color is spread evenly throughout the stone. This type is quite valuable.
<i>Zi er cui</i>	High-grade jadeite mined from rivers. Because of its high translucency, it is also known as <i>bing zhong</i> (“ice”).
<i>Lao keng bo li zhong</i>	Old-mine “glassy” (finer texture, more translucent) jadeite (see figure 18). In Imperial green, this type is the most valuable jadeite.
<i>Fei yu</i>	Red jadeite, named after a red-feathered bird
<i>Hong pi</i>	“Red skin” jadeite, cut from the red skin of a boulder (see figure 1)
<i>Jin fei cui</i>	Golden or yellow jadeite
<i>Shuangxi</i>	Jadeite with both red and green
<i>Fu lu shou</i>	Jadeite with red, green, and lavender
<i>Da si xi</i>	Highly translucent jadeite with red, green, lavender, and yellow
<i>Wufu linmen</i>	Jadeite with red, green, lavender, and yellow, as well as white as the bottom layer

^aBased on Ho (1996).

modifiers should be present in the finished piece.

- Saturation (*nong*): This is by far the most important element of green and lavender jadeite color. The finest colors appear intense from a distance (sometimes described as “penetrating”). Side-by-side comparisons are essential to judge saturation accurately. Generally, the more saturated the hue is, the more valuable the stone will be. A related factor is referred to as *cui* by the Chinese. Colors with fine *cui* are variously described as brilliant, sharp, bright, or hot. This is the quality that makes “shocking” pink shocking and “electric” blue electric.
- Tone (*xian*): The ideal tone is medium—not too light or too dark.
- Distribution (*jun*): Ideally, color should be completely even to the unaided eye, without spotting or veins. In lower qualities, fine root- or vein-like structures that contrast with the bodycolor of the stone may be considered attractive. However, dull veins or roots are less desirable. Any form of mottling, dark irregular specks, or blotches that detract from the overall appearance of the stone will reduce the value.

Clarity. This refers to imperfections that impair the passage of light. The finest jadeite has no inclusions or other clarity defects that are visible to the naked eye.

Typical imperfections are mineral inclusions, which usually are black, dark green, or brown, but may be other colors. White spots also are common, as are other intergrown minerals. The most severe clarity defects in jadeite are fractures (healed or unhealed), which can have an enormous impact on value because jadeite symbolizes durability and perfection (Ou Yang, 1999).

Translucency (Diaphaneity). This is another important factor in evaluating quality. The best jadeite is semi-transparent; opaque jadeite or material with cloudy patches typically has the least value.

It is interesting to note that even if the overall color is uneven or low in saturation, jadeite can still be quite valuable if it has good transparency. The “glass” jade bangles in figure 18 sold for U.S. \$116,000 at the November 1999 Christie’s Hong Kong auction.

Texture (*zhong*). In jadeite, texture is intimately related to transparency. In the authors’ experience, typically the finer the texture is, the higher the



Figure 17. This necklace, which contains a total of 65 beads (7.8–9.8 mm in diameter) and two matching hoops, illustrates the optimum “vivid emerald green” color in fine jadeite. Note also the very fine “old mine” texture and translucency. Photo courtesy of and © Christie’s Hong Kong and Tino Hammid.

transparency will be. Further, the evenness of the transparency depends on the consistency of the grain size. Our observations also suggest that coarse-grained jadeite tends to have more irregularities, blotches, or discolorations.

Texture is key to the classification of fashioned jadeite into three categories: fine (*lao keng*, or “old mine”), medium (*jiu keng*, or “relatively old mine”), and coarse (*xin keng*, or “new mine”), as described by Ho (1996). “Old mine” is considered the best, with the finest texture, translucency, and luster (again, see figures 17 and 18). Note that Chinese jadeite dealers also use the terms “old mine” (*keng zhong*) and “new mine” (*xin shan zi*) to describe rough. This is not really an expression of the age or location where the jadeite is mined, but more an indication of texture and translucency, with old-mine jadeite having a higher quality, being of finer grain size, and having greater luster and translucency (Ho, 1996). It probably derives from the belief that jade that is more compact and of finer texture is of greater age.



Figure 18. Referred to as “glass” jadeite, this rare pair of bangles (both 53.4 mm in interior diameter, with thicknesses of 9.6 and 9.7 mm) shows extraordinary translucency. Photo courtesy of and © Christie’s Hong Kong and Tino Hammid.

Fashioning. More so than for most gem materials, fashioning plays a critical role in jadeite beauty and value. Typically, the finest qualities are cut for use in jewelry—as cabochons, bracelets, or beads. Cutters often specialize: one may do rings, another carvings, and so on.

Polish is particularly important with jadeite. Fine polish results in fine luster, so that light can pass cleanly in and out of a translucent or semi-

transparent piece. One method of judging the quality of polish is to examine the reflection of a beam of light on the surface of a piece of jadeite. A stone with fine polish will produce a sharp, undistorted reflection, with no “orange-peel” or dimpling visible.

Following are a few of the more popular cutting styles of jadeite.

Cabochons. The finer qualities are usually cut as cabochons (see figure 1). One of the premium sizes—the standard used by many dealers’ price guides—is 14 × 10 mm (Samuel Kung, pers. comm., 1997). Material used for cabochons is generally of higher quality than that used for carvings (Ou Yang, 1999), although there are exceptions.

With cabochons, the key factors in evaluating cut are the contour of the dome, the symmetry and proportions of the cabochon, and its thickness. Cabochon domes should be smoothly curved, not too high or too flat, and should have no irregular flat spots. Proportions should be well balanced, not too narrow or wide, with a pleasing length-to-width ratio (Ng and Root, 1984). The best-cut cabochons have no flaws or unevenness of color that is visible to the unaided eye.

Since the 1930s, double cabochons, shaped like the Chinese ginko nut, have been considered the ideal for top-grade jadeite, since the convex bottom is said to increase light return to the eye, thus intensifying color (Christie’s, 1996). Stones with poor transparency, however, are best cut with flat bases, since any material below the girdle just adds to the bulk without increasing beauty. Hollow cabochons are considered least valuable (Ou Yang, 1999).

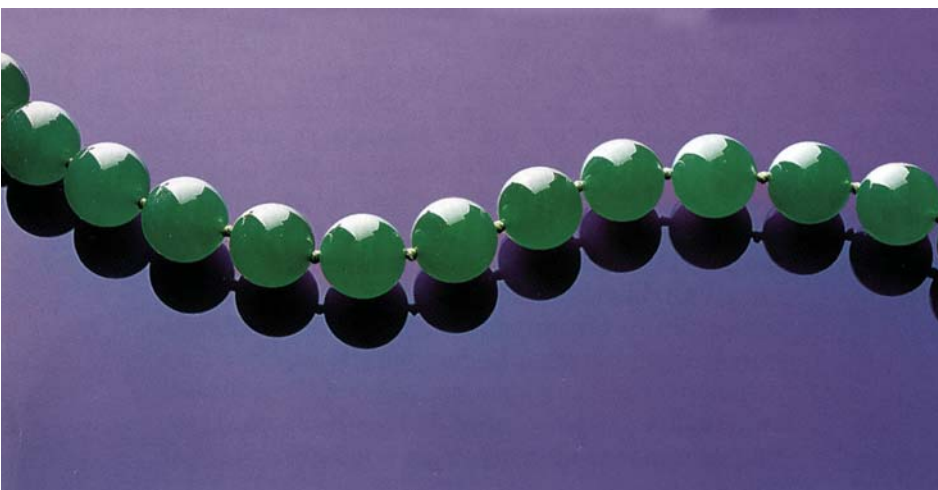


Figure 19. Uniformity of a fine “emerald” green color, superb translucency, size, and symmetry all come together to produce the necklace known as the Doubly Fortunate. The 27 beads, which range from 15.09–15.84 mm, were all cut from the same piece of rough, a 1 kg portion of a much larger boulder. The name derived from the fact that the necklace’s owners “doubled their fortunes” every time the boulder was cut (Christie’s, 1997, p. 70). The necklace sold in 1997 for approximately US\$9.3 million. Photo courtesy of and © Christie’s Hong Kong and Tino Hammid.

Traditionally, when fine jadeite cabochons are mounted in jewelry, they are backed by metal with a small hole in the center. The metal acts as a foilback of sorts, increasing light return from the stone. Also, with the hole one can shine a penlight through the stone to examine the interior, or probe the back with a toothpick to determine the contours of the cabochon base (Ng and Root, 1984). When this hole is not present, one needs to take extra care, as the metal may be hiding some defect or deception.

Beads. Strands of uniform jadeite beads are in greater demand than those with graduated beads. The precision with which the beads are matched for color and texture is particularly important, with greater uniformity resulting in greater value (figure 19). Other factors include the roundness of the beads and the symmetry of the drill holes. Because of the difficulties involved in matching color, longer strands and larger beads will carry significantly higher values. Beads should be closely examined for cracks. Those cracked beads of 15 mm diameter or greater may be recut into cabochons, which usually carry a higher value than a flawed bead (Ng and Root, 1984).

Bangle Bracelets. Bangles are one of the most popular forms of jadeite jewelry, symbolizing unity and eternity. Even today, it is widely believed in the Orient that a bangle will protect its wearer from disaster by absorbing negative influences. For example, if the wearer is caught in an accident, the bangle will break so that its owner will remain unharmed. Another common belief is that a spot of fine color in a bangle may spread across the entire stone, depending on the *fuqi*—good fortune—of the owner (Christie's, 1995a). In the past, bangles (and rings) were often made in pairs, in the belief that good things always come in twos (Christie's, 1997).

Because a single-piece bangle requires a large quantity of jadeite relative to its yield, prices can be quite high, particularly for fine-quality material. The bangle in figure 20 sold for US\$2,576,600 at the Christie's Hong Kong November 1999 auction. Multi-piece bangles are worth less than those fashioned from a single piece, because the former often represent a method of recovering parts of a broken bangle. Mottled material is generally used for carved bangles, as the carving will hide or disguise the imperfections. When a piece is carved from high-quality material, however, it can be a true collector's item (Ng and Root, 1984).



Figure 20. Believed to date back at least four millennia in China, the jade bangle is both one of the oldest and one of the most important pieces of jewelry in the Chinese culture. This superb jadeite bangle sold for US\$2,576,600 at the Christie's Hong Kong November 1999 auction. The interior diameter is 49.50 mm; the jadeite is 8.36 mm thick. Photo courtesy of and © Christie's Hong Kong and Tino Hammid.

Huaigu (pi). The Chinese symbol of eternity, this is a flat disk with a hole in its center, usually mounted as a pendant or brooch. Ideally, the hole should be one-fifth the diameter of the entire disk and exactly centered. Small pairs are often used in earrings or cufflinks (figure 21).

Saddle Rings (su an). Carved from a single piece of jadeite, these look like a simple jadeite band onto which a cabochon has been directly cut (figure 22). Saddle rings allow the most beautiful area to be positioned on top of the ring, while the lower part is relatively hidden, whereas a standard jadeite band should have uniform color all around. *Saddle tops* are the top piece of a saddle ring, without the band portion (again, see figure 21).

Double Hoop Earrings (lian huan). These require a large amount of rough relative to their yield, since they are cut from two pieces of the same quality, each of which must produce two hoops. A pair of these earrings (figure 23) sold for US\$1.55 million at Christie's April 29, 1997, Hong Kong sale (Christie's, 1997).



Figure 21. These fine matched huaigu (each approximately 19×4.5 mm) have been set as cufflinks, with diamonds inserted into their center holes. Each is linked to a saddle top of comparable material. Photo courtesy of and © Christie's Hong Kong and Tino Hammid.

Carvings. For the most part, the jadeite used in carvings is of lower quality than that used for other cutting styles, but nevertheless there are some spectacular carved jadeite pendants and *objets d'art*. The intricacy of the design and the skill with which it is executed are significant factors in determining the value of the piece. Carving is certainly one area where the whole equals more than the sum of the parts.

Recut Recovery Potential. As with many other types of gems, the value of poorly cut or damaged pieces is generally based on their recut potential. For example, it might be possible to cut a broken bangle into several cabochons. Thus, the value of the broken bangle would be the value of the cabochons into which it was recut (Ng and Root, 1984). If three cabochons worth \$500 each could be cut from the bangle, its value would be about \$1,500.

Enhancements and Imitations. *Enhancements.* Jadeite historically has been subjected to various enhancements to “finish” it, “clean” surface and interior stains, and even dye it to change the color altogether. In recent years, a three-part—A through

C—classification system has been used in Hong Kong and elsewhere to designate the treatment to which an item has been subjected (Fritsch et al., 1992).

A-Jade is jadeite that has not been treated in any way other than cutting and polishing. Surface waxing is generally considered part of the “traditional” finishing process. Used to improve luster and fill surface fractures and pits, wax dipping is the final step in finishing virtually all cut jadeite (figure 24).

As noted above, much jadeite is discolored by rust-like oxidation stains. *B-Jade* is jadeite that has been soaked in chemical bleaches and/or acids for an extended period to remove brown or yellow impurities from between grain boundaries and cracks. Because this treatment process leaves voids in the jadeite, the bleached jadeite is subsequently impregnated with paraffin wax or, most commonly, a clear polymer resin. The result is usually a significant improvement in both transparency and color. However, detection of this enhancement requires infrared spectroscopy, a sophisticated technique that usually must be performed in a gemological laboratory. (See Fritsch et al., 1992, for a full description of both the treatment and its identification.)

Figure 22. Note the small patches of a slightly paler color on the shank of one of these “emerald” green saddle rings (21.27 and 21.65 mm, respectively, in longest dimension). Photo courtesy of and © Christie's Hong Kong and Tino Hammid.



C-Jade, jadeite that has been artificially stained or dyed, also has a long history. Green, lavender, and even orange-brown (Wu, 1997) colors are produced by staining suitable pale-colored material with vegetable or other organic dyes, a process that has been performed on jadeite since at least the 1950s. The methods used in Hong Kong have been described by Ehrmann (1958), Ng and Root (1984), and Ho (1996).

The authors have seen fading in both dyed green and dyed lavender jades, but the green dyes tend to fade more readily. Generally, dyeing is identified with a microscope and a spectroscope: The color tends to concentrate in veins throughout the stone, in surface cracks, and along grain boundaries; also, a broad band from about 630 to 670 nm in the red region of the visible spectrum is considered proof of dye in green jadeite (see, e.g., Hobbs, 1982). Some of the newer dyes may also show a weaker band at 600 nm. Because some stones are only partially dyed, the entire piece must be checked.

Assembled Stones and Other Imitations. There are many assembled stones that resemble jadeite. These include triplets made by taking a highly translucent piece of pale-colored jadeite and cutting it as a thin, hollow cabochon. A second cabochon is cut to fit snugly into the first, with a green cement or jelly-like substance placed between the two. A third, flat piece of jadeite of lower transparency is then cemented onto the base. Another type of assembled stone is that made with a piece of extremely dark green jadeite hollowed out to eggshell thickness. This allows light to pass through, creating the appearance of fine Imperial jade. To strengthen the piece, the hollow back is filled with an epoxy-like substance; and to hide the deception, the piece is then mounted in jewelry with the back hidden (Kammerling and McClure, 1995; Hughes and Slavens, 1999).

At Mandalay's jadeite market, two of the authors (RWH and FW) noticed many pale jadeite cabochons that had been coated on their upper surface with green plastic (Hughes, 1987). Another convincing imitation is produced by first placing a dye layer on the piece and then overlaying it with varnish (Koivula et al., 1994).

Repairs. Bangles in particular that have been broken during wear are sometimes cleverly reassembled with glue. UV fluorescence is a good method of detecting such fraud, since the glues often fluoresce



Figure 23. The well-matched hoops and cabochons in these double hoop earrings set with rose-cut diamonds have been dated to the Qing dynasty (1644–1912). They sold for US\$1.55 million in 1997. Courtesy of Christie's Hong Kong; photo by Tino Hammid.

(commonly blue; DelRe, 1992). Gas bubbles also may be seen in the cement portions (Hughes and Slavens, 1999).

Assembled Rough. The authors have observed several types of assembled rough. One type involves grinding away the skin of a jade boulder, painting or staining the surface green, and then "growing" a new skin via immersion in chemicals, which deposit a new oxidation layer on the outside. Unlike the skin on genuine jadeite boulders, which is extremely tough and can be removed only by grinding, the fake skins are soft and easily taken off. Another type involves sawing or drilling a core out of a jade boulder, inserting a green filling and a reflector, and then covering the hole with a combination of epoxy and grindings from the surface of jade boulders.

In certain cases, even the cut windows of jadeite boulders may be faked. One method involves simply



Figure 24. A process commonly used to enhance polished jadeite, waxing (or “wax dipping”) is actually a simple procedure. First (top left), the bangles are soaked in a warm alkaline solution about 5–10 minutes to clean the residue left behind during polishing. Next they are rinsed, dried, and then soaked in an acidic “plum sauce” to remove any residue from the alkaline solution. Then, they are rinsed, dried, and placed in boiling water for several minutes (top right) to open the “pores” in the jadeite and bring it to the right temperature (to avoid cracking) before it is placed in a pre-melted wax solution for several minutes to several hours (bottom left). After waxing, the items are polished with a clean cloth to reveal their best luster (bottom right). Photos and description by Benjamin So.

applying a superficial stain to the window area. Another is to break off a chip, stain it green and glue it back onto the boulder. When a window is then cut on the boulder, it “reveals” a fine green color.

JADEITE AUCTIONS

At many of the early auctions, buyers would examine the jade and make offers to the seller using hand signals under a handkerchief (see, e.g., Ng and Root, 1984, for an illustration of these “finger signs”). This system, which has been used historically at the mines as well as in China, allows the seller to realize the highest price for each lot without letting others know the actual amount paid. Thus, the buyer can resell the material at whatever price the market will bear (Allan K. C. Lam, pers. comm., 1997). This technique can still be seen every morning in Hong Kong’s Canton Road jade market. However, it is no longer used at the jadeite mines.

Recognizing the importance of the market for jadeite jewelry, Sotheby’s Hong Kong initiated specialized jadeite jewelry auctions in November 1985 with just 25 pieces. Christie’s Hong Kong followed suit in 1994 with a sale of 100 pieces. Since then, thousands of pieces have been auctioned off by Christie’s Hong Kong in what are now biannual auctions of magnificent jadeite jewelry.

To give some idea of the importance of this market, the Mdivani necklace (Lot 898), which contains 27 beads (15.4 to 19.2 mm in diameter),

sold for US\$3.88 million at the October 1994, Christie’s Hong Kong sale. The record price for a single piece of jadeite jewelry was set at the November 1997 Christie’s Hong Kong sale: Lot 1843, the “Doubly Fortunate” necklace of 27 approximately 15 mm jadeite beads, sold for US\$9.3 million (again, see figure 19). These auctions clearly show that jadeite is among the most valuable of all gemstones.

SUMMARY AND CONCLUSION

Jade (primarily nephrite) has been prized in China for thousands of years. Yet the finest jade—jadeite—has been a part of the Chinese culture only since the late 18th century, when the mines in what is today north-central Myanmar were opened. As the first Western gemologists to enter the remote jadeite mining area in more than three decades, the authors witnessed tens of thousands of miners working the rivers, Uru conglomerate, and *in-situ* deposits in search of jadeite. Backhoes, trucks, pneumatic drills, and rudimentary tools are all enlisted in the different mining operations.

Identification of jadeite in a boulder requires both luck and skill (and the presence of windows or “eyes”), although many dealers simply grind off the skin of the boulder or cut it in half. Once the taxes are paid (and the boulders marked accordingly), the rough jadeite is sold primarily to Chinese buyers who carry it to Hong Kong and elsewhere

in China for resale and fashioning. Color, clarity, transparency, and texture are the key considerations in evaluating fine jadeite, which is cut into many different forms—such as cabochons, bangles, saddle rings, disks, and double hoop earrings, as well as carved for use as pendants or *objets d'art*.

The finest Imperial jadeite is a rich “emerald” green color that is highly translucent to semi-transparent, with a good luster. With both rough and fashioned jadeite, purchasers must be cautious about manufactured samples or enhancements. Although “waxing” of jadeite has been an accepted practice for many years, the more recent “B” jade—by which the stone is cleaned with acid and then impregnated with a paraffin wax or polymer—will affect the value of the piece. Jadeite is often dyed, and plastic-coated cabochons were seen even in the Myanmar markets. Also of concern, because of durability, are those jadeite pieces that have been cut very thin and then “backed” or filled with an epoxy-like substance.

The prices received at the Hong Kong auctions held specifically for jade indicate that for many people, especially in the Orient, jadeite holds a higher value than almost any other gem material. From humble beginnings as an encrusted boulder to its exquisite emergence as a fashioned piece, jadeite truly is an inscrutable gem.

Acknowledgments: Richard Hughes thanks Robert Weldon and Jewelers' Circular-Keystone for making his first trip possible. Thanks also to Robert Frey for a careful reading of the manuscript, Elaine Ferrari-Santhon of the Richard T. Liddicoat Library and Information Center for helpful research on jade, and Dr. Edward Gübelin, whose earlier accounts of the mines provided inspiration. Olivier Galibert thanks the following: C. K. Chan of Chow Tai Fook, Edmond Chin of Christie's Hong Kong, Garry Dutoit of the AGTA Gemological Testing Center, Lisa Hubbard of Sotheby's Hong Kong, Benjamin So and Judith Grieder Jacobs of the Hong Kong Jade and Jewellery Association, Samuel Kung, Dominic Mok, and Eric Nussbaum of Cartier Geneva. George Bosshart thanks his wife, Anne, an outstanding trekking companion. Fred Ward and Richard Hughes thank Georg Muller, television producer and friend with enough foresight, insight, and connections to get his colleagues and himself into the Myanmar jade localities. George Harlow and Richard Hughes also thank William Larson of Pala International for his help and advice. Photographer Tino Hammid was very helpful in providing photos of the Christie's Hong Kong auction items, and Harold and Erica Van Pelt supplied figures 1 and B-3, as well as the cover.

This article is dedicated to our colleague and co-author, Dr. Thet Oo, who suffered a series of strokes after his second trip to the mines. A finer traveling companion does not exist. We wish him a speedy recovery.

REFERENCES

- The art of feeling jade (1962) *The Gemmologist*, Vol. 31, No. 372, pp. 131–133 (reprinted from *Gems and Minerals*, No. 286, July 1961, pp. 28–29).
- Bender F. (1983) *Geology of Burma*. Gebrüder Borntraeger, Berlin, 260 pp.
- Bleek A.W.G. (1907) Die Jadeitlagerstätten in Upper Burma. *Zeitschrift für praktische Geologie*, Vol. 15, pp. 341–365.
- Bleek A.W.G. (1908) Jadeite in the Kachin Hills, Upper Burma. *Records, Geological Survey of India*, Vol. 36, No. 4, pp. 254–285.
- Chhibber H.L. (1934a) *The Geology of Burma*. Macmillan, London, 538 pp.
- Chhibber H.L. (1934b) *The Mineral Resources of Burma*. Macmillan, London, 320 pp.
- Christie's (1995a) *Magnificent Jadeite Jewellery*. Catalog for Christie's Hong Kong, May 1, 1995 auction.
- Christie's (1995b) *Magnificent Jadeite Jewellery*. Catalog for Christie's Hong Kong, October 30, 1995 auction.
- Christie's (1996) *Magnificent Jadeite Jewellery*. Catalog for Christie's Hong Kong, November 5, 1996 auction.
- Christie's (1997) *Magnificent Jadeite Jewellery*. Catalog for Christie's Hong Kong, April 29, 1997 auction.
- Cummings J., Wheeler T. (1996) *Lonely Planet Travel Survival Kit: Myanmar (Burma)*, 6th. ed. Lonely Planet, Hawthorn, Australia, 393 pp.
- Damour A. (1863) Notice et analyse sur le jade vert: réunion de cette matière minérale à la famille des wernerites. *Comptes Rendus des Séances de l'Académie des Sciences*, Vol. 56, pp. 861–865.
- Deer W.A., Howie R.A., Zussman J. (1963) *Rock-forming Minerals*. Vol. 2, *Chain Silicates*. John Wiley and Sons, New York.
- DelRe N. (1992) Gem Trade Lab notes: Repaired jadeite. *Gems & Gemology*, Vol. 28, No. 3, pp. 193–194.
- Ehrmann M.L. (1958) A new look in jade. *Gems & Gemology*, Vol. 9, No. 5, pp. 134–135, 158.
- Eldridge F. (1946) *Wrath in Burma*, 1st ed. Doubleday & Co., Garden City, NY, 320 pp.
- Fritsch E., Wu S.-T.T., Moses T., McClure S.F., Moon M. (1992) Identification of bleached and polymer-impregnated jadeite. *Gems & Gemology*, Vol. 28, No. 3, pp. 176–187.
- Goette J. (n.d.) *Jade Lore*. Reynal & Hitchcock, New York, 321 pp.
- Griffith W. (1847) *Journals of Travels in Assam, Burma, Bootan, Affghanistan, and the Neighbouring Countries*. Bishop's College Press, Calcutta, reprinted in 1971 by Ch'eng Wen Publishing Co., Taipei, 529 pp.

- Gübelin E.J. (1964–65) Maw-sit-sit: A new decorative gemstone from Burma. *Gems & Gemology*, Vol. 11, No. 8, pp. 227–238, 255.
- Gübelin E.J. (1965a) Jadealbit: Ein neuer Schmuckstein aus Burma. *Zeitschrift der Deutschen Gesellschaft für Edelsteinkunde*, No. 51, pp. 4–22.
- Gübelin E.J. (1965b) Maw-sit-sit—A new decorative gemstone from Burma. *Journal of Gemmology*, Vol. 9, No. 10, pp. 329–344.
- Gübelin E.J. (1965c) Maw-sit-sit proves to be jade-albite. *Journal of Gemmology*, Vol. 9, No. 11, pp. 372–379.
- Gump R. (1962) *Jade: Stone of Heaven*. Doubleday & Co., Garden City, NY, 260 pp.
- Hänni H.A., Meyer J. (1997) Maw-sit-sit (kosmochlore jade): A metamorphic rock with a complex composition from Myanmar (Burma). *Proceedings of the 26th International Gemmological Conference*, Idar-Oberstein, Germany, pp. 22–24.
- Hansford S.H. (1950) *Chinese Jade Carving*, 1st ed. Lund Humphries & Co., London, 145 pp.
- Harlow G.E., Olds E.P. (1987) Observations on terrestrial ureyite and ureyitic pyroxene. *American Mineralogist*, Vol. 72, pp. 126–136.
- Harlow G.E., Sorensen S.S. (in press) Jade: Occurrence and metasomatic origin. *Extended Abstracts of the 25th International Geological Congress*, August 2000, Rio de Janeiro, Brazil.
- Healy D., Yu R.M. (1983) Quality grading of jadeite. *Lapidary Journal*, Vol. 36, No. 10, pp. 1670–1674.
- Hertz W.A. (1912) *Burma Gazetteer: Myitkyina District*. Superintendent, Government Printing and Stationery, Rangoon, Volume A, reprinted 1960, 193 pp.
- Hind Co. Map (1945) Mogaung Sheet, Hind 1095 Sheet 92C, First Edition Unlayered.
- Ho L.Y. (1996) *Jadeite*, English ed. Transl. by G.B. Choo, Asiapac, Singapore, 127 pp.
- Hobbs J.M. (1982) The jade enigma. *Gems & Gemology*, Vol. 18, No. 1, pp. 3–19.
- Htein W., Naing A.M. (1994) Mineral and chemical compositions of jadeite jade of Myanmar. *Journal of Gemmology*, Vol. 24, No. 4, pp. 269–276.
- Htein W., Naing A.M. (1995) Studies on kosmochlor, jadeite and associated minerals in jade of Myanmar. *Journal of Gemmology*, Vol. 24, No. 5, pp. 315–320.
- Hughes R.W. (1987) The plastic coating of gemstones. *Australian Gemmologist*, Vol. 16, No. 7, pp. 259–261.
- Hughes R.W. (1999) Burma's jade mines: An annotated accidental history. *Journal of the Geo-Literary Society*, Vol. 14, No. 1, pp. 15–35.
- Hughes R.W., Slavens C. (1999) Tales from the Crypt—GQI lab news: Jadeite—Repaired, assembled, treated. *GQ Eye*, Vol. 2, No. 1, pp. 10–11.
- Jackson J.A., Ed. (1997) *Glossary of Geology*, 4th ed. American Geological Institute, Alexandria, VA, 769 pp.
- Johnson M.L., Koivula J.I., Eds. (1998) Gem news: Jadeite boulder fakes. *Gems & Gemology*, Vol. 34, No. 2, pp. 141–142.
- Kammerling R.C., Koivula J.I., Johnson M.L., Eds. (1995) Gem news: Jade market in Mandalay. *Gems & Gemology*, Vol. 31, No. 4, pp. 278–279.
- Kammerling R.C., McClure S.F. (1995) Gem Trade Lab notes: Jadeite jade assemblages. *Gems & Gemology*, Vol. 31, No. 3, pp. 199–201.
- Keller P.C. (1990) *Gemstones and Their Origins*. Van Nostrand Reinhold, New York, 144 pp.
- Koivula J.I., Kammerling R.C., Fritsch E., Eds. (1994) Gem news: Coated jadeite. *Gems & Gemology*, Vol. 30, No. 3, p. 199.
- Lee R. (1956) Jade cutting in Orient. *The Mineralogist*, Vol. 24, No. 3, March, pp. 138–140.
- Lintner B. (1994) *Burma in Revolt*. Westview Press, Boulder, CO, 514 pp.
- Lintner B. (1996) *Land of Jade: A Journey from India through Northern Burma to China*, 2nd rev. ed. White Orchid Press, Bangkok, 380 pp.
- Mével C., Kiéna J.R. (1986) Jadeite-kosmochlor solid solution and chromian sodic amphiboles in jadeitites and associated rocks from Tawmaw (Burma). *Bulletin de Minéralogie*, Vol. 109, pp. 617–633.
- Mining Journal Annual Review* (1970) Diamonds, gemstones and abrasives: Other gemstones. *Mining Journal, London*, June, p. 124.
- Morimoto N., Fabries J., et al. (1988) Nomenclature of pyroxenes. *American Mineralogist*, Vol. 73, pp. 1123–1133.
- Myanma jade (1991) Myanma Gems Enterprise, WPD, Yangon, unpublished report.
- Ng J.Y., Root E. (1984) *Jade for You: Value Guide to Fine Jewelry Jade*. Jade N Gem Corp. of America, Los Angeles, CA, 107 pp.
- Noetling F. (1893) Note on the occurrence of jadeite in Upper Burma. *Records, Geological Survey of India*, Vol. 26, pp. 26–31.
- Ou Yang C.M. (1993) Microscopic studies of Burmese jadeite jade-1. *Journal of Gemmology*, Vol. 23, No. 5, pp. 278–284.
- Ou Yang C.M. (1995) *Jadeite Appreciation*. Cosmos Books Ltd., Hong Kong, 191 pp. [in Chinese].
- Ou Yang C.M. (1999) How to make an appraisal of jadeite. *Australian Gemmologist*, Vol. 20, No. 5, pp. 188–192.
- Ponahlo J. (1999) Cathodoluminescence du jade. *Revue de Gemmologie A.F.G.*, No. 137, pp. 10–16.
- Rossmann G.R. (1974) Lavender jade: The optical spectrum of Fe³⁺ and Fe²⁺-Fe³⁺ inter-valence charge transfer in jadeite from Burma. *American Mineralogist*, Vol. 59, pp. 868–870.
- Soe Win (1968) The application of geology to the mining of jade. *Union of Burma Journal of Science and Technology*, Vol. 1, pp. 445–456.
- Sorensen S.S., Harlow G.E. (1998) A cathodoluminescence (CL)-guided ion and electron microprobe tour of jadeite chemistry and petrogenesis. *Abstracts with Programs, 1998 Annual Meeting, Geological Society of America*, Vol. 30, p. A-60.
- Sorensen S.S., Harlow G.E. (1999) The geochemical evolution of jadeite-depositing fluids. *Abstracts with Programs, Annual Meeting of the Geological Society of America*, Vol. 31, p. A-101.
- Thin N. (1985) *Petrologic-Tectonic Environment of Jade Deposits, Phakant-Tawmaw Jade Tract, Burma*. Department of Geology, University of Rangoon.
- Tröger W.E. (1967) *Optische Bestimmung der gesteinsbildenden Minerale*. E. Schweizerbart'sche Verlagsbuchhandlung, Stuttgart, Teil 2.
- United Nations (1979) *Geological Mapping and Geochemical Exploration in Mansi-Manhton, Indaw-Tigyain, Kyindwe-Longyi, Patchaung-Yane and Yezin Areas, Burma*. Mineral Exploration Burma, Technical Report 7, United Nations Development Programme, 13 pp., 6 maps in body.
- Wang C. (1994) Essence and nomenclature of jade—A problem revisited. *Bulletin of the Friends of Jade*, Vol. 8, pp. 55–66.
- Wu S.T. (1997) The identification of B + C jade. *Journal of the Gemmological Association of Hong Kong*, Vol. 20, pp. 27–29.

LAPIS LAZULI FROM THE COQUIMBO REGION, CHILE

By Robert R. Coenraads and Claudio Canut de Bon

Lapis lazuli has been mined from the Coquimbo Region of Chile since 1905. Some of this material approaches the quality of fine lapis lazuli from Afghanistan. The Chilean material is composed of blue lazurite, together with wollastonite, calcite, haüyne, diopside, pyrite, and minor quantities of other minerals. The deposit is located in the Andes Mountains at an elevation of 3,500 m; it is hosted by a contact-metamorphosed limestone that was later metasomatized to introduce sulfur, a necessary component for the formation of lazurite. Two companies are currently mining the deposit, Las Flores de Los Andes S.A. and Compañía Minera LapisChile S.A., and today they produce about 150 tonnes of material annually. Much of the lapis lazuli is processed locally, for use in fine jewelry, ornamental objects, and building materials such as table-tops or tiles.

ABOUT THE AUTHORS

Dr. Coenraads (coenraad@firstnet.com.au) is a consulting geologist, geophysicist, and gemologist, based in Sydney, Australia; a research associate with the Australian Museum in Sydney; and a lecturer for the Gemmological Association of Australia. Dr. Canut de Bon is a lecturer at the University of La Serena, La Serena, Quinta Region, Chile.

Please see acknowledgments at the end of the article.

*Gems & Gemology, Vol. 36, No. 1, pp. 28–41
© 2000 Gemological Institute of America*

Lapis lazuli is a rock composed of lazurite—the source of the blue color—with variable amounts of other minerals depending on its origin and, typically, small particles of pyrite. Prized for its attractive blue color, lapis lazuli was used in jewelry by some of the world's most ancient civilizations. The stone is mined at relatively few locations, some of which have been worked since the fifth millennium BC (von Rosen, 1990).

Considering the extensive history and romance attached to this ornamental gem material, the Chilean deposit is a relative newcomer. The first reference to Chilean lapis lazuli dates back to the 19th century (Field, 1850a and b). Another early mention was made by Ignacio Domeyko (1860), a Polish immigrant and mining engineer who became the first director of the School of Mines at La Serena (about 140 km from the workings). The first detailed geologic studies of the deposit and mine workings were carried out by German geologist J. Bruggen (1921, 1926), who identified the host rock as contact-metamorphosed limestone. Lapis lazuli was officially recognized as the national gemstone of Chile in 1984.

The Coquimbo Region is the only known source of lapis lazuli in Chile. Although reference is sometimes made to another Chilean deposit at Vicuña Mackenna Mountain near Antofagasta (Webster, 1994; Sofianides and Harlow, 1990), this material has been identified as dumortierite by Canut de Bon (1991). Once considered a minor or unimportant locality, with the lapis lazuli described as “at best mediocre” (Wyart et al., 1981), the Chilean deposit has produced significant quantities of attractive material in recent years. Today, Chilean lapis lazuli is exported in the rough, or incorporated into jewelry (see, e.g., figure 1), carvings, and decorative building materials by local artisans. This article will review the historical significance of lapis lazuli, and examine the geologic setting and gemological characteristics of material from Chile.

Figure 1. Chilean lapis lazuli is currently used in a variety of ways, but the finer-quality material is incorporated into jewelry. This sterling silver brooch (3.8 × 2.5 cm) was manufactured by Chilean artisans. Photo by Maha Tannous.



HISTORICAL BACKGROUND

Lapis lazuli was one of the first gem materials used for adornment and as an ornamental stone in the Middle East, Asia, and Europe. Most of the material used by these ancient civilizations is believed to have originated from the Sar-e-Sang deposit in present-day Badakhshan, Afghanistan (Wyart et al., 1981).

Mesopotamia. The earliest archeological evidence for lapis lazuli's use was traced back to the 5th millennium BC by von Rosen (1990), who recorded the discovery of beads at a cemetery outside the temple walls of Eridu (Sumer) in southern Babylonia (later known as Mesopotamia; now Iraq).

The earliest known written reference to lapis lazuli is found in the Sumerian *Poem of Gilgamesh*, which was recovered on 12 engraved clay tablets from the ruins of the palace library of the Assyrian King Ashurbanipal in Nineveh (near present-day Al Mawsil in northern Iraq; Heidel, 1946). The hero, Gilgamesh, was a king in southern Mesopotamia who actually lived sometime between 2700 and 2500 BC (Tiglay, 1982). In the epic, the goddess of love offers to be the wife of Gilgamesh, and promises "a chariot of lapis lazuli and gold." Artistic works containing lapis lazuli from this period were recovered in the 1920s, during excavations of the ancient Chaldean city of Ur (near present-day An Nasiriyah in southern Iraq). The most famous of these were recovered from the royal tomb of Queen Pu-abi (2500 BC), including three gold headdresses and two bead necklaces (Sofianides and Harlow, 1990; Sutherland, 1991), as well as two statues of male goats with fleece, shoulders, eyes, and horns of lapis lazuli (see, e.g., figure 2).

Egypt. Lapis lazuli was used for scarabs, pendants, beads, and inlaid jewelry in Egypt prior to 3100 BC (Sofianides and Harlow, 1990). The tombs of Ramses II (circa 1279 BC) and Tutankhamun (1361–1352 BC) revealed rings and other jewelry made of lapis lazuli. In fact, the golden mask over the head and shoulders of Tutankhamun's mummy has eyebrows and areas around the eyes that are inlaid with lapis lazuli (Silverman, 1978).

China. The use of lapis lazuli was mentioned in Chinese annals of the sixth and eighth centuries BC, as the stone was a favorite with Chinese carvers (Bowersox and Chamberlin, 1995). Some Chinese hair and belt ornaments carved from lapis lazuli have been dated to 551–479 BC (Sofianides and Harlow, 1990).

Europe. Curiously, most modern Bibles use the term *sapphire* to denote lapis lazuli (Douglas, 1980). This is because *sappir* and *sappheiras* were used in the early Old Testament Massoretic and Septuagint texts, respectively (Douglas, 1980). It is generally recognized that true sapphire was scarcely known to the ancients, and that the "sapphire" of antiquity was in fact lapis lazuli that contained golden specks of pyrite (Burnham, 1886). The term *lapis lazuli* came into use in the Middle Ages and derives from the ancient Persian *lazhuward* (blue) and Arabic *lazaward* (heaven, sky, or blue; Sofianides and Harlow, 1990). Historically, lapis lazuli was crushed for use as a blue pigment, "ultramarine," until 1826 when an inexpensive substitute was developed by J. B. Guimet (Wyart et al., 1981).



Figure 2. Several artistic works were recovered in the 1920s during excavations of the Chaldean city of Ur (in southern Iraq). This statue of a goat (42.6 cm tall), called “Ram Caught in a Thicket,” dates back to the mid-3rd millennium BC and is made of gold, silver, ornamental stone, and lapis lazuli and shell that are set in bitumen. Photo courtesy of the University of Pennsylvania Museum (#T4-1000).

During the Renaissance, lapis lazuli was used for cups, bowls, and urns, and was inlaid into clock faces and tables. The popular flower, bird, and butterfly mosaics of Florence used lapis lazuli, along with carnelian, malachite, and agate, skillfully set into a background of black Belgian marble (Hinks, 1975). In Renaissance Russia, lapis lazuli was used as a decorative stone, as at the Winter Palace in St. Petersburg and the Palace of Catherine the Great in Tsarskoe-Selo (now the city of Pushkin; Bauer, 1904).

More recently, at the turn of the 20th century, French jeweler and artist Peter Carl Fabergé (1846–1920) used lapis lazuli in many of his major works. Among these was one of his 58 Imperial Easter Eggs—a gift from Czar Nicholas II of Russia to Czarina Alexandra in 1912 (figure 3).

LAPIS LAZULI IN THE AMERICAS

Three lapis lazuli deposits are known in North America (Sinkankas, 1997): Italian Mountain in Colorado (Christopher, 1977; Hogarth and Griffin 1980; Schultz, 1981), the San Gabriel Mountains in California (Rogers, 1938), and Baffin Island in Canada (Hogarth and Griffin, 1978). These have been mined sporadically during this century, primarily for local ornamental use, although some blocks of “azure-blue material” from Italian Mountain have been sent to Idar-Oberstein, Germany, for carving (Sinkankas, 1997).

In South America, there have been several recent references to the use of lapis lazuli by the Moche (800–100 BC) and Inca (1100–1537 AD) cultures, which occupied present-day Peru, Ecuador, Bolivia, northern Chile, and northwestern Argentina (e.g., Sofianides and Harlow, 1990). However, the accuracy of these identifications has been questioned by one of the authors (Canut de Bon, 1991), who has not confirmed any archeological evidence of the

Figure 3. Intricate gold work is combined with lapis lazuli in this “Imperial Czarevitch Easter Egg” (12.5 × 8.9 cm), made in 1912 by Peter Carl Fabergé. Courtesy of the Virginia Museum of Fine Arts, Richmond. Bequest of Lillian Thomas Pratt. Photo: Katherine Wetzel. © Virginia Museum of Fine Arts.





Figure 4. The lapis lazuli mining area is located at the headwaters of the Tascadero River, near the border between Chile and Argentina, in the Coquimbo Region of Chile. Modified after Cuitiño (1986).

early use of lapis lazuli from Chile. In fact, pre-Columbian artifacts from both national and foreign museums that were studied at the University of La Serena have been found to contain sodalite or other blue minerals, but not lapis lazuli (Canut de Bon, 1991). The Moche use of sodalite is consistent with the observation that the peoples of the Bolivian and Peruvian altiplano commonly used this mineral for beads and carvings (Brendler, 1934). However, evidence of human activity near the lapis lazuli mining area—including flint arrowheads in an old campsite just 300 m from the mine, and pre-Columbian ceramic fragments near Punta Negra, about 5 km away—does suggest that the deposit could have

been known to early inhabitants of the region (S. Rivano, pers. comm., 2000; see also Rivano, 1975a and b; Rivano and Sepúlveda, 1991). Further research is needed to determine conclusively if the Coquimbo lapis lazuli deposit was indeed worked by ancient cultures before its modern discovery in the mid-19th century.

THE CHILEAN DEPOSIT

Location and Access. The mining area lies in the Andes Mountains at an altitude of 3,500 m (11,480 feet). Geographically, it is located southeast of Montepatria, in Chile's Coquimbo Region (figure 4), at the headwaters of Lapislazuli Creek, a tributary

of the Tascadero River. The deposit is situated on the steep slopes of an east-facing glacial cirque (figure 5), approximately 500 m from the Andean watershed that defines the international border between Chile and Argentina.

Access to the mining area from the regional center of La Serena is via paved road to Ovalle, and then by dirt road through Montepatria, Carén, Tulahuén, Las Ramadas, and El Polvo (again, see figure 4). A four-wheel-drive dirt track from Montepatria follows Tascadero River and Lapislázuli Creek to the mining area. The deposit is accessible only during the Chilean summer, from January to April. From May to September, the roads and workings are covered with up to 4 m (13 feet) of snow; and from October to December, the road is flooded by melt water. Typically much of January is spent repairing the road and removing ice from the mining pits (R. Vega E., pers. comm., 1993).

The deposit is mined in a linear array of small pits over a distance of about 600 m (2,000 feet). These pits are covered by three mining concessions—Flor de Los Andes, San Marcelo, and Seguridad. Flor de Los Andes is the oldest concession, established in 1952, and is controlled by the company Las Flores de Los Andes S.A.; this concession was visited by the senior author in 1993. In 1995, a group of Chilean companies consolidated to form Compañía Minera LapisChile S.A., which now

controls the San Marcelo and Seguridad concessions (J. Muxi, pers. comm., 1999). The formation of LapisChile S.A. and its entry into the marketplace was chronicled by Ward (1996).

Geology and Occurrence. Chilean lapis lazuli formed through the metasomatic introduction of sulfur into impure limestone that was previously metamorphosed by granitic intrusives (Rivano, 1975a and b; Cuitiño, 1986). Its origin is probably similar to that of Italian Mountain, Colorado (Hogarth and Griffin, 1980). In contrast, the lapis lazuli deposits at Sar-e-Sang, Baffin Island, and Lake Baikal (Russia) probably formed during regional metamorphism of shale and dolomitic evaporite deposits (Hogarth and Griffin, 1978; see also Ivanov, 1976; Kulke, 1976).

The Chilean lapis lazuli is hosted by the outermost of three contact-metamorphic zones associated with the intrusion of the Río Las Cuevas granite into Mesozoic limestones of the Río Tascadero formation, 24 million years ago (Rivano, 1975a and b; Cuitiño, 1986). These metamorphic zones are visible in the steep slopes of the glacial cirque (again, see figure 5). The innermost zone adjacent to the granite intrusion, about 40–50 m wide, is a hornfels (a fine-grained metamorphic rock) that contains clinopyroxene, plagioclase, quartz, and magnetite. The second zone, a skarn about 80–100 m wide, is

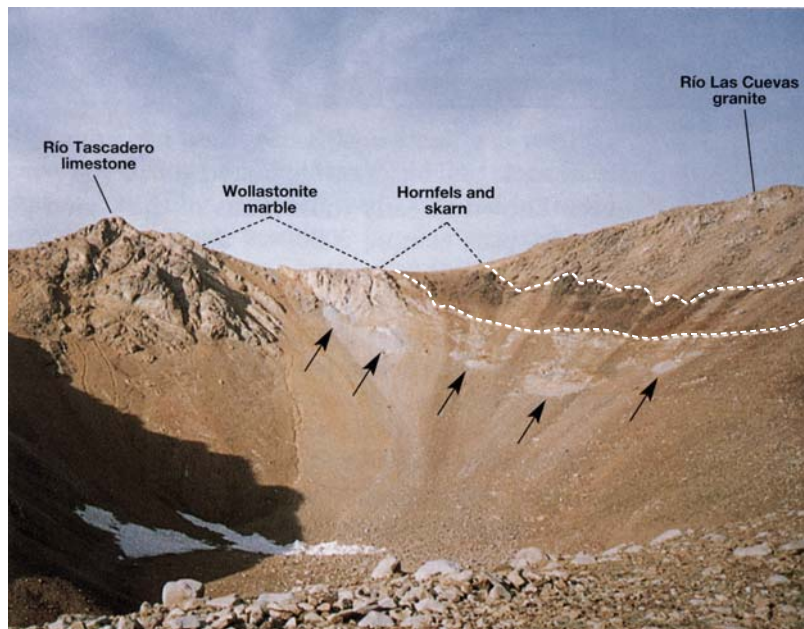


Figure 5. The geology is well exposed in the steep north and east faces of the glacial cirque that hosts the lapis lazuli deposits. Two of the three contact-metamorphic zones adjacent to the granite are distinguishable. The innermost hornfels zone and the second skarn zone form a dark band, with an irregular contact against the gray-colored granite. The outer zone is a “cream”-colored wollastonite marble displaying a sharp, straight contact with the second zone. The marble hosts local lenses of lapis lazuli exposed by a linear array of mining cuts with blue-tinged dumps (arrows), barely visible near the top of the scree slopes. The contact between the outermost marble zone and the limestone is obscured by scree.

BOX A: MINERALOGY OF LAPIS LAZULI

Lazurite is a member of the sodalite group, which has the general formula: $\text{Na}_6(\text{Na,Ca})_2(\text{Al}_6\text{Si}_6\text{O}_{24})\text{X}_{1-2} \cdot n\text{H}_2\text{O}$, where X = Cl, OH, SO_4 , and/or S, and n = 0 or 1 (Gaines et al., 1997). Lazurite is anhydrous and contains both Na and Ca, with S and SO_4 occurring in the X site. The other members of the sodalite group are sodalite, nosean, and haüyne. All of these minerals crystallize in the cubic system, and can show blue color; lazurite has commonly been confused with sodalite (see, e.g., table A-1). However, the "bright azure" or "ultramarine blue" of fine lazurite is somewhat distinctive, and is the most highly prized color attained by minerals of the sodalite group.

Using microscopic observation of thin sections, as well as X-ray diffraction and microprobe analyses, Cuitiño (1986) identified the following constituents in Chilean lapis lazuli: lazurite (39%–66%), wollastonite (20%–43%), calcite (1%–21%), haüyne (2%–6%), diopside (2%–5%), pyrite (1%–4%), and scapolite (0.3%–4%), with traces (<1%) of siderite, epidote, plagioclase, tremolite, sodalite, afghanite, allanite, arsenopyrite, pyrrhotite, and chalcopyrite. It is interesting to compare these with the list of minerals identified in lapis lazuli from Afghanistan by Wyart et al. (1981): lazurite, calcite, and dolomite, associated with forsterite, plagioclase, diopside, scapolite, phlogopite, and pyrite. Electron microprobe analyses of the lazurite in Chilean lapis lazuli revealed that the greater the sulfur content was, the darker the blue color appeared; chlorine was noted in the greenish blue varieties (Cuitiño, 1986).

TABLE A-1. Properties of lazurite and sodalite^a.

Property	Lazurite	Sodalite
Crystal system	Cubic	Cubic
Formula	$\text{Na}_6\text{Ca}_2(\text{Al}_6\text{Si}_6\text{O}_{24})\text{S}_2$	$\text{Na}_8(\text{Al}_6\text{Si}_6\text{O}_{24})\text{Cl}_2$
Habit	Dodecahedra or cubo-octahedra up to 5 cm; more commonly compact, massive; often with pyrite and calcite	Dodecahedra, cubo-dodecahedra, octahedra; usually massive
Twinning	Common on {111}, but generally not apparent	Common on {111}, forming pseudo-hexagonal prisms
Color	Blue, white, gray, yellow, greenish blue, colorless	Colorless, gray, white, greenish or yellowish white, light to medium blue, violet blue, pink
Luster	Dull to vitreous	Vitreous to greasy
Streak	Bright blue	White or very pale blue
Diaphaneity	Translucent to opaque	Transparent to translucent
Cleavage	{110} distinct	{110} poor to distinct
Fracture	Uneven, brittle	Uneven to conchoidal, brittle
Hardness	5–5.5	5.5–6
Specific gravity	2.38–2.45	2.14–2.30
Refractive index	1.500–1.522	1.483–1.487
Fluorescence		
Short-wave UV	None	Intense orange to orange-red
Long-wave UV	None	Intense orange to orange-red
Phosphorescence	None	Often short-lived yellowish white
Distinguishing features	Bright blue streak; H_2S (rotten egg smell) liberated upon application of HCl	Absence of pyrite (except rare cases), almost white streak

^aReferences: Deer et al., 1963; Schumann, 1997; Anthony et al., 1995; Webster, 1994; Gaines et al., 1997.

characterized by the presence of andradite-grossular garnet. In the outermost zone, about 300 m wide, the limestone has been altered to wollastonite marble. Small, irregular lenses of lapis lazuli occur locally in the wollastonite marble, in a chemical environment undersaturated in silica. These lenses range up to 2 m (6.5 feet) long and 10 cm (4 inches) wide, with local concentrations up to 40 cm in diameter.

Both Rivano (1975a and b) and Cuitiño (1986) believe that the Río Las Cuevas granitic intrusion by itself was not sufficient to form the lapis lazuli, but that a vital second stage was required. The formation of lazurite, rather than another member of the sodalite group (see Box A), required the introduction of sulfur. This probably occurred as a result

of hydrothermal alteration associated with the Portezuelo del Azufre intrusion, which is exposed 3 km south of the lapis lazuli workings, and was emplaced about 10–11 million years ago (Rivano and Sepúlveda, 1991). This superposition of two unrelated geologic events explains the uniqueness of this lapis lazuli deposit in the Andean Cordillera of South America.

Mining. The irregular lenses of lapis lazuli are mined in small cuts or quarries (see, e.g., figure 6). Prior to 1996, explosives were used at all three concessions; however, the artisans reported that the lapis lazuli tended to fail along fractures and blamed the use of explosives in the extraction process (W. Vega A., pers. comm., 1993). Las Flores de Los Andes now

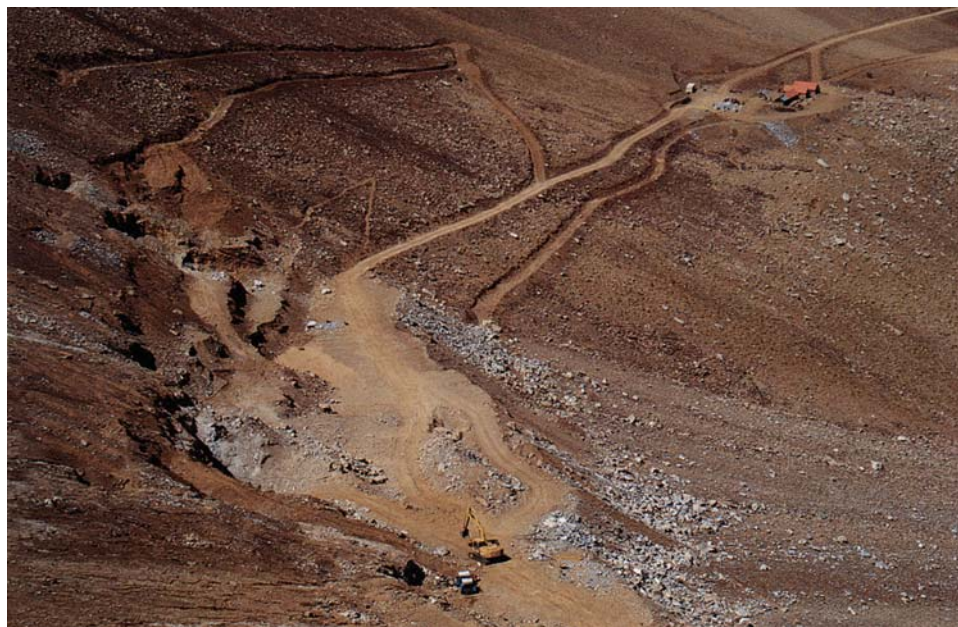


Figure 6. This view of the Flor de los Andes concession shows a series of small cuts that have been explored and mined for lapis lazuli. Photo © 2000 Fred Ward.

uses only a limited amount of explosives to break away large blocks of lapis lazuli along lines of closely spaced drill holes (J. Correa, pers. comm., 2000). Some of the blocks recovered are more than 2 m across. In 1996, granite, marble, and jade quarrying techniques were introduced by LapisChile using expertise from the Canadian nephrite mines (Ward, 1996). LapisChile does not use explosives, but rather diamond-impregnated cable saws in conjunction with drill holes and wedges (J. Muxi, pers. comm., 1999). Las Flores de Los Andes currently employs 20 workers, and LapisChile about 10 workers, in the mining and processing of the material (J. Correa, pers. comm., 2000; B. Lepe, pers. comm., 1999). The ore is hand sorted on site before being transported by truck to Santiago, where it undergoes further processing (figure 7).

Production. Between 1905 and 1910, about 10 tonnes of lapis lazuli from the Coquimbo Region were sent to Germany (Canut de Bon, 1991). Later, small, hand-selected pieces of high-quality lapis lazuli were mined (Zeballos, 1973), and used to supply the local market. Transport at that time was only possible by mule; the journey from the mine to La Serena took two days, and each mule carried 100 kg. Until 1989, when the company constructed an access road navigable by truck, only about 20–30 tonnes of lapis lazuli were being removed annually from Flor de Los Andes (S. Rivano, pers. comm., 2000). Current production is about 150 tonnes a year of mixed-grade material. Of this amount, Las

Flores de Los Andes currently mines about 100 tonnes (J. Correa, pers. comm., 2000), and Lapis-Chile produces about 50 tonnes.

Because the full extent at depth of the lapis lazuli lenses has not been determined—and about 50% of the surface of the ore zone is covered by scree (landslide debris)—it is difficult to determine how much remains. Canut de Bon (1991) discovered traces of lapis lazuli 5.5 km north of the present workings and 2 km to the south in the same geologic formation. Drilling in 1993 at the Flor de Los Andes concession outlined more than 10,000 tonnes of proven reserves and 60,000 tonnes of probable reserves; more recent work indicates even greater reserves at the LapisChile concessions (S. Rivano, pers. comm., 2000).

PROCESSING AND EVALUATION

Quality Considerations. The term *lapis lazuli* has been applied to a broad range of material, from pure lazurite to pieces of gray marble that contain less than 30% lazurite. For the purpose of comparing parameters in a simple grading system, we define *lapis lazuli* as an ornamental stone that contains varying quantities of lazurite (blue), wollastonite (white), calcite (white to gray), specks of pyrite (“golden” yellow), and minor quantities of other minerals. The key factors in evaluating the quality of lapis lazuli are the percentage and color of the lazurite, as well as the combination and distribution of the colors of the associated minerals.

Since the blue color of lapis lazuli is due to

lazarite, the maximum amount of this mineral is desirable. In the rare case that a specimen is composed of an aggregate of *pure* lazurite, it is still called lapis lazuli (rather than lazurite), in the same way that a metamorphic rock consisting of an aggregate of *pure* calcite is still termed a marble.

The most desirable color of lazurite is a bright, saturated blue “of extraordinary depth and intensity” (Webster, 1994, p. 263), to which the terms *ultramarine blue* and *azure blue* have been applied (Arem, 1987; Anthony et al., 1995). The lighter blues, dull dark blues, and green-blues are less desirable.

The mixtures of colors from the main minerals present also influence the quality of lapis lazuli. White and dark blue make a pleasing combination, as does the presence of tiny specks of golden pyrite, whereas a gray and blue combination is far less desirable. The colors should be distributed evenly, and large areas of color other than blue are not desirable. Patchy color variation, veining, and mineral aggregations may be used to good effect by skilled artisans, although such material is generally considered difficult to work. Evenly distributed, fine-grained pyrite is desirable, whereas sizable aggregates of pyrite devalue the material.

Grading. Using the factors described above, one of the authors developed a four-category scheme for quality grading Chilean lapis lazuli (Canut de Bon, 1991) that is currently used by Las Flores de Los Andes. *First-quality* material (figure 8) consists predominantly of dark blue to “ultramarine” blue lazurite, with no gray calcite; small white spots and finely dispersed pyrite may be present. *Second-quality* lapis lazuli (figure 9, left) is composed predominantly of dark blue to medium blue lazurite, along with significant amounts of white spots and fine specks of pyrite, and minor gray calcite. *Third-quality* material (figure 9, center) is composed of deep blue to pale blue lazurite, together with appreciable amounts of gray and white minerals and local aggregates of pyrite (or other trace minerals). *Fourth-quality* lapis lazuli (figure 9, right) contains subordinate amounts of lazurite in various tones of blue, with most of the remainder being gray calcite.

LapisChile uses different categories for their products; these categories are based predominantly on the percentage of lazurite present in the piece. They have found that most carvers and jewelry manufacturers will not use pieces of lapis lazuli with less than 70% lazurite, although 50%–70% lazurite is acceptable for carving in

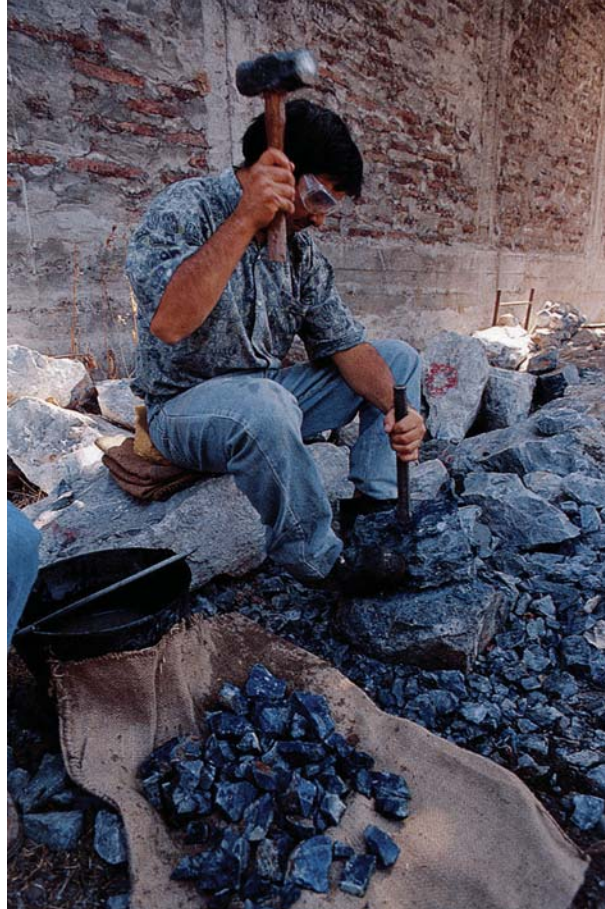


Figure 7. Workers at the LapisChile factory in Santiago break apart blocks containing lapis lazuli to extract the higher-quality material. The pieces are dipped in water to help reveal their colors and textures. Photo © 2000 Fred Ward.

Figure 8. Portions of these brightly colored pieces of lapis lazuli from the San Marcelo claim would be considered “first-quality” according to the grading system used by Las Flores de Los Andes. Note the intense blue color and general lack of impurities in these areas. Photo © 2000 Fred Ward.

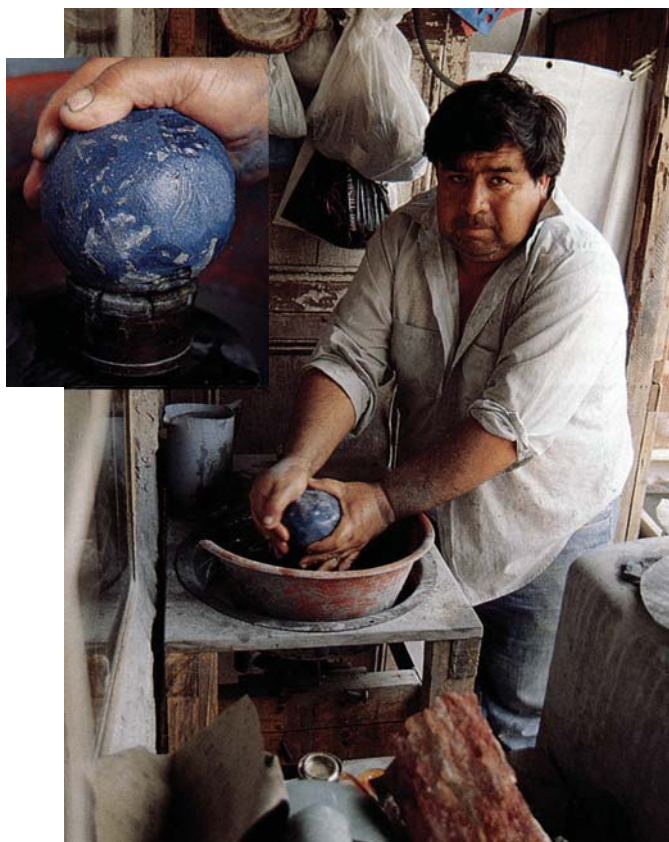




Figure 9. These slabs constitute some of the samples obtained for this study, and illustrate three of the quality grades of lapis lazuli used by Las Flores de Los Andes (see text for discussion); left—second quality (19 × 11 cm), center—third quality (18 × 9 cm), and right—fourth quality (21 × 13 cm).

some markets. Material with less than 50% lazurite is used only for construction materials, such as slabs, countertops, or tiles (J. Muxi, pers. comm., 1999).

Figure 10. This Chilean artisan is forming a sphere of lapis lazuli at his home in La Serena. The sphere-making machinery uses an old diamond-coring bit (inset); the sphere weighs 1.5 kg.



MARKETING AND DISTRIBUTION

Both LapisChile and Las Flores de Los Andes supply lapis lazuli to the wholesale and retail markets, and also sell processed products—including jewelry, doorknobs, pens, glasses, clocks, spheres, carvings, tabletops, and tiles (see, e.g., LapisChile’s Web site, www.cepri.cl/lapislaz/company.html). Most of the lapis lazuli mined by Las Flores de Los Andes is sold as rough material, by the kilogram, in a range of sizes. The majority is processed domestically, with the remainder going primarily to Germany, Italy, and the U.S.

A thriving industry of local Chilean artisans work individually, or in small family groups, to manufacture jewelry and other ornamental objects (figure 10). During a 1993 visit to Chile by the senior author, “Keop’s” in Ovalle was one of the largest local buyers; they purchased several thousand kilograms of material annually from Las Flores de Los Andes. The principal artisan, Wellington Vega A., created carvings using fine electric saws and drills, while his employees used the off-cuts to produce cabochons and tumbled pieces. The carvings frequently show interesting patterns created by the spots and veins of associated minerals (figure 11).

Before trucks could access the mining area starting in 1989, lower-quality lapis lazuli was rarely mined. Now that the material can be extracted in larger blocks, today it is being exploited profitably by both LapisChile and Las Flores de Los Andes. Much of this is cut into slabs for use as building products (J. Muxi, pers. comm., 1999). In 1998, Lapis Pigment S.A., a subsidiary of Las Flores de Los Andes, began producing the natural blue pigment “ultramarine” using Chilean lapis lazuli (J. Correa, pers. comm., 2000).

GEMOLOGICAL TESTING

Materials and Methods. Lapis lazuli samples representing all four qualities (and rejects) were obtained from the Las Flores de Los Andes processing warehouse in La Serena, and examined at the Australian Museum and Gemmological Association of Australia laboratories in Sydney. The samples consisted

Figure 11. This 17-cm-high figurine of a man smoking a pipe is fashioned from third-quality lapis lazuli. Note how the light-colored areas of the rock are effectively used to highlight portions of the man's clothing and the bowl of his pipe. Oriental themes in carved Chilean lapis lazuli are popular, with finished works being sent to Japan, as well as Italy, France, and Germany.



Figure 12. These samples represent the graded material studied by the authors. From left to right: first-quality (150 g), second-quality (100 g), third-quality (100 g), fourth-quality (170 g), and reject material (180 g).

of 700 g of graded rough (figure 12), five polished slabs totaling 1.8 kg (see, e.g., figure 9), four free-form cabochons, and a 1.5 kg sphere (figure 10). The Chilean material was compared with four samples of Afghan lapis lazuli from the Australian Museum's collection: a 150 g piece of rough and a 14.38 ct cabochon (both "first-quality"), and two specimens with dodecahedral lazurite crystals in a matrix of white calcite and pyrite. Cabochons fashioned from sodalite (17.14 ct) and the following lapis lazuli imitations (loaned from the GIA collection) were also studied: barium sulfate (4.18 ct), Gilson-created (2.63 ct), and plastic (1.82 and 5.09 ct).

All samples were examined with a 45× binocular microscope, and viewed in a darkened room with a Raytech short- and long-wave ultraviolet lamp. The colors of the different samples were referenced to a Munsell Color Chart and described using the three independent parameters: hue, tone (cf., lightness or darkness value), and saturation (cf., chroma). We used a Topcon refractometer to obtain spot refractive index readings on the Chilean cabochons, and an Oertling R42 hydrostatic balance to determine the specific gravity of most of the samples. Small pieces of first-quality lapis lazuli from Chile and Afghanistan were crushed for powder X-ray diffraction (XRD) analysis at the Australian Museum, and the results were compared to reference diffraction patterns by Diffraction Technology, Australia.

Characteristics of Chilean Lapis Lazuli. Overall, the Chilean lapis lazuli samples varied from light blue

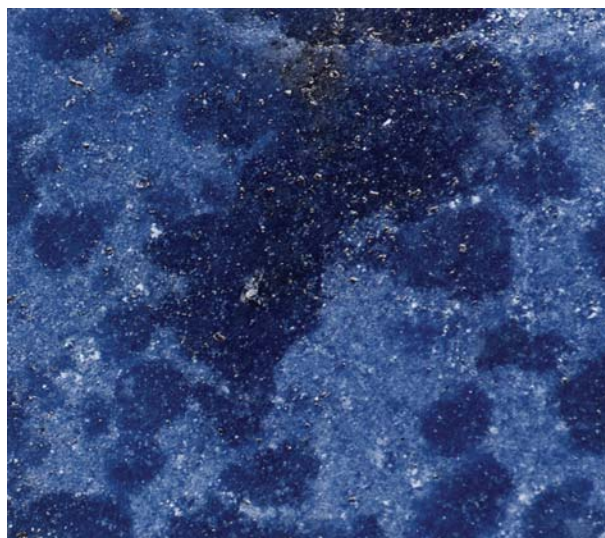


Figure 13. The overall darkness or lightness of blue depends on the number of lazurite grains per given area of the white wollastonite matrix, as shown in this sample (left, 4 × 5 cm; photo by Maha Tannous). The less lazurite there is, the lighter the overall appearance of the lapis lazuli will be (right; photomicrograph by John I. Koivula, magnified 20×).

to dark blue (Munsell tone = 2 to 6), typically within a narrow hue range of violetish blue (Munsell hue = 5PB to 6PB); some also showed greenish blue. The Afghan samples, as well as the lapis imitations and the sodalite, were visibly more violet in hue (7.5PB to 8.5PB).

Even small samples of Chilean lapis lazuli showed slightly different tones of blue within a single piece (see, e.g., figure 13 left). When these pieces were examined with magnification (figure 13 right), it was evident that the apparent darkness or lightness of blue depended on the amount of white or colorless minerals (particularly wollastonite) mixed with the lazurite, rather than on the hue of the lazurite itself. Those areas that contained fewer grains of light-colored minerals appeared a darker blue.

Pyrite inclusions in the Chilean material occurred in many different sizes, shapes, and forms. Most commonly, the grains were rounded or displayed highly irregular or “stretched” shapes (figure 14). In the lower-grade polished slabs, the pyrite showed a patchy distribution, often forming irregular bands and aggregates.

Exposure of the Chilean samples to UV radiation confirmed their heterogeneous nature. The lazurite was inert to UV, while the accompanying fluorescent minerals stood out as spots, patches, and veins that fluoresced strong blue-white to short-wave UV, with different areas or veins showing strong orange-yellow to long-wave UV. On the basis of Cuitiño

(1986) and our observations with magnification, these fluorescent minerals are most likely wollastonite, calcite, and haüyne.

S.G. and R.I. are not always useful for identifying lapis lazuli, since it is an aggregate of different minerals. Measurements of 46 Chilean samples (4 to 22 g) of varying quality yielded a mean S.G. value of 2.77, with a standard deviation of ±0.06. This is greater than the reported value for lazurite (2.38–2.45), but it falls within the range reported for commercial grades of lapis lazuli (2.7–2.9; Arem, 1977; Webster, 1994). A spot R.I. of about 1.50 was obtained from the cabochons. This is consistent with the reported R.I. values for lazurite (1.500–1.522), and it is identical to the R.I. for lapis lazuli reported by Webster (1994).

X-ray diffraction analysis identified lazurite and wollastonite as the principal minerals in samples of first-grade lapis lazuli from both Chile and Afghanistan. Additional peaks for plagioclase and calcite were observed in the scans of the Afghan material. These mineral assemblages are consistent with previous investigations, except that wollastonite was not documented in Afghan lapis lazuli by Wyart et al. (1981).

SEPARATION FROM SODALITE, LAPIS SIMULANTS, AND AFGHAN LAPIS LAZULI

Lazurite vs. Sodalite. Lazurite is easy to distinguish from sodalite (see Box A) by its higher refractive index (1.500–1.522, compared to 1.483–1.487) and

its higher specific gravity (2.38–2.45, compared to 2.14–2.30). Most massive lazurite contains at least traces of pyrite, which further increases its apparent specific gravity relative to sodalite. The presence of brassy specks of pyrite, however, is not diagnostic, as pyrite has also been reported in sodalite (Webster, 1994). Lazurite is inert to UV radiation, whereas sodalite may show an intense orange to orange-red fluorescence to both short- and long-wave UV. Lazurite is also distinguishable by its bright blue streak (compared to the white or pale blue streak of sodalite), and the liberation of hydrogen sulfide gas (with its distinctive rotten egg odor) when hydrochloric acid is applied, or when it is worked on grinding and polishing laps.

Chilean Lapis Lazuli vs. Simulants. Magnification is the most useful tool for this separation. At 10×–45× magnification, the blue color of the natural material was nonhomogeneous, whereas the simulants studied all showed a homogeneous bright, saturated blue coloration that was more purple than the Chilean material. The different minerals in Chilean lapis lazuli were clearly visible as intricate spots, patches, and veinlets, both in daylight and with UV radiation. In particular, the rounded or highly irregular forms displayed by the pyrite inclusions in Chilean lapis lazuli were usually distinct from the equant, straight-edged brassy inclusions commonly seen in the lapis lazuli imitations.

A number of materials have been used as lapis lazuli simulants. As described in Webster (1994) and supplemented by our tests on three samples, these may be distinguished from natural lapis lazuli—regardless of the locality of origin—as follows:

1. *Gilson-created lapis* shows a stronger reaction to hydrochloric acid (HCl) and is more porous (and thus shows a marked increase in weight after immersion in water). Crushed pyrite grains, if added, are very regular in shape and size, and tend to pluck out during polishing. This simulant is considerably lower in hardness (about 3 on the Mohs scale, compared to 5.5 for lapis lazuli) and S.G. (average 2.35).
2. “*Swiss/German lapis*” (i.e., dyed jasper) appears red with the Chelsea filter (as compared to no reaction for the natural samples), has a higher R.I. (1.54), displays an inferior blue color, does not contain pyrite or react with HCl, and will stain a swab moistened with acetone (as will dyed natural lapis lazuli).



Figure 14. Pyrite exhibits many forms in Chilean lapis lazuli. In addition to the disseminated, fine-grained pyrite with rounded edges, this sample shows pyrite with highly irregular “stretched” shapes. Photomicrograph by John I. Koivula; magnified 40×.

3. *Sintered cobalt-colored blue synthetic spinel* has significantly higher values for S.G. (3.52) and R.I. (1.725), appears red with the Chelsea filter, displays cobalt lines in its absorption spectrum, and does not react to HCl. Specks of gold are often added to simulate pyrite.
4. *Barium sulfate imitation lapis* has a lower S.G. (2.33 measured on the sample we tested), is semi-translucent to strong light, and is indented by the thermal reaction tester, producing a whitish discoloration and a weak acrid odor (see also Koivula and Kammerling, 1991). Although it typically contains crushed pyrite in realistic-looking “veins,” the grains are usually very regular in shape and size.
5. *Plastic* is very soft (a Mohs hardness of 1.5–3), has a lower S.G. (2.47 measured on the sample we tested, which contained pyrite), may be more porous, and indents when tested with the thermal reaction tester (emitting an acrid odor).

Chilean vs. Afghan Lapis Lazuli. None of the Chilean samples studied had the prized “azure” or “ultramarine” hue of the high-quality Afghan material we examined. Our findings are consistent with earlier observations that Chilean lapis lazuli is more spotted (Schumann, 1997) or less pure (Webster, 1994) than Afghan material. Webster (1994) reported that Chilean lapis lazuli, when viewed with UV

Figure 15. Attractive jewelry is manufactured in Chile using higher-quality lapis lazuli. The bracelet and earrings shown here feature Chilean lapis lazuli and Chilean malachite. Photo by Robert Weldon.



radiation, shows more pronounced spots and streaks of orange or “copper”-colored fluorescence than the Afghan material. Our observations indicate that these fluorescent patches are nearly ubiquitous in Chilean lapis lazuli, and correspond to areas of wollastonite, calcite, and haüyne.

SUMMARY AND CONCLUSION

Since the deposits were first discovered in the mid-19th century, hundreds of tonnes of lapis lazuli have been mined from the Coquimbo Region in the Chilean Cordillera. Field mapping and drilling projects indicate that substantial reserves of lapis lazuli are still present in the traditional mining area. Two companies—Las Flores de Los Andes S.A. and Compañía Minera LapisChile S.A.—are currently mining the lapis lazuli and supplying raw and finished material to local and international markets. Higher-quality lapis lazuli is used for jewelry (figure 15) or for carvings; lower-quality material is carved or used in various ornamental building materials.

Chilean lapis lazuli consists mainly of lazurite, wollastonite, and calcite. It can be readily

distinguished from similar-appearing rocks and manufactured imitations by standard gemological techniques.

Acknowledgments: The authors thank Ramon Vega E., Coquimbo, Chile, for providing samples of lapis lazuli and for access to the Las Flores de Los Andes processing plant in La Serena. The authors are also indebted to Wellington Vega A. of Taller Keop's, Ovalle, Chile, and his staff—Teresa Vega A., Elsa Vega A., and Pamela Eriza V.—for their hospitality and assistance during the field visit, as well as to Paola Yéñez R., Maudy Tabilo M., and Amy Melling of the La Serena Information Center. Invaluable assistance with samples and XRD analyses was provided by Ross Pogson and David Colchester of the Australian Museum, Sydney. Updated information on mining techniques and marketing strategies was provided by Jorge Correa, general manager of Las Flores de Los Andes S.A., Jorge Muxi Balsells, managing director of LapisChile S.A., Bernadita Lepe, a manager at LapisChile S.A., and Dr. Sergio Rivano G. of the University of Chile, a consulting geologist to LapisChile S.A.

REFERENCES

- Anthony J.W., Bideaux R.A., Bladh K.W., Nichols M.C. (1995) *Handbook of Mineralogy—Vol. 2: Silica, Silicates*, Part 2. Mineral Data Publishing, Tucson, AZ.
- Arem J.E. (1987) *Color Encyclopedia of Gemstones*, 2nd ed. Van Nostrand Reinhold, New York.
- Bauer M. (1904) *Precious Stones, Their Characters and Occurrence*. Charles Griffen and Co., London.
- Bowersox G.W., Chamberlin B.E. (1995) *Gemstones of Afghanistan*. Geoscience Press, Tucson, AZ.
- Brendler W. (1934) Sodalite from Bolivia. *American Mineralogist*, Vol. 19, pp. 28–31.
- Burnham S.M. (1886) *Precious Stones in Native Art and Literature*. Bradlee Whidden, Boston, MA.
- Bruggen J. (1921) Informe geológico sobre el yacimiento de lapislázuli Flor de Los Andes del Señor Santiago M. Merry [Geological report on the Flor de Los Andes lapis lazuli deposit of Mr. Santiago M. Merry]. Unpublished report, Santiago, Chile, 10 pp.
- Bruggen J. (1926) Segundo informe geológico sobre las minas de lapislázuli de Ovalle [Second geological report on the Ovalle lapis lazuli mines]. Unpublished report, Santiago, Chile, 8 pp.
- Canut de Bon C. (1991) Apreciaciones sobre las reservas de lapislázuli de yacimientos chilenos [Reserve estimates for the Chilean lapis lazuli deposits]. Unpublished report for El Servicio Nacional de Geología y Minería, December 9, 1991.
- Christopher G.W. (1977) Colorado's blue stone of the ancients. *Western and Eastern Treasures*, Vol. 11, No. 5, pp. 38–40.
- Cuitiño L. (1986) Mineralogía y genesis del yacimiento de lapislázuli, Flor de los Andes, Coquimbo, norte de Chile [Mineralogy and genesis of the Flor de los Andes lapis lazuli deposit, Coquimbo, northern Chile]. *Revista Geológica de Chile*, Vol. 27, pp. 55–67.
- Dana E.S. (1892) *The System of Mineralogy*, 6th ed. John Wiley & Sons, New York.
- Deer W.A., Howie R.A., Zussman J. (1963) *Rock Forming Minerals, Vol. 4, Framework Silicates*. Longmans, Green and Co., London, pp. 289–302.
- Domeyko I. (1860) *Elementos de Mineralogía*, 2nd ed. Imprenta del Ferrocarril (Railway Press), Santiago, Chile.
- Douglas J.D., Ed. (1980) *The Illustrated Bible Dictionary*. Intervarsity Press, Sydney.
- Field F. (1850a) Análisis de lapislázuli de Elqui [Analysis of lapis lazuli from Elqui]. *Los Anales de la Universidad de Chile por 1850*, p. 386.
- Field D.F. (1850b) Mineralogía.—Lapis lazuli en Chile. Comunicado en una carta escrita al Secretario de la Facultad de Ciencias. *Chile Universidad Anales*, p. 340.
- Gaines R.V., Skinner H.C.W., Foord E.E., Mason B., Rosenzweig A. (1997) *Dana's New Mineralogy*, 8th ed. John Wiley & Sons, New York, pp. 1623–1628.
- Heidel A. (1946) *The Gilgamesh Epic and Old Testament Parallels*. University of Chicago Press, Chicago and London.
- Hinks P. (1975) *Nineteenth Century Jewellery*. Faber and Faber, London, p. 56.
- Hogarth D.D., Griffin W.L. (1978) Lapis lazuli from Baffin Island—a Precambrian meta-evaporite. *Lithos*, Vol. 11, No. 1, pp. 37–60.
- Hogarth D.D., Griffin W.L. (1980) Contact-metamorphic lapis lazuli: The Italian Mountain deposits, Colorado. *Canadian Mineralogist*, Vol. 18, Part 1, pp. 59–70.
- Ivanov V.G. (1976) The geochemistry of formation of the rocks of the lazurite deposits of the southern Baykal Region. *Geochemistry International*, Vol. 13, No. 1, pp. 26–31.
- Koivula J.I., Kammerling R.C., Eds. (1991) Gem news: Imitation lapis lazuli. *Gems & Gemology*, Vol. 27, No. 1, p. 54.
- Kulke H.H.G. (1976) Metamorphism of evaporitic carbonate rocks (NW Africa and Afghanistan) and the formation of lapis lazuli. *Abstracts, International Geological Congress* (Sydney, Australia), No. 25, Vol. 1, Section 3B, pp. 131–132.
- Rivano S. (1975a) Reconocimiento geológico de las nacientes del río Grande Alta Cordillera de Ovalle, entre los 30°30' and 31°20' latitud sur, Provincia de Coquimbo [Reconnaissance geology of the headwaters of the Grande Alta Cordillera de Ovalle River, between latitude 30°30'S and 31°20'S, Coquimbo Province]. Unpublished thesis, Departamento de Geología, Universidad de Chile, Santiago.
- Rivano S. (1975b) El lapislazuli de Ovalle (Provincia de Coquimbo, Chile) [The lapis lazuli from Ovalle (Coquimbo Province, Chile)]. *6º Congreso Geológico Argentino*, Vol. 3, pp. 165–177.
- Rivano S., Sepúlveda P. (1991) *Hoja Illapel. Serie Carta Geológica de Chile, escala 1:250000 [Illapel 1:250,000 Geological Map Sheet, Chile]*. SERNAGEOMIN (Servicio Nacional de Geología y Minería de Chile), Santiago, Chile.
- Rogers A.F. (1938) Lapis-lazuli from San Bernardino County, California. *American Mineralogist*, Vol. 23, pp. 111–113.
- Schultz P.R. (1981) Colorado lapis lazuli from the Blue Winkle Mine in Gunnison County. *Lapidary Journal*, Vol. 34, No. 11, pp. 2344, 2346.
- Schumann W. (1997) *Gemstones of the World*. Sterling Publishing Co., New York.
- Silverman D.P. (1978) *50 Wonders of Tutankhamun*. An Artabras Book, Crown Publishers, New York.
- Sinkankas J. (1997) *Gemstones of North America*, Vol. 3. Geoscience Press, Tucson, AZ.
- Sofianides A.S., Harlow G.E. (1990) *Gems & Crystals from the American Museum of Natural History*. Simon and Schuster, New York.
- Sutherland L. (1991) *Gemstones of the Southern Continents*. Reed Books, Sydney, Australia.
- Tiglay J.H. (1982) *The Evolution of the Gilgamesh Epic*. University of Pennsylvania Press, Philadelphia.
- von Rosen L. (1990) Lapis lazuli in archaeological contexts. In P. Astrom, Ed., *Studies in Mediterranean Archaeology, Pocketbook 93*, Jonsered, Foerlag, Sweden.
- Ward F. (1996) Atop the Andes—Mining Chile's mountain-high lapis. *Lapidary Journal*, Vol. 50, No. 3, pp. 36–40.
- Webster R. (1994) *Gems, Their Sources, Descriptions and Identification*, 5th ed. Rev. by P.G. Read, Butterworth-Heinemann, Oxford, England.
- Wyart J., Bariand P., Filippi J. (1981) Lapis-lazuli from Sar-e-Sang, Badakhshan, Afghanistan. *Gems & Gemology*, Vol. 17, No. 4, pp. 184–190.
- Zeballos J. (1973) Estudio geológico preliminar del yacimiento de lapislázuli de Río Tascadero, Ovalle [Preliminary geological study of the Tascadero River lapis lazuli deposit, Ovalle]. Unpublished report for Empresa Nacional de Minería, ENAMI, Santiago, Chile, 41 pp.

SPECTROSCOPIC EVIDENCE OF GE POL HPHT-TREATED NATURAL TYPE IIa DIAMONDS

By David Fisher and Raymond A. Spits

Results from spectroscopic analyses of GE POL high-pressure high-temperature (HPHT) annealed nominally type IIa diamonds are presented, and these spectral characteristics are compared with those of untreated diamonds of similar appearance and type. Absorption spectroscopy reveals that any yellow coloration in such HPHT-treated diamonds is due to low concentrations of single nitrogen, which have not been observed in untreated type IIa diamonds. Laser-excited photoluminescence spectroscopy reveals the presence of nitrogen-vacancy centers in most, but not all, HPHT-treated stones. When these centers are present, the ratio of the 575:637 nm luminescence intensities offers a potential means of separating HPHT-treated from untreated type IIa diamonds. The total absence of luminescence may be another important indicator of HPHT treatment.

The announcement in March 1999 that Lazare Kaplan International (LKI) subsidiary Pegasus Overseas Limited (POL) planned to market diamonds that had undergone a new "process" developed by General Electric (GE) led to widespread unease throughout the diamond industry. Of particular concern were the statements made then and subsequently that the process—to improve color and brilliance—was irreversible and undetectable. Since this announcement, a number of articles have shown the potential for detection of such material,

on the basis of both gemological and spectroscopic features (Shigley et al., 1999; Moses et al., 1999; Chalain et al., 1999 and 2000). GE has confirmed that the process involves high-temperature annealing at high pressure (HPHT), and LKI has said that brown diamonds are used as the starting material (Moses et al., 1999; figure 1 inset).

De Beers's own extensive research program, including studies begun in the 1980s, has enabled us to compare spectroscopic observations made on several GE POL-treated samples with data obtained on experimental samples that had been HPHT-treated at the De Beers Diamond Research Laboratory (DRL) in Johannesburg. These DRL samples were treated purely for research and only to help establish identification techniques. This article will highlight spectral features that we believe are potentially indicative of such HPHT-treated diamonds. Comparison with similar natural untreated samples is very important in this respect, and this has formed a significant part of our continuing research.

ABOUT THE AUTHORS

Dr. Fisher is a research scientist at the De Beers DTC Research Centre, Maidenhead, United Kingdom. Dr. Spits is a principal research officer at the De Beers Diamond Research Laboratory, Johannesburg, South Africa.

Please see acknowledgments at end of article.

Gems & Gemology, Vol. 36, No. 1, pp. 42–49.

© 2000 Gemological Institute of America

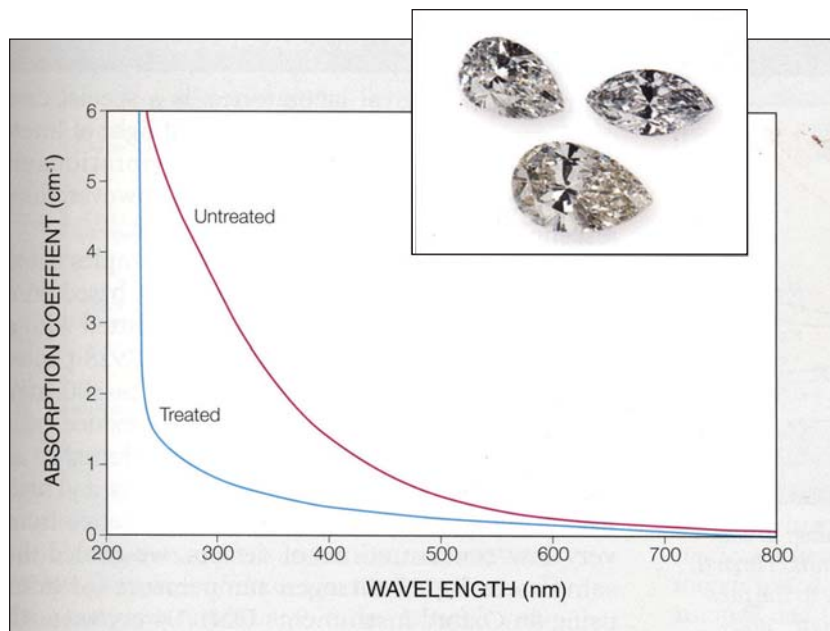


Figure 1. High-pressure, high-temperature treatment—such as that used by General Electric in their GE POL diamonds—can effectively reduce the coloration of some type IIa brown diamonds to colorless. In this UV/Vis/NIR absorption spectrum, note the increasing absorption at lower wavelengths of an untreated type IIa brown diamond. After HPHT treatment at the De Beers Diamond Research Laboratory, the same sample (now colorless) showed a significant reduction in that absorption. The inset shows three GE POL diamonds in a range of color grades: Top left = I color, 0.50 ct; top right = E color, 0.45 ct; bottom = J color, 0.77 ct. Photo by Elizabeth Schrader.

MATERIALS AND METHODS

Samples Examined. The Gemological Institute of America (GIA) has published demographic information on 858 GE POL diamonds (Moses et al., 1999). Almost all of these samples were nominally type IIa diamonds. While GIA records infrared (IR) spectra on some of the diamonds submitted to the Gem Trade Laboratory, the laboratory uses transparency to short-wave ultraviolet radiation, and the presence of a cross-hatched (“tatami”) strain pattern seen with crossed polarizers, as a practical means of distinguishing type IIa diamonds during its normal diamond grading procedure (J. Shigley, pers. comm., 2000). Technically, type IIa diamonds are defined as those that have no detectable nitrogen in that part of the IR absorption spectrum between 1332 and 400 cm^{-1} , the so-called single-phonon region, where absorption due to vibration of impurity atoms is present. (A phonon is a quantum of lattice vibration within a crystal; see, e.g., Collins, 1982. For more on diamond types, see, e.g., Fritsch and Scarratt, 1992.) Most of the 858 samples were colorless or near-colorless, although some had a distinct yellow hue.

For the present study, we examined 16 commercially purchased GE POL diamonds ranging in color from D to U/V and in weight from 0.36 to 4.09 ct. All were laser-inscribed “GE POL” and accompanied by GIA Gem Trade Laboratory grading reports. Some showed distinctive internal features such as discoid fractures around solid inclusions and partial graphitization of pre-existing fractures; all showed banded or cross-hatched strain patterns when viewed between

crossed polarizers with a microscope, as described by Moses et al. (1999). All these samples were nominally type IIa. By “nominally” we mean that there was no easily detectable nitrogen-related absorption between 1332 and 400 cm^{-1} . However, as is described below, careful high-resolution IR measurements did, in some cases, detect features due to single substitutional nitrogen atoms (i.e., where a nitrogen atom substitutes for a carbon atom, hereafter referred to as “single nitrogen”), which typically are not seen in untreated type IIa diamonds.

We also analyzed samples that had been subjected to what we believe are similar HPHT conditions using technology developed at the DRL. Seventeen originally brown, type IIa rough diamonds were treated. In some cases, multiple samples were cut from the same piece of rough before treatment, so that the total number of DRL-treated pieces studied was 23 (visually estimated to be 18 colorless, 5 near-colorless). Parallel windows were polished on opposite sides of each sample to permit accurate absorption spectroscopy measurements. Nine of these samples were fully characterized before HPHT treatment, and all were fully characterized after treatment.

Five additional brown (14 total) and 16 colorless type IIa rough diamonds were examined fully for comparison with the HPHT-treated samples. These samples were also windowed to permit accurate absorption measurements. One advantage of using rough diamonds taken directly from De Beers mines is that we can guarantee absolutely that our comparison samples were untreated.

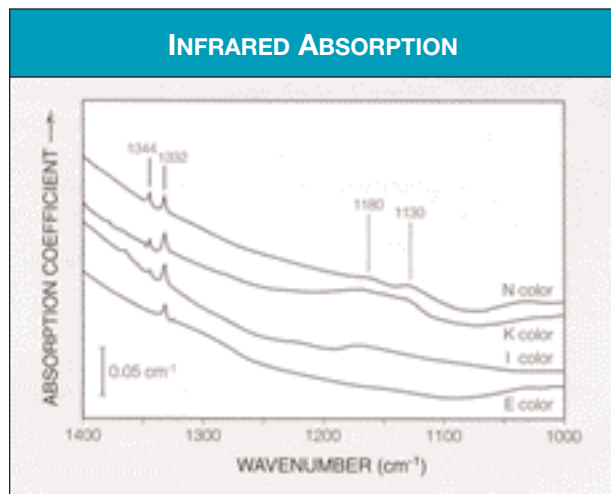


Figure 2. These IR absorption spectra were taken in the single-phonon region on four GE POL diamonds. Three (I, K, and N colored samples) show features due to the presence of single nitrogen (i.e., the peak at 1344 cm^{-1} and broad band at 1130 cm^{-1}), and weak absorption at about 1180 cm^{-1} due to low concentrations of B-centers. The sharp peak at 1332 cm^{-1} is observed in most diamonds.

Absorption Spectroscopy. Room-temperature infrared spectra were recorded on all samples with a Nicolet Magna-IR 750 Fourier-transform IR spectrometer. We used a Perkin-Elmer Lambda 19 spectrophotometer for ultraviolet/visible/near-infrared (UV/Vis/NIR) absorption measurements on all samples. Faceted samples were mounted in such a way as to allow the beam to pass through the sample, usually through opposite pavilion facets. IR spectra were acquired at a resolution of 0.5 cm^{-1} to allow increased sensitivity to very low concentrations of lattice defects. Quantitative information from the IR spectra was obtained by normalizing the spectra to the intrinsic diamond absorption between 2664 and 1500 cm^{-1} , the so-called two-phonon absorption. In this region, the IR spectrum, expressed as absorption coefficient, is the same for all diamonds. For spectra in the UV/Vis/NIR range, a semi-quantitative approach was adopted, whereby the sample was mounted in the same configuration as in the IR spectrometer and the same factor as determined from the intrinsic IR absorption was assumed for conversion to absorption coefficient.

Photoluminescence. The photoluminescence (PL) technique measures the intensity of light emitted from a sample, as a function of wavelength, in response to excitation by UV radiation or visible light. In general, different wavelengths of excitation will produce different PL spectra. Laser Raman microspectrometry, a standard analytical technique

in many gemological laboratories, is a special case of PL spectroscopy where the emitted light of interest is produced by characteristic vibrations of molecules and crystals. In this study, however, fluorescence was the emitted light of interest.

For this study, we tested all of the samples listed above with custom-built PL equipment based on a Spex 1404 double-grating spectrometer fitted with a thermoelectrically cooled Hamamatsu R928 photomultiplier detector. A Spectra-Physics 300 mW multi-line argon ion laser was used to produce excitation at 488 and 514.5 nm (hereafter referred to as “514 nm”). To achieve the high sensitivity and high resolution necessary to reveal luminescence from very low concentrations of defects, we cooled the samples to liquid-nitrogen temperature (-196°C) using an Oxford Instruments DN1704 cryostat. All the PL spectra were normalized to the intensity of the first-order Raman peak.

RESULTS

Absorption Spectroscopy. UV/Vis/NIR spectra recorded on an initially brown diamond before and after treatment at the DRL are shown in figure 1. The absorption, which steadily rises with decreasing wavelength, is responsible for the initial brown color. This absorption decreased substantially following

TABLE 1. Single substitutional nitrogen concentrations calculated for the 16 GE POL diamonds, by color grade.

Color grade	Single nitrogen concentration (ppm)	
	Infrared ^a	Ultraviolet/visible ^b
D	—	<0.01
E	—	<0.02
E	—	0.04
E	—	<0.01
F	—	0.03
F	—	<0.01
F	—	<0.02
I	0.21	0.20
J	0.11	0.06
K	0.17	0.26
K	0.35	0.32
L	0.28	0.31
L	0.45	0.52
M	0.21	0.23
N	0.42	0.48
U/V	0.35	0.48

^a Calculated after Kiflawi et al. (1994) from the 1344 cm^{-1} peak.

^b Calculated after Chrenko et al. (1971) from the 270 nm peak.

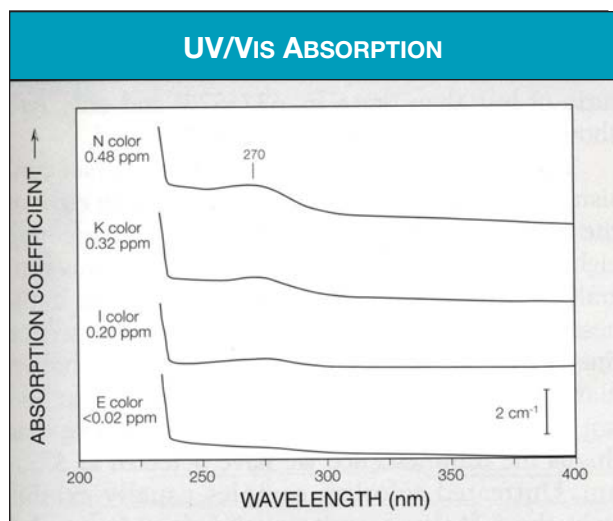


Figure 3. The broad peak at 270 nm in the UV/Vis absorption spectra of these four GE POL diamonds (same samples as in figure 2) is due to single substitutional nitrogen. Note that the strength of this peak increases as the color increases.

HPHT treatment, resulting in a colorless diamond.

IR absorption spectra from four GE POL stones (color graded E, I, K, and N) are shown in figure 2. All four spectra show a sharp line at 1332 cm^{-1} , which is often observed at very low intensity in untreated type IIa diamonds. The spectra of the I, K, and N color samples also show, albeit very weakly, a broad absorption feature peaking at 1130 cm^{-1} and a sharp line at 1344 cm^{-1} . This line would not have been detectable in all cases at a resolution lower than 0.5 cm^{-1} . The shape of the 1344 and 1130 cm^{-1} absorption is consistent with that due to single nitrogen. Kiflawi et al. (1994) determined conversion factors to relate the strength of the 1130 cm^{-1} absorption to the concentration of nitrogen, and we used these conversions to calculate the concentration figures presented in table 1. From the infrared spectra, we determined single-nitrogen concentrations ranging from about 0.5 atomic parts per million (ppm) down to about 0.1 ppm in the near-colorless GE POL samples. We also detected an additional weak, broad peak at 1180 cm^{-1} in some samples that was due to the presence of low concentrations of B-centers (aggregates of nitrogen consisting of four nitrogen atoms and a vacancy).

Single nitrogen gives a characteristic broad absorption peak at 270 nm in the UV region (Dyer et al., 1965). UV/Vis spectra for the same E, I, K, and N color samples are given in figure 3. Although spectra often are distorted due to reflections within the sample, the single nitrogen signature can be clearly detected for the I, K, and N color samples.

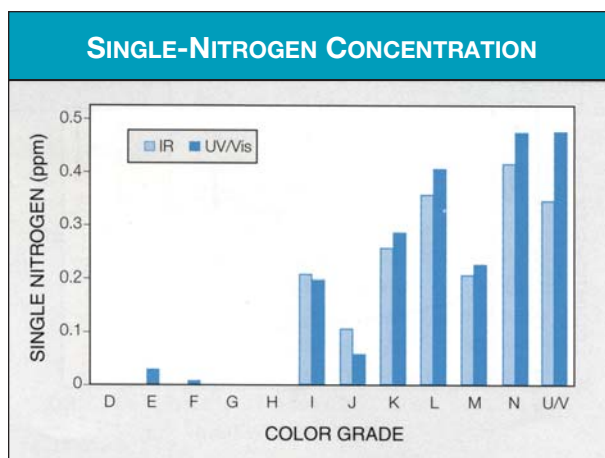


Figure 4. This bar chart illustrates the variation in single-nitrogen concentration with intensity of color (indicated here by color grade) for the GE POL diamonds tested. The nitrogen values were calculated using IR and UV/Vis absorption features (see table 1). No samples with G and H color were examined; no single nitrogen was detected in the one D color sample. Average values are shown for the E ($n = 3$), F ($n = 3$), K ($n = 2$), and L ($n = 2$) colored samples.

Only a hint of the 270 nm peak was detected in the E color diamond, for which the nitrogen concentration was estimated to be no more than 0.02 ppm.

For comparison with the IR values, we determined nitrogen concentrations from this absorption using the formula published by Chrenko et al. (1971), with modifications to allow for any additional absorption in the UV region that our own experimental work had shown to be necessary.

These values show reasonable agreement with those obtained from IR absorption (again, see table 1). As a general trend, single-nitrogen concentration increases as color becomes more evident (figure 4).

Photoluminescence. *488 nm Ar Ion Laser Excitation.* Figure 5 presents spectra acquired from the four GE POL samples (E, I, K, and N color) cited above, in this case using 488 nm excitation from the argon ion laser. The dominant feature in most cases was the H3 luminescence. This can be distinguished from other centers that give sharp-line luminescence at 503 nm by the structure of the associated vibronic band (Collins, 1982). Our annealing experiments on initially brown samples showed that there is a decrease in the H3 luminescence on HPHT annealing. In some, but not all, cases, additional features were observed. The lines at 575 and 637 nm are due to emission from the nitrogen-vacancy center in its neutral, $(\text{N-V})^0$, and negative, $(\text{N-V})^-$, charge state, respectively (Mita, 1996).

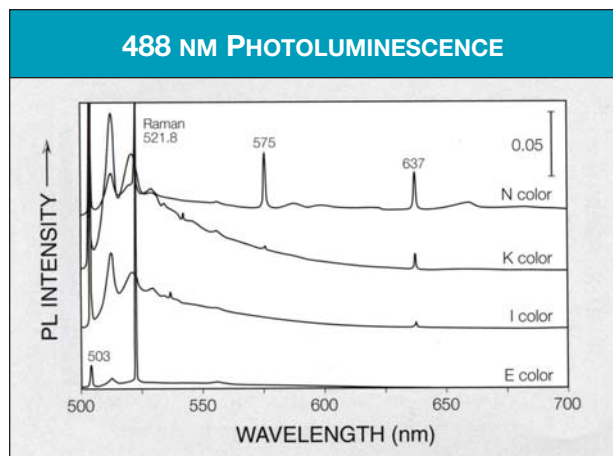


Figure 5. These photoluminescence emission spectra of four GE POL diamonds (same as in figure 2) were obtained at liquid-nitrogen temperature using 488 nm Ar ion laser excitation. The dominant features are luminescence from the H3 center (503 nm) and from the nitrogen-vacancy center in its neutral (575 nm) and negative (637 nm) charge states. The line at 521.8 is the first-order Raman peak.

514 nm Ar Ion Laser Excitation. The first room-temperature PL spectra of GE POL diamonds under 514 nm excitation using a Raman spectrometer were published by Chalain et al. (1999 and 2000). Liquid-nitrogen temperature PL spectra from the E, I, K, and N color GE POL samples are shown in figure 6, and table 2 presents a summary of the main features observed in the range of samples studied under these conditions. All the spectra we obtained showed the first-order Raman line at 552.4 nm and the second-order Raman spectrum between 578 and 597 nm. In some cases, a line was observed at 535.8 nm. The defect responsible for this luminescence has not been identified, but emission at this wavelength has been observed in untreated type Ia brown diamonds and in type Ia diamonds that have been irradiated and annealed (see, e.g., Anderson, 1963; Collins, 1982).

The key GE POL features are lines at 575 and 637 nm related to the N-V center. Chalain et al. (2000) noted an increase in intensity of the 637 nm luminescence with more strongly colored samples. Although there was such a trend in most of the GE POL diamonds we examined, we did not observe a strict correlation of 637 nm emission with either color grade or single-nitrogen content.

However, we did observe that the ratio of the 575:637 nm emission intensities in HPHT-treated diamonds was, in general, lower than that typically found in untreated colorless type IIa diamonds. Of the 14 GE POL diamonds examined with detectable 575 and 637 nm luminescence, 12 had a 575:637 nm

ratio of less than one (i.e., $637 > 575$) and only two showed a ratio greater than one (i.e., $575 > 637$).

The luminescence at around 575 nm in fact consisted of two lines, at 574.8 and 575.8 nm, in eight of the 16 GE POL samples examined. In the remaining eight samples, the 575.8 nm luminescence was generally absent in samples where the 574.8 nm luminescence was weak or also absent. A luminescence line at 575 nm has been observed in type Ia brown diamonds that show yellow luminescence to 365 nm excitation (Jorge et al., 1983); it is possible that this is the luminescence we have detected at 575.8 nm. Untreated colorless samples usually exhibit only the 574.8 nm emission (of the 16 samples examined, 14 showed detectable 574.8 nm luminescence and none showed the 575.8 nm line). In contrast, most untreated type IIa brown diamonds exhibit either (1) both 574.8 and 575.8 nm luminescence, or (2) in more strongly colored samples, neither of these lines but instead a line at 578.8 nm. Strongly colored brown samples often reveal a line at 559.0 nm as well (see figure 7). Just two of our 14 type IIa brown samples showed only 574.8 nm luminescence. We are continuing to investigate whether this also might be a useful diagnostic characteristic.

The colorless HPHT-treated samples generally showed weaker luminescence than the near-colorless to yellow stones. For two of the seven GE POL diamonds of D to F color, and for 15 of the 18 DRL-treated samples of similar treated color, no significant luminescence was generated under these excitation and detection conditions. Conversely, none of our 16 colorless untreated type IIa diamonds or 14 type IIa brown diamonds showed the complete absence of luminescence features under such conditions. Therefore, the presence or absence of luminescence, in itself, is a useful diagnostic characteristic for a diamond that has been confirmed to be type IIa by IR spectroscopy.

DISCUSSION

Single Nitrogen. In the vast majority of natural diamonds, any hint of yellow color is due to the presence of N3 centers, and stones with strong N3 absorption are usually referred to as Cape diamonds (Collins, 1982). The N3 center consists of three nitrogen atoms surrounding a common vacancy (van Wyk, 1982). In contrast, our spectroscopic results show that those GE POL samples that appear pale yellow do so because of the presence of low concentrations of single nitrogen. Although single nitrogen has been found in natural diamond—in

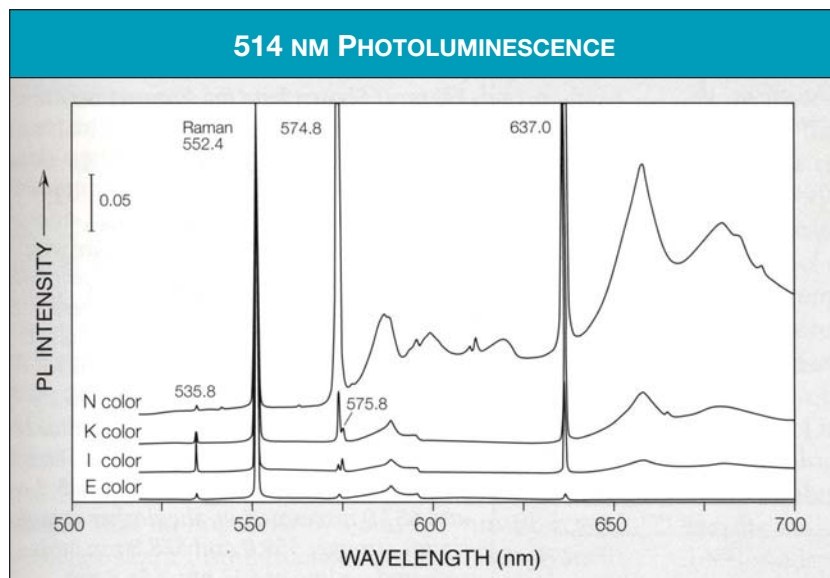


Figure 6. Photoluminescence emission spectra of the same four GE POL diamonds as in figure 5 were obtained at liquid-nitrogen temperature using 514 nm argon ion laser excitation. The 574.8 and 575.8 nm lines are clearly visible in the spectra of the I and K colored samples, and the stronger 637 nm—relative to the 575 nm—emission is evident. Also observable is a line at 535.8 nm.

so-called Canary yellows—it usually is present in samples that also contain significant concentrations of aggregated nitrogen; that is, the diamonds are of mixed type Ia/Ib. In the course of many years of research, we have never encountered a natural diamond that is nominally type IIa, but that contains sufficient single nitrogen to produce an observable yellow color. This includes not only the samples used in this research but also a suite of 50 type II or very weakly type Ia diamonds studied previously (the only non-type Ia diamonds found among 6,000 D to R color polished stones examined). As discussed below, the presence of single nitrogen in GE POL diamonds is important in the interpretation of other spectroscopic observations.

The single nitrogen in GE POL diamonds is probably the product of dissociation of aggregates of nitrogen that were initially present in small concentrations in the untreated sample. Brozel et al. (1978) have shown that it is possible to dissociate A-centers at temperatures over 1960°C and B-centers at temperatures above 2240°C. We believe that these temperatures are consistent with those used in the

GE POL treatment. (Over geological time, single nitrogen atoms in natural diamonds aggregate to form more complex defects. A-centers are pairs of nitrogen atoms; B-centers are formed of four nitrogen atoms surrounding a vacancy; see, e.g., Evans, 1991; Fritsch and Scarratt, 1992.) The presence of single nitrogen in nominally type IIa diamond provides an indication of HPHT treatment.

Nitrogen-Vacancy Centers. With 514 nm Ar ion laser excitation, most of the GE POL samples tested showed luminescence at 575 and 637 nm due to the neutral and negative charge states of the nitrogen-vacancy center. N-V centers will be produced by the combination of a proportion of single nitrogen with vacancies. The most probable source of these vacancies is dislocations. The starting specimens for the GE POL process, brown type IIa diamonds, have undergone plastic deformation as part of their geological history. The brown coloration is thought to be associated with the dislocations produced by the deformation (e.g., Wilks and Wilks, 1991). The reduction in color on annealing is presumably due to a modification of the structure of the defect that is responsible for the absorption states. It has been observed that GE POL diamonds exhibit a high degree of strain and that the pattern of strain birefringence is similar to that seen in brown type IIa diamonds (Moses et al., 1999).

Recently there have been reports of HPHT color alteration of type Ia brown diamonds (Moses and Reinitz, 1999; Collins et al., 2000). Here the color change is to yellowish green due to the production of H3 absorption and fluorescence. It is thought that during HPHT annealing, vacancies are generated at

TABLE 2. Summary of 575/637 nm luminescence in untreated and HPHT-treated type IIa samples.^a

Category	Total no.	Only 575 nm	Only 637 nm	Both 575/637	Neither 575/637	575<637
GE POL	16	0	0	14	2	12
DRL-treated	23	0	3	0	20	3
Colorless	16	7	0	7	2	1
Brown	14	2	4	4	4	4

^aLuminescence features generated by 514 nm Ar ion laser excitation.

514 NM PHOTOLUMINESCENCE COMPARISON SPECTRA

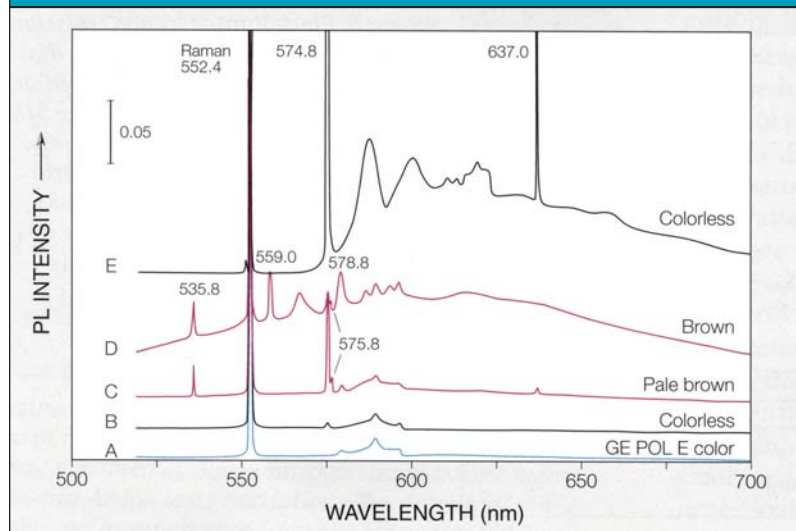


Figure 7. Shown here for comparison are photoluminescence emission spectra (at 514 nm excitation) for a range of type IIa diamonds. The E-color GE POL sample (A) shows no sharp luminescence lines, only Raman features. Spectra B and E are from two untreated type IIa colorless diamonds: B shows only the 574.8 nm line, whereas E shows strong emission at 574.8 and 637.0 nm from the neutral and negative nitrogen-vacancy center, respectively. Spectra C and D are from a pale brown and a darker brown type IIa sample, respectively. The pale sample shows stronger 574.8, 575.8, and 637.0 nm emission; the darker sample shows stronger 559.0 and 578.8 nm emission and no line at 637 nm; 535.8 nm emission is seen in both.

the dislocations, and these vacancies combine with pre-existing A-centers in the vicinity of the dislocations to produce the N-V-N centers. This is evidenced by the distribution of the resulting H3 luminescence in banded or cross-hatched patterns. We believe that a similar process has taken place in these type IIa diamonds to produce the observed N-V centers. In addition, both the 575 and 637 nm luminescence peaks, seen in some type IIa brown diamonds, may be preserved during annealing.

The ratio of the 575:637 nm emission intensities in GE POL diamonds varies considerably, but in most of the samples we tested the ratio was less than one (i.e., 637>575). This indicates that a significant proportion of the N-V centers are in their negative charge state. Because substitutional nitrogen in the diamond lattice acts as a deep donor, and a large proportion of these GE POL diamonds show detectable quantities of single nitrogen, one would expect negatively charged N-V centers to be present in them. However, we did not find a strict correlation between color grade (or single nitrogen concentration) and the 575:637 nm emission ratio; this may be due to the presence of other donor and/or acceptor centers that will affect the relative numbers of N-V centers in respective charge states.

Chalain et al. (2000) found that 637 nm photoluminescence was present in all five GE POL, and in three untreated brown type IIa, diamonds studied, but not in the seven D-color untreated type IIa diamonds that they tested. They therefore tentatively suggested that the presence of 637 nm PL in non-brown type IIa diamonds might be diagnostic of HPHT treatment. However, they make the point that this is a preliminary result based on the small number of samples,

and that further investigation is needed. They have now examined 14 GE POL samples in the D to L color range, all of which showed 637 nm luminescence (J.-P. Chalain, pers. comm., 2000).

In this work, we found two GE POL diamonds (D and F color) that did not show 637 nm PL. An analysis of GE POL diamonds that fall exclusively in this color range would probably yield a significant number of such samples, although detection of 637 nm PL will undoubtedly depend on the sensitivity of the instrument being used. The diamonds HPHT-treated at the DRL were carefully selected initially to ensure very low nitrogen content, and a high proportion of the resulting samples (20 out of 23) exhibited no 637 nm luminescence. We also found seven *untreated* colorless type IIa diamonds that did show 637 nm PL (see, e.g., figure 7E). So, although the presence of 637 nm PL may be used as an indication that further investigation is warranted, it cannot be regarded as a diagnostic characteristic on its own.

However, the ratio of the 575 to 637 nm luminescence, where present, might provide a more secure means of discriminating between untreated and treated samples. Note that the ratio we have reported here is that generated with 514 nm Ar ion laser excitation; a different ratio would be obtained under different excitation conditions. The detection response of the system will also influence the measured ratio, but a system giving a reasonably linear response over the short wavelength range between 575 and 637 nm should produce consistent results. Care must be taken to ensure that this was the case if the technique were to be transferred between laboratories.

Although there is certainly some overlap

between treated and untreated type IIa diamonds in the 575:637 nm luminescence ratio observed, in general the lower the 575:637 nm ratio the more likely it is that a particular diamond has been HPHT-annealed. This gives a more secure identification than observation of 637 nm luminescence alone. In the rare cases of untreated colorless diamonds that exhibit relatively strong 637 nm luminescence, additional spectral features should provide evidence that the diamond has not been treated. Investigation into the usefulness of such features forms a significant part of our continuing research in this area. In general, those HPHT-treated diamonds that do not show 575 and 637 nm PL reveal no other sharp luminescence features. This in itself is an important indication that a type IIa diamond might be HPHT-treated.

CONCLUSIONS

The spectroscopic data presented highlight some of the differences we have observed between natural type IIa diamonds and GE POL-treated diamonds. In particular, the presence of detectable quantities of single nitrogen and the relatively high levels of 637 nm luminescence relative to 575 nm luminescence, as observed with 514 nm Ar ion laser excitation, appear to be characteristic of some heat-treated samples. The total absence of luminescence with strong 514 nm excitation may

be another important indicator that a near-colorless type IIa diamond has been HPHT-treated.

At the time of the early POL announcements in spring 1999, it was thought in the trade that this HPHT treatment was undetectable. We believe that by using a combination of absorption features and the low-temperature, high-resolution PL results presented here, in conjunction with the gemological data presented by Moses et al. (1999), the vast majority of HPHT-treated diamonds can now be detected. De Beers is in close contact with the leading gemological laboratories. We hope that, through this collaboration, a practical application for these results will be devised shortly. This should be possible by adapting laser Raman microspectrometers, now available in many gemological laboratories, for use at low temperature and with appropriate lasers.

Acknowledgments: The authors are grateful to colleagues at both the DTC Research Centre and the Diamond Research Laboratory. In particular, we thank Dr. Simon Lawson, Samantha Quinn, and Dr. Paul Spear for assistance with spectroscopy; Chris Kelly, Andy Taylor, and Mike Crowder for sample preparation and characterization; Dr. Grant Summer-ton, Dennis Welch, and Dr. Robbie Burns for assistance with HPHT annealing experiments; and Dr. Chris Welbourn for supervising the work and assisting in the preparation of the manuscript.

REFERENCES

- Anderson B.W. (1963) Absorption spectra and properties of metamict zircons. *Journal of Gemmology*, Vol. 9, No. 1, pp. 1–11.
- Brozel M.R., Evans T., Stephenson R.F. (1978) Partial dissociation of nitrogen aggregates in diamond by high temperature-high pressure treatments. *Proceedings of the Royal Society of London A*, Vol. 361, pp. 109–127.
- Chalain J.-P., Fritsch E., Hänni H.A. (1999) Detection of GE POL diamonds: A first stage. *Revue de Gemnologie a.f.g.*, No. 138/139, pp. 30–33.
- Chalain J.-P., Fritsch E., Hänni H.A. (2000) Identification of GE POL diamonds: A second step. *Journal of Gemmology*, Vol. 27, No. 2, pp. 73–78.
- Chrenko R.M., Strong H.M., Tuft R.E. (1971) Dispersed paramagnetic nitrogen content of large laboratory diamonds. *Philosophical Magazine*, Vol. 23, pp. 313–318.
- Collins A.T. (1982) Colour centres in diamond. *Journal of Gemmology*, Vol. 18, No. 1, pp. 37–75.
- Collins A.T., Kanda H., Kitawaki H. (2000) Colour changes produced in natural brown diamonds by high-pressure, high-temperature treatment. *Diamond and Related Materials*, Vol. 9, pp. 113–122.
- Dyer H.B., Raal F.A., Du Preez L., Loubser J.H.N. (1965) Optical absorption features associated with paramagnetic nitrogen in diamond. *Philosophical Magazine*, Vol. 11, No. 112, pp. 763–773.
- Evans T. (1991) Diamond—a letter from the depths. In R.G. Chambers, J.E. Enderby, A. Keller, A.R. Lang, J.W. Steeds, Eds., *Sir Charles Frank, OBE, FRS: An Eightieth Birthday Tribute*, Adam Hilger, pp. 378–406.
- Fritsch E., Scarratt K. (1992) Natural-color nonconductive gray-to-blue diamonds. *Gems & Gemology*, Vol. 28, No. 1, pp. 35–42.
- Jorge M.I.B., Pereira M.E., Thomaz M.F., Davies G., Collins A.T. (1983) Decay times of luminescence from brown diamonds. *Portugaliae Physica*, Vol. 14, pp. 195–210.
- Kiflawi I., Mayer A.E., Spear P.M., van Wyk J.A., Woods G.S. (1994) Infrared absorption by the single nitrogen and A defect centres in diamond. *Philosophical Magazine B*, Vol. 69, No. 6, pp. 1141–1147.
- Mita Y. (1996) Change of absorption spectra in type-Ib diamond with heavy neutron irradiation. *Physical Review B*, Vol. 53, No. 17, pp. 11360–11364.
- Moses T.M., Reinitz I.R. (1999) Gem Trade Lab notes: Yellow to yellow-green diamonds treated by HPHT, from GE and others. *Gems & Gemology*, Vol. 35, No. 4, pp. 203–204.
- Moses T.M., Shigley J.E., McClure S.F., Koivula J.I., Van Daele M. (1999) Observations on GE-processed diamonds: A photographic record. *Gems & Gemology*, Vol. 35, No. 3, pp. 14–22.
- Shigley J., Moses T., McClure S., Van Daele M. (1999) GIA reports on GE POL diamonds. *Rapaport Diamond Report*, Vol. 22, No. 36, October 1, p. 1 *et passim*.
- van Wyk J.A. (1982) Carbon-13 hyperfine interaction of the unique carbon of the P2 (ESR) or N3 (optical) centre in diamond. *Journal of Physics C*, Vol. 15, pp. L981–L983.
- Wilks E., Wilks J. (1991) *Properties and Applications of Diamond*. Butterworth-Heinemann, Oxford, pp. 81–82.

PURPLE TO PURPLISH RED CHROMIUM-BEARING TAAFFEITES

By Karl Schmetzer, Lore Kiefert, and Heinz-Jürgen Bernhardt

Gemological, microscopic, chemical, and spectroscopic properties are given for eight purple to purplish red chromium (Cr)- and iron (Fe)-bearing taaffeites and, for comparison, two grayish violet Fe-bearing but Cr-free samples. The eight purple to purplish red stones represent the largest sample of this extremely rare (i.e., Cr-bearing) variety of taaffeite that has been included in a single study; these taaffeites contain up to 0.33 wt.% Cr₂O₃, 2.59 wt.% FeO, and 2.24 wt.% ZnO. The purple to purplish red color is a function of the relative amounts of Fe and Cr present. Apatite and zircon crystals are common inclusions in taaffeite. Also present were healed fractures that consisted of negative crystals with multiphase fillings that contain magnesite.

In October 1945, Count Edward Charles Richard Taaffe of Dublin, Ireland, was examining a parcel of faceted gems when he noted an unusual birefringent stone with a spinel-like bluish violet color. Extensive mineralogical characterization of the sample eventually led to the description of a new mineral species, which was named *taaffeite* (pronounced "tár-fite") in honor of its discoverer

(Anderson et al., 1951). This was the first time that a new mineral species was discovered in its faceted form. The first description of a red, Cr-bearing taaffeite was published 30 years later (Moor et al., 1981; sample F of this study). Until 1981, taaffeite was one of the rarest gem materials, with only about 20 faceted samples known, all of which were believed to originate from Sri Lanka. The greater awareness of taaffeite by miners and gem dealers that followed publication of the article by Moor et al. (1981), and subsequent research by one of the present authors (Schmetzer, 1983a and b), led to the identification of hundreds of faceted taaffeites from Sri Lanka.

Because of an error in the chemical formula published in the original description by Anderson et al. (1951) as BeMgAl₄O₈ (or Be₂Mg₂Al₈O₁₆), the Cr-bearing taaffeite described by Moor et al. (1981)—with the correct formula of BeMg₃Al₈O₁₆—was initially thought to be a new mineral species. The name *taprobanite* was approved by the International Mineralogical Association (IMA) Commission on

ABOUT THE AUTHORS

Dr. Schmetzer is a research scientist residing in Petershausen, near Munich, Germany. Dr. Kiefert is a research scientist at the SSEF Swiss Gemmological Institute, Basel, Switzerland. Dr. Bernhardt is a research scientist at the Institute of Mineralogy of Ruhr University, Bochum, Germany.

Please see acknowledgments at end of article.

Gems & Gemology, Vol. 36, No. 1, pp. 50–59.

© 2000 Gemological Institute of America



Figure 1. Purple to purplish red, Cr-bearing taaffeite is a very rare gem. Six of the study samples shown here fall into this color range. The two largest show the grayish violet color that is more commonly seen in gem taaffeite; they were included in the study as comparison stones. From left to right, the samples are: G (1.23 ct), F (0.33 ct), I (1.78 ct), C (2.26 ct), A (grayish violet, 4.02 ct), H (1.04 ct), B (grayish violet, 3.17 ct), and J (0.89 ct). Photo by John Parrish.

New Minerals and Mineral Names. Later, when it was established that—ignoring trace-element contents—the chemical composition of this sample was identical to that of the first taaffeite (discovered by Count Taaffe), the IMA Commission decided that only the name *taaffeite* should be used in the future (Schmetzer, 1983a and b).

Over the past 20 years, faceted taaffeites have continued to appear in parcels of cut stones from Sri Lanka, and even some crystals have been discovered (Saul and Poirot, 1984; Kampf, 1991). Additionally, a gem-quality taaffeite from Myanmar has been mentioned (Spengler, 1983); and, recently, several samples from the Tunduru area of Tanzania were described (“Taaffeite found in Tunduru,” 1996; Burford, 1998). Nevertheless, red, pink, and purple (i.e., Cr-bearing) taaffeites are still extraordinarily rare, with only a few stones described in the literature since Moor et al. (1981). All of these have been reported from Sri Lanka: 1.25 ct (Schmetzer and Bank, 1985), 0.58 ct (Koivula and Kammerling, 1990, 1991), 0.78 and 2.59 ct (Ponahlo, 1993), and 1.07 ct (Burford, 1997).

Taaffeite is known to crystallize in metasomatized limestones or in high-grade amphibolite- or granulite-facies rocks (Kampf, 1991; Chadwick et al., 1993). The stones recovered thus far from Sri Lanka, especially the Cr-bearing samples, originate from secondary deposits, so the exact host rocks are still unknown.

Synthetic taaffeite has been grown experimentally by the floating-zone technique (Kawakami, 1983; Teraishi, 1984a), by the flux method (Teraishi,

1984b), and by flux pulling (Miyasaka, 1987). To the best of our knowledge, however, no synthetic gem material has been marketed thus far.

The present study provides a detailed description of Cr-bearing taaffeite, in response to problems associated with: (1) the distinction of faceted taaffeite from musgravite, a closely related mineral with a formula of $\text{BeMg}_2\text{Al}_6\text{O}_{12}$ that is even more rare (Demartin et al., 1993; Johnson and Koivula, 1997; Kiefert and Schmetzer, 1998); and (2) the properties of a heat-treated sample of the taaffeite-musgravite group that was found to consist of intergrown lamellar taaffeite and spinel (Schmetzer et al., 1999). Occasionally, purple to purplish red taaffeite is submitted for testing as “musgravite,” because only a few gemological descriptions of taaffeites in this color range exist. The present article attempts to fill this gap in the gemological literature.

MATERIALS AND METHODS

To determine the gemological, physical, and chemical properties of the color range known at present for Cr-bearing taaffeite, we borrowed eight rough and faceted specimens of purple-to-red taaffeite (see, e.g., figure 1). Given the rarity of this material, we believe that this is the largest group of Cr-bearing taaffeites ever made available at a single time for detailed study and comparison.

Dr. E. Gübelin generously loaned us six faceted purple-to-red taaffeites from his collection. J. Ponahlo provided a faceted reddish purple taaffeite, and P. Entremont loaned us a fragment of a purple taaffeite crystal. For comparison, we also examined

Table 1. Physical and chemical properties of the 10 sample taaffeites.^a

Property	A	B	C	D	E	F	G	H	I	J
Color										
Daylight	Grayish violet	Grayish violet	Purple	Purple	Reddish purple	Red-purple	Reddish purple	Purple-red	Purple-red	Purplish red
Incandescent light	Violet	Violet	Reddish purple	Reddish purple	Red-purple	Purple-red	Red-purple	Purplish red	Purplish red	Red
Weight/shape	4.02 ct oval	3.17 ct oval	2.26 ct pear	10.40 ct rough	2.59 ct modified pear	0.33 ct round	1.23 ct oval	1.04 ct oval	1.78 ct oval	0.89 ct oval
Size (mm)	11.3 x 7.4	9.8 x 7.3	9.2 x 7.7	14.2 x 8.5 x 8.0	8.2 x 6.4	4.0	8.1 x 5.8	5.8 x 4.1	8.6 x 6.7	6.4 x 6.1
Microscopic features	None noted	Healed fractures with two-phase (fluid/magnesite) inclusions ^{c,d} corroded magnesite crystal ^c	Healed fractures with two-phase (fluid/magnesite) inclusions ^{c,d}	Growth planes to {1123} and {1123} twin(?) plane to (0001); healed fractures with two-phase inclusions; zircon crystals ^c with tension cracks	Irregular growth boundary ^b ; growth planes to (0001); zircon crystals ^c with tension cracks; apatite crystals ^c	None noted	Healed fractures with two-phase (fluid/magnesite) inclusions ^c	Zircon crystals ^c with tension cracks; apatite crystals ^c	Zircon crystals ^c with tension cracks; apatite crystals ^c	Zircon crystals with tension cracks; healed fractures with two-phase (fluid/magnesite) inclusions
Density (g/cm ³)	3.61	3.62	3.63	3.63	3.66	3.61	3.63	3.63	3.65	3.67
Refractive indices										
n _ω	1.720	1.722	1.722	1.724	1.728	1.722	1.722	1.723	1.725	1.728
n _ε	1.716	1.718	1.718	1.720	1.722	1.718	1.718	1.719	1.720	1.722
Birefringence	0.004	0.004	0.004	0.004	0.006	0.004	0.004	0.004	0.005	0.006
Microprobe analyses (wt.%)										
Al ₂ O ₃	72.14	72.12	72.77	72.62	71.12	72.90	72.62	72.13	71.88	71.31
Ga ₂ O ₃	0.05	0.04	0.04	0.03	0.04	0.03	0.02	0.05	0.04	0.02
V ₂ O ₃	0.01	0.01	0.01	0.01	0.02	0.01	0.01	0.02	0.01	0.04
Cr ₂ O ₃	0.01	0.01	0.10	0.11	0.14 ^b	0.13	0.13	0.21	0.18	0.33
TiO ₂	0.01	0.01	0.01	0.01	0.02	0.01	0.01	0.01	0.02	0.02
MgO	21.58	20.92	20.98	19.40	19.71	20.52	20.73	20.15	19.71	18.85
FeO ^e	0.80	2.10	1.89	2.21	2.05	1.37	1.54	1.52	2.59	2.09
ZnO	0.09	0.11	0.05	0.59	2.11	0.09	0.55	1.18	0.38	2.24
MnO	0.02	0.02	0.03	0.04	0.03	0.04	0.02	0.03	0.03	0.06
BeO ^f	4.45	4.46	4.49	4.43	4.40	4.46	4.47	4.44	4.42	4.39
Total	99.15	99.80	100.37	99.45	99.64	99.56	100.10	99.74	99.26	99.35
Sum ^g	0.99	2.30	2.13	3.00	4.41	1.68	2.28	3.02	3.25	4.80
Cations ^h										
Al	7.946	7.940	7.955	8.035	7.926	8.010	7.966	7.969	7.983	7.975
Ga	0.003	0.002	0.002	0.002	0.002	0.002	0.001	0.003	0.002	0.001
V	0.001	0.001	0.001	0.001	0.002	0.001	0.001	0.002	0.001	0.003
Cr	0.001	0.001	0.007	0.008	0.011	0.010	0.010	0.016	0.013	0.025
Ti	0.001	0.001	0.001	0.001	0.001	0.001	0.001	0.001	0.001	0.001
Mg	3.006	2.913	2.901	2.715	2.778	2.852	2.876	2.815	2.768	2.666
Fe	0.063	0.164	0.147	0.174	0.162	0.107	0.120	0.119	0.204	0.166
Zn	0.006	0.008	0.003	0.041	0.147	0.006	0.038	0.082	0.026	0.157
Mn	0.002	0.002	0.002	0.003	0.002	0.003	0.002	0.002	0.002	0.005

^aAll samples are reportedly from Sri Lanka except for sample A, which is reportedly from Myanmar.

^bThis color-zoned sample contained a smaller, more intense reddish purple area with 0.26 wt.% Cr₂O₃; the larger, lighter area contained 0.14 wt.% Cr₂O₃. The Cr content of this sample given in the original article by Ponahlo (1993) was found to be erroneous; a later analysis by X-ray fluorescence gave an average composition of 0.19 wt.% Cr₂O₃ (J. Ponahlo, pers. comm., 1999), which is consistent with our analyses of this zoned sample.

^cIdentified by Raman analysis.

^dIdentified by electron microprobe analysis.

^eTotal iron as FeO.

^fCalculated for 1 BeO per formula unit; for the theoretical composition of taaffeite (BeMg₃Al₆O₁₆) an amount of 4.52 wt.% BeO is required (beryllium is not detectable by microprobe analysis).

^gSum = sum of minor and trace elements (wt.%) calculated as (Ga₂O₃+V₂O₃+Cr₂O₃+TiO₂+FeO+ZnO+MnO).

^hCalculated on the basis of 16 oxygens assuming Be = 1.000.

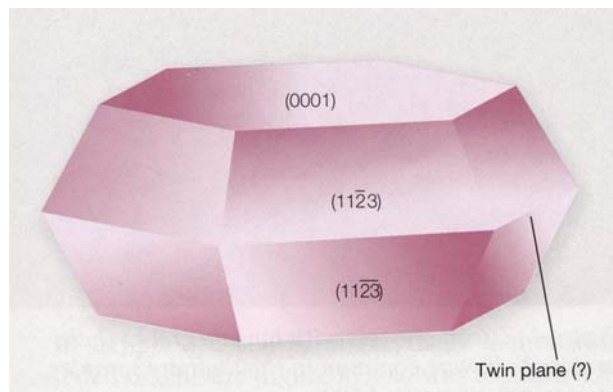


Figure 2. Growth structure analysis was used to extrapolate the crystal morphology of the water-worn purple taaffeite crystal fragment (sample D). The original crystal had basal $\{0001\}$ and pyramidal $\{11\bar{2}3\}$ faces; the sample is probably twinned on (0001) , along an equatorial twin plane.

two grayish violet faceted taaffeites, one of which was very light colored (again, see figure 1). These two samples represent the color typically seen in taaffeite. A complete description of these 10 stones is provided in table 1.

Nine of the 10 samples reportedly originated from Sri Lanka (taaffeites B to J), with one from Myanmar (sample A). All were tested by standard gemological methods for optical properties, fluorescence, and density. We examined the inclusions and internal growth patterns by standard microscopic techniques using different gemological microscopes and lighting conditions. Solid inclusions were identified with a Renishaw laser Raman microspectrometer and, for two faceted samples with inclusions exposed on the surface, by electron microprobe (see below). For those few inclusions that yielded no useful Raman spectra, identification was accomplished by direct comparison with known inclusions of similar appearance that were determined by analytical means in other taaffeites of our study.

For all samples, UV-visible spectra were recorded with a Leitz-Unicam SP 800 spectrophotometer. To determine quantitative chemical composition, we used a Cameca Camebax SX 50 electron microprobe, with one or two traverses of 50 point analyses each, measured across the tables of the nine faceted stones and across a polished window almost parallel to the basal plane of the rough taaffeite sample.

RESULTS

Visual Appearance and Gemological Properties. The rough taaffeite was a water-worn fragment of a crystal that was originally much larger. The sample had one basal termination, which revealed an irregularly stepped surface structure similar to that described by Kampf (1991) for taaffeite crystals from Sri Lanka. On the opposite side, parallel to the basal plane (0001) , a flat face had been polished in Sri Lanka for the measurement of refractive indices. Only one positive and one negative hexagonal pyramidal face were present. Because of the water-worn nature of the sample, it was impossible to determine the hexagonal pyramids directly by goniometric measurements.

However, when this sample was immersed in methylene iodide and examined in one particular orientation, growth planes parallel to one positive and one negative hexagonal dipyramid were visible. The angle between these two faces was measured at 50° , with an accuracy of $\pm 2^\circ$. From this, we determined that the hexagonal pyramids were $(11\bar{2}3)$ and $(11\bar{2}\bar{3})$, respectively, which requires an angle of 51.34° , and we could extrapolate that the original crystal appeared as pictured in figure 2. This morphology is different from that of other water-worn taaffeite samples from Sri Lanka, for which the main hexagonal pyramids were determined by Kampf (1991) as $\{11\bar{2}4\}$ and $\{11\bar{2}2\}$ (based on theoretical angles of 65.30° and 35.52° , respectively).

At the intersection of the $(11\bar{2}3)$ and $(11\bar{2}\bar{3})$ faces of our rough sample was a small groove, which corresponded to an internal (0001) plane within the complete crystal. This plane appeared slightly reflective in the microscope and is probably a twin plane, with the crystal twinned by reflection on a basal (0001) plane.

All samples revealed a small shift of color between day (or fluorescent) light and incandescent light (table 1). The seven Cr-bearing samples (C to J) ranged from purple to purplish red in daylight and from reddish purple to red in incandescent light (again, see figure 1). The two nearly Cr-free samples (A and B) were grayish violet to violet; taaffeite A was light colored. (Note that in this article, the daylight color is used when describing the samples.) Pleochroism in Cr-free samples was absent (taaffeite A) or extremely weak (taaffeite B); in all Cr-bearing samples, pleochroism was weak to moderate with a light pink to pinkish red seen parallel to the c-axis and a more intense purple, reddish purple, or purplish red visible perpendicular to c. All

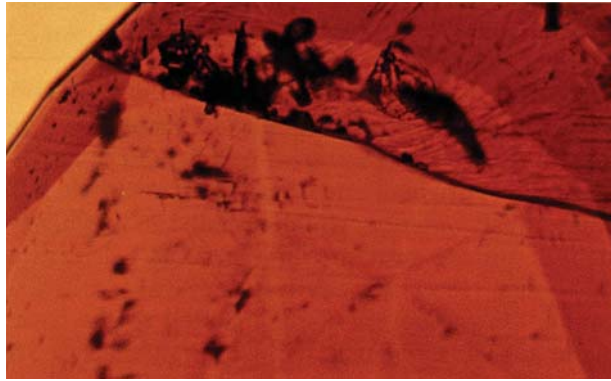


Figure 3. An irregular growth boundary in this reddish purple taaffeite (sample E) separates a lighter from a more intensely colored area of the stone. Immersion, magnified 60 \times .

the taaffeites were inert to long- and short-wave ultraviolet radiation.

The refractive indices varied from 1.716–1.720 and 1.722–1.728, with a birefringence between 0.004 and 0.006; the light-colored nearly Cr-free sample had the lowest R.I. values. The density values ranged from 3.61 to 3.67 g/cm³ (table 1). The correlation of the chemical composition with refractive index and density will be described below.

Features Seen with the Microscope. Microscopic properties of the 10 taaffeites examined in this study are described below and summarized in table 1.

Structural Features. Only two samples revealed growth patterns. The rough sample (D) was described above. In sample E we saw a series of growth planes parallel to the basal plane {0001}, as well as an irregular growth boundary separating a lighter from a more intensely colored area of the stone (figure 3; see also table 1 for chemical zoning).

Figure 5. Rounded, transparent apatite crystals were noted in three of the taaffeite samples. Sample H; magnified 50 \times .

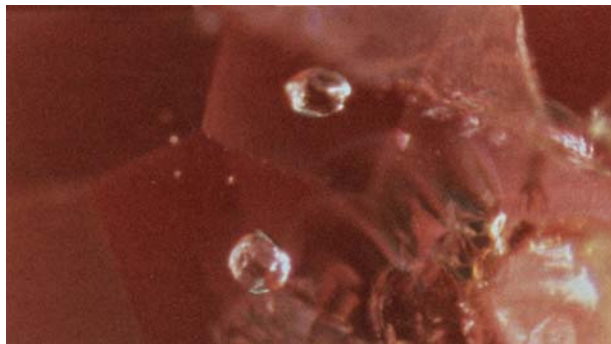


Figure 4. Zircon crystals with tension cracks (here, in sample I) were common in the taaffeite samples. Immersion, magnified 100 \times .

Inclusions. Five samples contained numerous zircon inclusions surrounded by tension cracks (see, e.g., figure 4). In addition, many small, somewhat rounded apatite crystals were found in three stones (see, e.g., figure 5).

The most characteristic inclusions—present in five of the 10 taaffeite samples—were healed fractures that usually consisted of numerous elongated negative crystals with multiphase fillings (figure 6). Examination with crossed polarizers revealed a solid birefringent mineral in each cavity (figure 7). Microprobe analysis of some of these tiny crystals revealed only the presence of magnesium. Raman analysis proved that these inclusions are magnesite (MgCO₃) crystals. Analyses of numerous inclusions in three samples consistently identified only magnesite. Consequently, we do not believe that other carbonates, such as dolomite or calcite, are present. (For the distinction of different carbonates by Raman analysis, see Herman et al., 1985, 1987; Gillet et al., 1993.)

Figure 6. Healed fractures in the taaffeite samples typically appeared as groups of negative crystals with multiphase fillings. Sample G; magnified 200 \times .



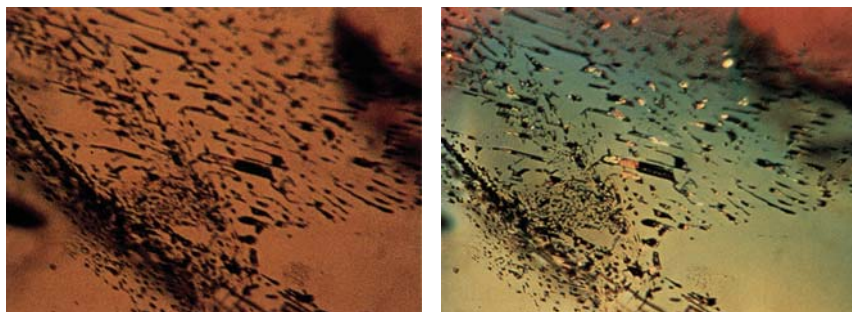


Figure 7. Healed fractures in taaffeite have been noted in the literature, but without identifying the the solid phase in the negative crystals as magnesite. Left: the healed fractures with standard illumination. Right: tiny birefringent crystals are visible in the negative crystals with crossed-polarized light. Immersion, magnified 80 \times .

In sample B, a comparatively large inclusion of corroded magnesite (figure 8) also was identified by Raman analysis. We were not able to identify some small black particles included in a few of the taaffeites.

Chemical Properties. As reported in table 1, the microprobe analyses proved that nine samples were more or less homogeneous in composition. Only sample E revealed a chemical zoning of its Cr contents, which is consistent with its color zoning (again, see figure 3).

All of the samples contained iron (0.80–2.59 wt.% FeO) and widely varying concentrations of zinc (0.05–2.24 wt.% ZnO). Samples A and B were essentially Cr-free, and the remaining eight taaffeites revealed 0.10–0.33 wt.% Cr₂O₃. Only trace amounts of gallium, titanium, vanadium, and manganese were detected.

The cation proportions of (Mg+Fe+Zn+Mn) : (Al+Ga+V+Cr+Ti) were always close to the theoretical ratio of 3:8 (see table 1). These results clearly indicate that all samples were taaffeite, rather than musgravite (which has a corresponding theoretical ratio of 2:6).

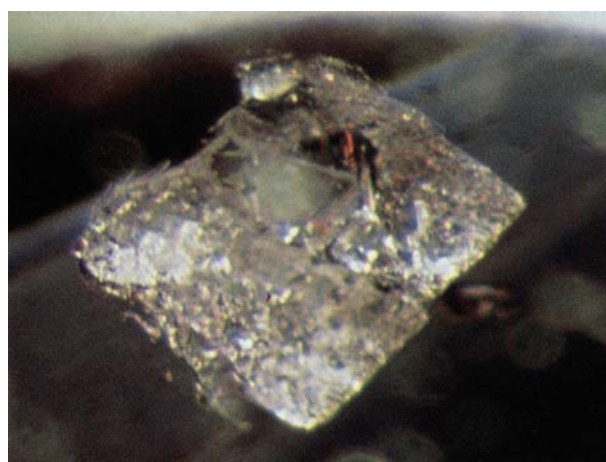
A plot of the minor- and trace-element concentrations (calculated as the sum of Ga₂O₃, V₂O₃, Cr₂O₃, TiO₂, FeO, ZnO, and MnO) versus refractive index and density is shown in figure 9. Both of these properties rise as the trace-element contents increase. The R.I. and S.G. values were mainly influenced by Fe and Zn, which were the predominant elements that are not present in the pure mineral.

Spectroscopic Properties. The absorption spectra of all the Fe- and Cr-bearing taaffeites (samples C to J) consisted of the basic iron absorption spectrum of Cr-free taaffeite (e.g., samples A and B), over which were superimposed the absorption bands of Cr³⁺ (figure 10; for the assignment of absorption bands, see table 2). The absorption spectra of Fe-bearing taaffeite samples A and B are consistent with those

described by Schmetzer (1983a) and Bank and Henn (1989), as well as with the spectra of about 20 grayish violet to violet taaffeites from Sri Lanka measured over time by one of the authors (KS, unpublished data). In Cr-bearing taaffeites, the spectral features appear to be related to the Fe:Cr ratio of the sample. In those samples with high Fe and low Cr (C, D, and E), the iron spectrum was dominant. In samples with distinctly lower Fe contents (F and G) and/or with higher Cr concentrations (H, I, and J), the chromium-related absorption bands were stronger, or dominant throughout the entire absorption spectrum.

Unfortunately, we could not obtain any Cr-bearing taaffeites that were completely Fe-free, so a pure spectrum of chromium in taaffeite was not observed. Taaffeite spectra, however, are similar to the absorption spectra of Fe- and/or Cr-bearing spinels (Schmetzer, 1983a). Consequently, the characteristics of spinel absorption spectra can be helpful for interpreting the absorption features of

Figure 8. This corroded magnesite crystal was observed in sample B. The rhombohedral habit of the crystal is clearly visible. Photomicrograph by H. A. Hänni; magnified 100 \times .



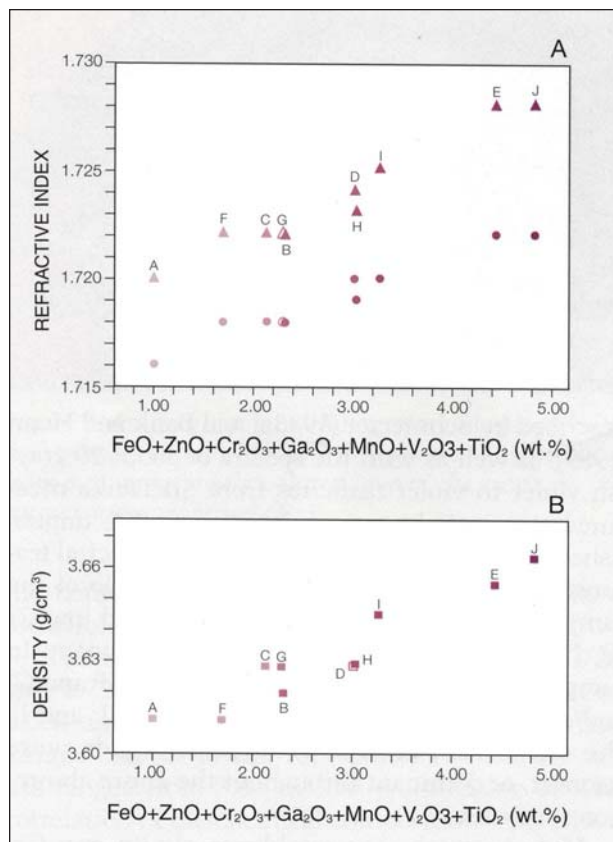


Figure 9. Refractive index (A) and density (B) values are plotted against the sum of the minor- and trace-element contents for all 10 taaffeite samples studied (see table 1). With significant increases in the sums of these elements, we recorded higher R.I. ($\blacktriangle = n_o$, $\bullet = n_e$) and density values.

taaffeite (see table 2; Schmetzer et al., 1989). Specifically, the strong absorption band in the 545 nm range is assigned to Cr^{3+} , and a second strong chromium absorption band should be present in the 400 nm range. In Cr-bearing taaffeite, however, this band is evidently superimposed by iron-related absorption maxima (figure 10). All other absorption bands in the taaffeite spectra are assigned to iron. A more detailed assignment of the taaffeite absorption features is impossible without further study (e.g., Mössbauer spectroscopy).

The variability in the taaffeite spectra can be attributed to the contents of Fe and Cr in the individual samples (table 1). For samples C, D, and E—which have relatively low Cr contents and high Fe contents (table 1)—the iron spectrum is dominant. For samples F and G—with Cr contents in the same range, but distinctly lower Fe concentrations—the chromium bands are stronger. For samples H and J—which have higher amounts of Cr, and moderate

Fe contents—the chromium bands are dominant. The spectrum of sample I is intermediate between the last two types of spectra mentioned.

The pleochroism in the eight Cr-bearing samples (C to J) correlates with the absorption at slightly different peak positions at orientations parallel and perpendicular to the c-axis. It is also related to the variable intensity of the chromium absorption band in the yellow to green spectral range (i.e., 500–600 nm; again, see figure 10).

DISCUSSION

The most characteristic internal feature of the nine taaffeites from Sri Lanka were healed fractures consisting of negative crystals, with magnesite as a solid component of the multiphase fillings. Healed fractures with the same visual characteristics frequently have been reported in taaffeite from Sri Lanka (Liddicoat, 1967; Fryer, 1982; Gunawardene, 1984a and b; McDowell, 1984; Bank and Henn, 1989; Kampf, 1991). However, in our samples we did not identify spinel in any of the multiphase inclusions, as was described by Gunawardene (1984a and b).

Apatite and zircon crystals were common. Apatite inclusions in taaffeite have been mentioned by various authors (Koivula, 1980, 1981; Gunawardene, 1984a and b; Gübelin and Koivula, 1986; Kampf, 1991; Burford, 1997). Zircon was observed by Kampf (1991) and Burford (1997). Another mineral, surrounded by tension cracks, was described by Gübelin and Koivula (1986). Although this inclusion was identified as monazite by analytical means (E. Gübelin, pers. comm., 1998), Raman analysis did not reveal monazite in any of the 10 samples we studied. Black inclusions also have been mentioned by various authors, and described as uraninite or graphite (Bank and Henn, 1989; Koivula and Kammerling, 1990, 1991; Kampf, 1991). However, we could not identify the small black inclusions seen in some of our samples. Although phlogopite inclusions have been described by various authors (Gunawardene, 1984a and b; Gübelin and Koivula, 1986; Bank and Henn, 1989), we did not observe this mineral in any of the sample taaffeites.

Our chemical analyses of the eight purple to purplish red taaffeites expand the compositional range that was previously reported for taaffeites from Sri Lanka (Schmetzer, 1983a and b; Schmetzer and Bank, 1985; Bank and Henn, 1989; Ponahlo, 1993). The highest Fe content measured to date for Sri Lankan taaffeite was in sample I of this study (2.59 wt.% FeO). The highest Zn content reported thus far

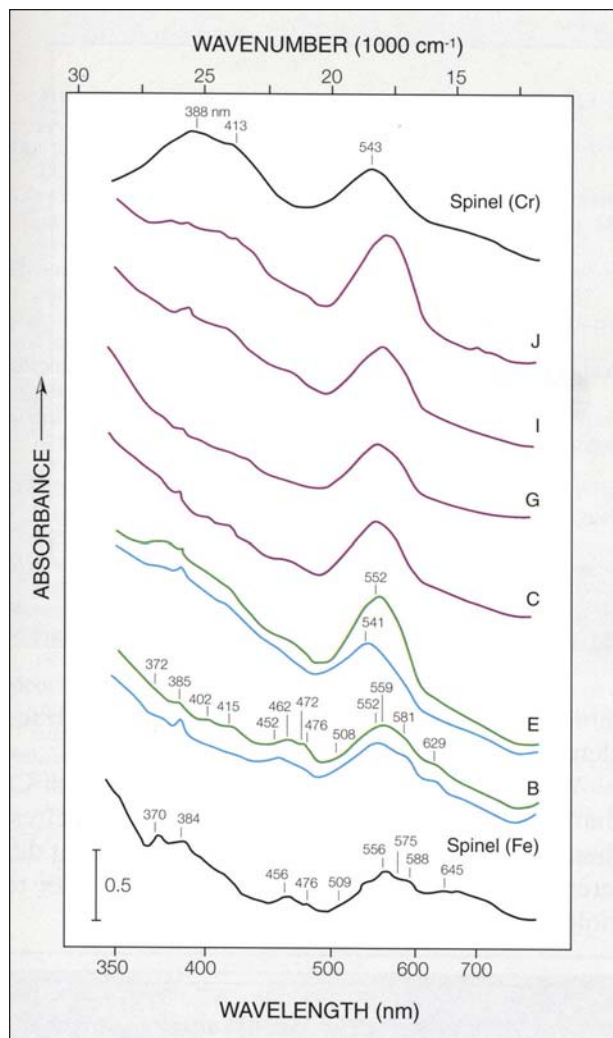


Figure 10. These absorption spectra of Fe- and Cr-bearing taaffeites from Sri Lanka (samples E, C, G, I, and J) show distinct features when compared with Cr-free taaffeite (sample B). All spectra are unpolarized except for samples B and E (green line = perpendicular to the c-axis, blue line = parallel to the c-axis). Two absorption spectra for spinel are shown for comparison: (top) a Cr-bearing, Fe-free red spinel from Mogok, Myanmar; (bottom) an Fe-bearing, Cr-free bluish violet spinel from Sri Lanka.

(4.66 wt.% ZnO) was in a sample with refractive indices of 1.726–1.730 (Schmetzer and Bank, 1985). It is probable that the taaffeite described by Burford (1997), with refractive indices of 1.725–1.730, is also a high Fe- and/or Zn-bearing sample. The highest Cr content reported so far was in the purplish red taaffeite in this study (sample J, with 0.33 wt.% Cr₂O₃). Unfortunately, no chemical or spectroscopic data are available for the deep red taaffeite described by Koivula and Kammerling (1990, 1991).

The color of Cr-bearing taaffeite is a function of the Cr and Fe contents (figure 11). Samples C, D, and E—which have relatively high Fe and low Cr concentrations—are purple or reddish purple in daylight. Taaffeites F and G, which contain similar amounts of Cr, but lower levels of Fe, are reddish purple or red-purple. Samples H, I, and J—which have higher Cr contents and various amounts of Fe—are purple-red to purplish red (for the designation of colors, see the hue circle on p. 256 of the Winter 1998 issue of *Gems & Gemology*).

All the Cr-bearing samples revealed a strong chromium-iron absorption band, with a maximum in the greenish yellow region around 545 nm (figure 10) and two minima in the red and blue regions (see also Bank and Henn, 1989). These spectral features are similar to those of minerals that reveal a distinct color-change between daylight and incandescent light (Schmetzer et al., 1980). However, the absorption maximum at about 545 nm in taaffeite is found at a somewhat lower wavelength than the absorption maximum (i.e., between 562 and 578 nm) in minerals that show an alexandrite-like color change, such as chrysoberyl, garnet, sapphire, spinel, kyanite, and diaspore. Thus, only a slight change of color between daylight and incandescent light is observed in taaffeite (see table 1).

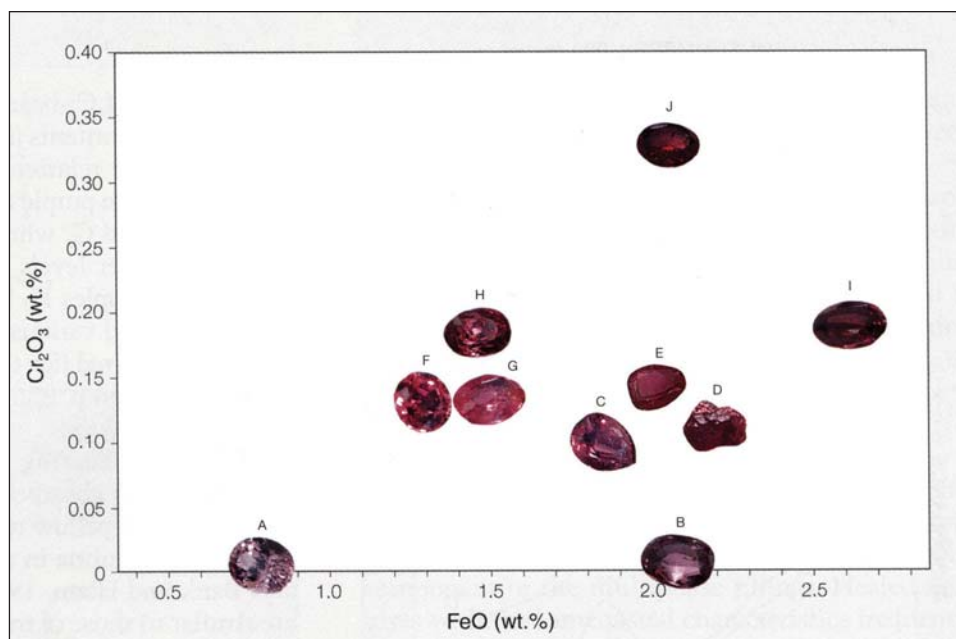
TABLE 2. Spectroscopic properties of iron- and chromium-bearing taaffeite and spinel.

Taaffeite absorption maxima (nm)		Spinel absorption maxima (nm) ^a	Assignment
c	⊥c		
541	552	543	Chromium ^b
Superimposed by iron absorption bands	Superimposed by iron absorption bands	413	
		388	
629	629	645	Iron
581	581	588	
		575	
552	559	556	
	508	509	
476	472	476	
452	462	456	
415	415		
	402		
385	385	384	
372	372	370	

^aFrom Schmetzer et al. (1989).

^bA sharp chromium line was observed in taaffeite sample J at 687 nm, which is identical with the R emission line of Cr³⁺ measured by Ponahlo (1993) in the cathodoluminescence spectrum of Cr-bearing taaffeite; the R line is observed in the absorption spectrum of spinel at 683 nm (Sviridov et al., 1973).

Figure 11. Color in Fe- and Cr-bearing taaffeites is related to their chemical composition. With increasing Cr and decreasing Fe, the red color component of the purple to purplish red stones is intensified. Note: size of samples not to scale.



CONCLUSIONS

Although this study of nine taaffeites from Sri Lanka and one from Myanmar did not reveal any inclusion that was specific to Cr-bearing samples as compared to grayish violet or violet Cr-free taaffeites, it did confirm the presence of internal features such as zircon, apatite, and healed fractures with tiny magnesite crystals (as solid components of multiphase inclusions), which are common for samples from Sri Lanka. The absorption spectra of Cr- and Fe-bearing samples are similar to those of Cr- and Fe-containing spinels. The color of the purple to purplish red samples is a function of the

relative amounts of the two color-causing trace elements, Cr and Fe.

With the exception of the small amounts of Cr that add a red color component to the taaffeites, there does not appear to be any other significant difference from the more common grayish violet to violet samples examined to date.

Acknowledgments: For the loan of samples used in this study, the authors are grateful to Prof. Dr. E. Gübelin of Lucerne, Switzerland; Dr. J. Pohnhlo of Vienna, Austria; and P. Entremont of Paris, France.

REFERENCES

- Anderson B.W., Payne C.J., Claringbull G.F., Hey M.H. (1951) Taaffeite, a new beryllium mineral, found as a cut gem-stone. *Mineralogical Magazine*, Vol. 29, pp. 765–772.
- Bank H., Henn U. (1989) Changierender Taaffeit aus Sri Lanka. *Zeitschrift der Deutschen Gemmologischen Gesellschaft*, Vol. 38, No. 2/3, pp. 89–94.
- Burford M. (1997) Two zirconian rarities. *Canadian Gemmologist*, Vol. 18, No. 4, pp. 105–110.
- Burford M. (1998) Gemstones from Tunduru, Tanzania. *Canadian Gemmologist*, Vol. 19, No. 4, pp. 108–110.
- Chadwick B., Friend C.R.L., George M.C., Perkins W.T. (1993) A new occurrence of musgravite, a rare beryllium oxide, in the Caledonides of north-east Greenland. *Mineralogical Magazine*, Vol. 57, pp. 121–129.
- Demartin F., Pilati T., Gramaccioli C.M., de Michele V. (1993) The first occurrence of musgravite as a faceted gemstone. *Journal of Gemmology*, Vol. 23, No. 8, pp. 482–485.
- Fryer C., Ed. (1982) Gem Trade Lab notes: World's largest taaffeite? *Gems & Gemology*, Vol. 18, No. 1, p. 49.
- Gillet P., Biellmann C., Reynard B., McMillan P. (1993) Raman spectroscopic studies of carbonates. Part I: High-pressure and high-temperature behaviour of calcite, magnesite, dolomite and aragonite. *Physics and Chemistry of Minerals*, Vol. 20, No. 1, pp. 1–18.
- Gübelin E.J., Koivula J.I. (1986) *Photoatlas of Inclusions in Gemstones*. ABC Edition, Zurich, pp. 174, 426.
- Gunawardene M. (1984a) Inclusions in taaffeites from Sri Lanka. *Gems & Gemology*, Vol. 20, No. 3, pp. 159–163.
- Gunawardene M. (1984b) Die innere Paragenese von Taaffeiten aus Sri Lanka. *Zeitschrift der Deutschen Gemmologischen Gesellschaft*, Vol. 33, No. 3/4, pp. 91–95.
- Herman R.G., Bogdan C.E. (1985) Laser Raman microprobe study of the identification of some carbonate and aluminosilicate minerals. *Materials Science Research, Advanced Materials Characterization 2*, Vol. 19, pp. 113–130.
- Herman R.G., Bogdan C.E., Sommer A.J., Simpson D.R. (1987) Discrimination among carbonate minerals by Raman spectroscopy using the laser microprobe. *Applied Spectroscopy*, Vol. 41, No. 3, pp. 437–440.
- Johnson M.L., Koivula J.I., Eds. (1997) *Gem News—Musgravite:*

- A rarity among the rare. *Gems & Gemology*, Vol. 33, No. 2, pp. 145–147.
- Kampf A.R. (1991) Taaffeite crystals. *Mineralogical Record*, Vol. 22, No. 5, pp. 343–347.
- Kawakami S. (1983) *Manufacture of Single Crystal of Taaffeite* [in Japanese]. Japanese Patent Application, open-laid No. 58-55396, April 1.
- Kiefert L., Schmetzer K. (1998) Distinction of taaffeite and musgravite. *Journal of Gemmology*, Vol. 26, No. 3, pp. 165–167.
- Koivula J.I. (1980–1981) Gübelin identifies apatite in taaffeite. *Gems & Gemology*, Vol. 16, No. 12, pp. 409.
- Koivula J.I., Kammerling R.C., Eds. (1990) Gem news: Red taaffeite. *Gems & Gemology*, Vol. 26, No. 1, pp. 102–103.
- Koivula J.I., Kammerling R.C. (1991) Gemological examination of a red taaffeite. *Zeitschrift der Deutschen Gemmologischen Gesellschaft*, Vol. 40, No. 1, pp. 33–37.
- Liddicoat R.T., Jr. (1967) Developments and highlights at the Gem Trade Lab in Los Angeles: Taaffeite proves largest. *Gems & Gemology*, Vol. 12, No. 7, pp. 212–215.
- McDowell R.B. (1984) A recent find of taaffeite. *Journal of Gemmology*, Vol. 19, No. 1, pp. 9–13.
- Miyasaka H. (1987) *Production of Taaffeite Single Crystal* [in Japanese]. Japanese Patent Application, open-laid No. 62-187200, August 15.
- Moor R., Oberholzer W.F., Gübelin E. (1981) Taprobanite, a new mineral of the taaffeite-group. *Schweizerische Mineralogische und Petrographische Mitteilungen*, Vol. 61, pp. 13–21.
- Ponahlo J. (1993) Kathodolumineszenz (KL) und KL-Spektren von Edelsteinen (Ausgewählte Beispiele) Teil II. *Zeitschrift der Deutschen Gemmologischen Gesellschaft*, Vol. 42, No. 4, pp. 149–162.
- Saul J., Poirot J.-P. (1984) Le premier cristal de taaffeite gemme? *Revue de Gemmologie a.f.g.*, No. 78, p. 28.
- Schmetzer K. (1983a) Crystal chemistry of natural Be-Mg-Al-oxides: taaffeite, taprobanite, musgravite. *Neues Jahrbuch für Mineralogie Abhandlungen*, Vol. 146, No. 1, pp. 15–28.
- Schmetzer K. (1983b) Taaffeite or taprobanite—a problem of mineralogical nomenclature. *Journal of Gemmology*, Vol. 18, No. 7, pp. 623–634.
- Schmetzer K., Bank H. (1985) Zincian taaffeite from Sri Lanka. *Journal of Gemmology*, Vol. 19, No. 6, pp. 494–497.
- Schmetzer K., Bank H., Gübelin E. (1980) The alexandrite effect in minerals: Chrysoberyl, garnet, corundum, fluorite. *Neues Jahrbuch für Mineralogie Abhandlungen*, Vol. 138, No. 2, pp. 147–164.
- Schmetzer K., Bernhardt H.-J., Medenbach O. (1999) Heat-treated Be-Mg-Al oxide (originally musgravite or taaffeite). *Journal of Gemmology*, Vol. 26, No. 6, pp. 353–356.
- Schmetzer K., Haxel C., Amthauer G. (1989) Colour of natural spinels, gahnospinel and gahnites. *Neues Jahrbuch für Mineralogie Abhandlungen*, Vol. 160, No. 2, pp. 159–180.
- Spengler W. (1983) Burmese parcel reveals rare find. *Jewellery News Asia*, Vol. 1, No. 1, p. 39.
- Sviridov D.T., Sevastyanov B.K., Orekhova V.P., Sviridova R.K., Veremeichik T.F. (1973) Optical absorption spectra of excited Cr³⁺ ions in magnesium spinel at room and liquid nitrogen temperatures. *Optics and Spectroscopy*, Vol. 35, No. 1, pp. 59–61.
- Taaffeite found in Tunduru (1996) *Jewellery News Asia*, No. 142, p. 58.
- Teraishi K. (1984a) *Taaffeite Mineral Crystal* [in Japanese]. Japanese Patent Application, open-laid No. 59-137391, August 7.
- Teraishi K. (1984b) *Synthesis of Artificial Taaffeite Single Crystal* [in Japanese]. Japanese Patent Application, open-laid No. 59-141484, August 14.



Calling All GIA Gemologists, Graduate Gemologists,
Graduate Jewelers and Graduate Jeweler Gemologists

You are invited to attend

GIA's Commencement 2000

A formal graduation ceremony held in your honor

Saturday, June 10, 2000

3:00 PM

GIA's Robert Mouawad Campus
Carlsbad, California, USA

Please join fellow graduates from GIA's international campuses and distance education programs in a celebration of your achievement. Festivities will include a gala reception and dinner dance, class reunions and a host of activities in keeping with this auspicious occasion.

To receive a formal invitation,
or for more information, please call:

800-421-7250 ext. 4321

Outside U.S. and Canada:

760-603-4321 Fax: 760-603-4456

E-mail: grad2000@gia.edu

Or visit our website at www.gia.edu.



Editors

Thomas Moses, Ilene Reinitz, and
Shane F. McClure
GIA Gem Trade Laboratory

Contributing Editors

G. Robert Crowingshield
GIA Gem Trade Laboratory, East Coast
Karin Hurwit, Mary L. Johnson,
and Cheryl Y. Wentzell
GIA Gem Trade Laboratory, West Coast

DIAMONDS**Chameleon, with Blue-to-Violet
"Transmission" Luminescence**

Chameleon diamonds are popular with colored-diamond collectors primarily for two reasons. First, these diamonds, which range from greenish gray or brownish greenish yellow to yellowish green, with medium-to-dark tones and moderate to high saturation (figure 1), are among that fraction of colored diamonds for which the green component can be determined to be of natural origin. Second, chameleon diamonds show photochromic and thermo-chromic behavior; that is, they change to a yellow to orangy yellow color when held in darkness for a few days or gently

heated. The original greenish color returns after less than one minute of exposure to light or on cooling to room temperature.

Both labs regularly see chameleon diamonds, and we described a particularly large one, a 22.28 ct heart brilliant, in this section in 1992 (Gem Trade Lab Notes, Summer 1992, p. 124). This past winter the East Coast lab examined several examples with strong blue-to-violet luminescence to visible light (violet "transmission"), a gemological property that is uncommon in such diamonds. Chameleon diamonds typically show a number of diagnostic properties: a moderate to strong absorption line at 415 nm, and a weak one at 425 nm, in a desk-

model spectroscope; and moderate to very strong yellow fluorescence—with strong, persistent yellow phosphorescence, often lasting more than 60 seconds—to both long- and short-wave UV. There is usually no observable luminescence to strong visible light. When a diamond in the color range described above shows these properties, it is safe to test it for thermochromic behavior to complete the identification. (Diamonds of greenish color that do not show a line at 425 nm and strong, persistent phosphorescence may have their color permanently altered by heating.)

A 0.74 ct Fancy Dark gray–yellowish green marquise (figure 1, top) first focused our attention on this unusual property. While examining its reaction to long-wave UV, we observed clouds of blue fluorescence mixed with the typical yellow, as well as strong, long-lasting yellow phosphorescence; it exhibited a yellow fluorescence and phosphorescence to short-wave UV, which is typical for chameleon diamonds. The violet transmission luminescence that appeared when the stone was placed on the base of our desk-model spectroscope was quite striking. It was unevenly distributed, forming a wedge on one side and a stripe on the other. Although this property was atypical, the others, including a 425 nm line seen with the desk-model



Figure 1. These two diamonds, 0.74 (top) and 31.10 ct, are typical of the yellowish green to greenish yellow colors seen in chameleon diamonds.



Editor's note: The initials at the end of each item identify the editor(s) or contributing editor(s) who provided that item.

Gems & Gemology, Vol. 36, No. 1, pp. 60–65
©2000 Gemological Institute of America

spectroscope, indicated a chameleon diamond, and we observed a good color change to orangy yellow on gentle heating with an alcohol lamp.

We saw a more striking example a few weeks later, a 31.10 ct Fancy Dark gray–greenish yellow oval modified brilliant (figure 1, bottom). This stone also fluoresced yellow with blue clouds to long-wave UV, with the typical phosphorescence and reaction to short-wave UV. Over the base of the desk-model spectroscope, it displayed strong blue-to-violet transmission with weak orange areas (figure 2). This chameleon diamond showed a strong color change to orangy yellow; it took several minutes to heat up and cool down because of its large size.

Valerie Chabert and IR

With Evidence of Another New Diamond Treatment

At the recent Tucson shows, John Haynes of InColor Diamonds, a long-time acquaintance of the GIA Gem Trade Laboratory, loaned us nine samples that showed evidence of yet another new diamond treatment. The treated polished diamonds include both black and green colors and ranged from 0.05 to 1.38 ct (see, e.g., figure 3).

The “black” diamonds appeared opaque black when examined over diffused light, but were actually very dark brown and semi-transparent to transparent when viewed with a fiber-optic illuminator. In reflected light, the faceted surfaces showed high luster, which appeared metallic and yellowish brown on the table facet. Although the abundant inclusions of natural-color black diamonds typically lead to poor polish, these samples revealed an uneven surface texture, even between fractures. When we looked through the pavilion at the table of the most transparent stone, we observed many fine dark brown spots surrounded by lighter brown areas. However, when we viewed it with Nomarski differential interference contrast microscopy (described by J. H. Richardson on pp. 243–256 of *Handbook for the Light Microscope*,

Noyes Publications, Park Ridge, New Jersey, 1991; see also figures 6–8, pp. 194–195 of the Winter 1987 *Gems & Gemology*), we noted deep polishing lines and subtle traces of a very thin material at the surface. There was no reaction to either long- or short-wave UV, and a synthetic sapphire point (hardness 9) did not scratch the surfaces of the stones. We recorded moderate to strong electrical conductivity.

The green samples showed a very slight unevenness of color. When the stones were observed over diffuse transmitted light, immersed in methylene iodide, the color appeared strongest around the girdle and along the pavilion facets. These diamonds, too, showed a metallic luster in reflected light (on all facets). With darkfield illumination, they revealed a highly distinctive feature: a display of iridescent colors along the facets of the pavilion that were seen easily near the culet (figure 4). While such iridescence also suggests a surface coating, Nomarski microscopy showed only polishing lines on these diamonds; again, the 9 hardness point did not scratch them. The reactions of the different diamonds to ultraviolet radiation ranged from inert to moderate blue to long-wave UV, and from inert to weak yellow or blue to short-wave UV. All the green samples showed a 415 nm line in the handheld spectroscope, which confirmed that they were natural diamond.

Infrared spectroscopy showed that all the samples, green and black,



Figure 2. The 31.10 ct chameleon diamond showed strong blue-to-violet and weak orange transmission luminescence to the strong visible light of a desk-model spectroscope.

were type Ia diamond with varying amounts of nitrogen at various aggregation states. Visible spectra of the green samples showed the Cape lines typical of natural yellow diamonds, with a peak at 741 nm that indicated that they had been exposed to ionizing radiation. None of the samples showed any residual radioactivity.

To continue the characterization, we turned next to energy-dispersive X-ray fluorescence (EDXRF) analysis, as well as to laser Raman microspectrometry of the surface of the diamonds. No elements were detected with EDXRF, but the Raman spectra gave some interesting results. The spectra of the green samples showed a sharp peak at 1330 cm^{-1} , and features at 2459 cm^{-1} and 2666 cm^{-1} , characteristic of diamond itself; a peak at 773 cm^{-1} was observed in one sample,

Figure 3. New diamond treatments produced the black and green colors of these round brilliants, which range from 0.08 to 0.23 ct.



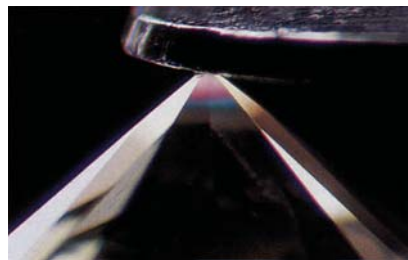


Figure 4. Bright iridescence, seen here with darkfield illumination reflected in the culet of a 0.18 ct round brilliant, is a characteristic property of the treated-color green diamonds shown in figure 3. Magnified 20 \times .

suggesting a possible carbide compound. The black diamonds showed a similar sharp peak at 1330 cm^{-1} , but also a broad peak centered at 1500 cm^{-1} , which indicates the presence of diamond-like carbon (DLC). The experimental use of DLC to coat gemstones other than diamond was reported in the Fall 1991 Gem News section (p. 186).

Examination of more samples, further testing, and discussion with the developer of the treatment will be

needed before we fully understand how these diamonds have been treated. However, the unusual aspects of their appearance make them straightforward to identify as treated.

*IR, John I. Koivula,
Shane Elen, Peter Buerki,
and Sam Muhlmeister*

Light Blue Synthetic

Early this year, three pale blue round brilliants, which weighed 0.10, 0.14, and 0.21 ct (figure 5), were submitted to the East Coast lab for colored diamond identification and origin-of-color reports. In this case, the identification portion of this service proved to be more essential than finding the cause of (or grading) the blue color.

When examined with magnification, two of the three stones displayed large metallic inclusions (figure 6) that appeared similar to the flux inclusions seen in the earliest blue synthetic diamonds from the General Electric Company (see G. R. Crowningshield, "General Electric's cuttable synthetic diamonds," *Gems & Gemology*, Summer 1971, pp. 302–314). The third diamond showed an unusual opaque cloud (figure 7), along with pinpoint-like inclusions arranged somewhat randomly throughout the

stone. Such pinpoints have been observed in yellow synthetic diamonds (J. E. Shigley et al., "The gemological properties of the De Beers gem-quality synthetic diamonds," *Gems & Gemology*, Winter 1987, pp. 187–206).

All three diamonds showed a very weak reaction to long- and short-wave UV radiation, but all did phosphoresce a moderate to strong yellow for longer than two minutes to both wavelengths. They also showed orangy yellow phosphorescence after exposure to strong visible light, such as that used in a desk-model spectroscope. Although persistent phosphorescence to short-wave UV radiation has been seen in natural IIb diamonds, the fact that we observed persistent phosphorescence to both wavelengths is another important indication (i.e., in addition to the metallic flux inclusions) that the material is synthetic diamond. In addition, these diamonds were drawn readily to a strong magnet. All three samples were identified as synthetic diamond on the basis of this combination of properties.

Most synthetic blue diamonds we have seen are a moderately saturated color with medium to dark tone. These synthetics were considerably paler and less saturated than the equivalent of a "Fancy" grade. Both the depth of the blue color and the degree of semi-conductivity are related to the boron content of the diamond, whether natural or synthetic. We measured moderate electrical conductivity in these three round brilliants, within the normal range for natural blue diamonds and unlike the high conductivity recorded for most of the synthetic blue diamonds we have examined previously.

Thomas Gelb

Figure 5. As seen both face-up and through the pavilion, the three synthetic blue diamonds on the left (0.10, 0.14, and 0.21 ct) are considerably paler than most of the synthetic blue diamonds seen in the laboratory to date. Nevertheless, their blue color is clearly evident when compared to the near-colorless diamond on the far right.



DUMORTIERITE

As the "Island of Gems," Sri Lanka is the source of many rare and unusual stones. Recently, Dunil Palitha Gunasekera, a gemologist in Ratnapura, Sri Lanka, called our attention to a 0.79 ct dark blue emerald cut



Figure 6. This inclusion in a 0.10 ct synthetic blue diamond has a shape that is both rod-like and globular, and displays the metallic luster that is typical of flux inclusions in synthetic diamonds. Magnified 63 \times .

stone (figure 8) that came from recently discovered material. This turned out to be an unusually large example of the rare gem dumortierite, so we took the opportunity to examine it in detail.

The transparent stone measured 5.67 \times 5.26 \times 3.52 mm. It was evenly colored dark blue and pleochroic in very dark blue and very light blue (reminiscent of the dichroism in benitoite). It was also biaxial negative, with refractive indices from 1.672 to 1.690. The specific gravity (measured hydrostatically) was 3.42. The gem was inert to long-wave UV and luminesced very weak (but chalky) green to short-wave UV. With magnification, we saw one "fingerprint" inclusion. No spectrum was evident with a handheld spectroscope.

We performed several advanced tests on this sample, including energy-dispersive X-ray fluorescence (EDXRF) spectroscopy, X-ray powder diffraction analysis, laser Raman microspectrometry, and UV-visible and FTIR spectroscopy. Qualitative EDXRF spectroscopy revealed major aluminum and silicon and minor-to-trace amounts of calcium, titanium, iron, arsenic, zirconium, niobium, and antimony. The best match to our powder diffraction pattern was JCPDS pattern 12-0270, a dark reddish brown dumortierite from Sri Lanka.

Although no features were seen with the spectroscope, UV-visible spectroscopy revealed broad peaks centered at about 400 and 600 nm. The infrared spectrum was relatively featureless, but the Raman spectra showed strong peaks at 211, 290, 401 (with a shoulder at 374), 506, 568, 643, 812, 850, 950, and 1075 cm^{-1} . Peaks also were seen at 456 and 1005 cm^{-1} in some orientations; the 1075 cm^{-1} peak was not seen in these directions.

For comparison, we performed EDXRF and Raman analyses on a 0.23 ct light blue dumortierite from an unknown geographic source. The Raman spectrum was similar, but the EDXRF results lacked arsenic and antimony.

Dumortierite is an unusual rock-forming mineral that is rarely usable as a gem, as it generally occurs as fibrous masses; it is a (sometimes hydrous) aluminum borosilicate that can have considerable variation in its chemical composition and hence its physical properties. Most dumortierite seen in the gem trade occurs as massive blue or pink material, or as inclusions in quartz. Some faceted examples are known, however. In his *Color Encyclopedia of Gemstones* (2nd ed., Van Nostrand Reinhold Co., New York, 1987), Joel Arem notes that facetable bluish green dumor-

Figure 7. The opaque dendritic cloud seen in this 0.21 ct synthetic blue diamond is reflected in the facets around the lower pavilion. Magnified 63 \times .



Figure 8. Sri Lanka is reportedly the source of this rare faceted 0.79 ct dumortierite. Stone courtesy of Dunil Palitha Gunasekera.

tierite occurs in Minas Gerais, Brazil, and that Sri Lanka provides transparent reddish brown material. However, in *Dana's New System of Mineralogy* (by R. V. Gaines et al., John Wiley & Sons, New York, 1997), dumortierite from Sri Lanka is stated to have up to 1.67 wt.% arsenic as As_2O_5 . Thus, the arsenic content, as well as the information that accompanied the stone, points to Sri Lanka as the source of this faceted blue dumortierite.

MLJ, John I. Koivula,
SFM, Sam Muhlmeister,
and Dino DeGhionno

Massive Pink HYDROGROSSULAR Carving

The challenges involved in identifying carved *objets d'art* are different from those encountered with a faceted gemstone. In particular, depending on the shape and artistry of the carving, delicate handling and special dexterity are required to perform standard gemological tests. This was certainly the case as the West Coast lab examined an intricately carved statue of an Asian woman (figure 9) that was submitted this winter for identification.

We were quite intrigued by the carving, which had been labeled as "rare jade." The figure itself measured approximately 12 \times 5 \times 2 cm, and was carved out of a single massive piece of translucent to semi-translucent purplish pink material with some areas



Figure 9. This carved statue, approximately $12 \times 5 \times 2$ cm, was identified as massive pink hydrogrossular.

of green coloration. The carving was beautifully finished with a very high polish. As is customary with such carvings, however, the flat base, designed to rest on a tightly fitting carved wooden stand, was left unpolished. Consequently, we could obtain a refractive index reading only by using the spot method on a carved part of the figure; a small area on the back of the statue yielded a reading of 1.71. This value is too high for either nephrite or jadeite jade.

Other standard gemological tests

did not provide any diagnostic information. There was no fluorescence to either long- or short-wave UV radiation, and the absorption spectrum did not show any characteristic features. Because of the size and delicacy of this statue, we could not obtain an accurate specific gravity determination. Instead we turned to laser Raman microspectrometry, which gave a spectrum that matched the reference we had for grossular garnet. Because this translucent material showed a low refractive index, below

the lower end (1.73) of the normal range for grossular, we identified it as hydrogrossular garnet. As the name implies, hydrogrossular is the water-bearing member of the garnet group, typically occurring in the massive form (R. Webster, *Gems*, 5th ed., 1994, Butterworth-Heinemann Ltd., Oxford, pp. 202–203).

Hydrogrossular is used only rarely as a carving material, and it occurs in pink hues even more rarely. However, this contributing editor recalled two similar items previously reported in the Lab Notes section: a carving of massive green grossular (Spring 1985, p. 44), and a strand of pink and green grossular beads that were also presented to that client as “rare jade” (Summer 1982, p. 103). KH

PEARLS

Black Cultured, from Baja California, Mexico

At this year’s Tucson shows, we saw attractive black cultured pearls that were harvested from Baja California in 1999. According to ITESM (the Monterrey Institute of Technology and Higher Education, in Mexico) these represent an unprecedented success in culturing pearls in the rainbow-lipped pearl oyster, *Pteria sterna*, which is native to the Gulf of California. We subsequently had the opportunity to examine a few smaller pearls in our laboratory.

The off-round pearls ranged from approximately 7 mm to 9 mm in diameter (figure 10). Their bodycolor mimicked the characteristic colors of the host oyster, primarily light and dark grays and browns, as well as black. In addition, some of the samples displayed strong purplish pink overtones, with green in some areas. The fine suture lines in the nacre, which cause the optical effects such as orient and overtone in pearls, were tightly spaced and very prominent in texture. All the cultured pearls showed a metallic luster.

X-radiography revealed the round bead nuclei used in the culturing process. The samples fluoresced a

distinctive red to long-wave UV, with some variation in intensity. This fluorescence serves as an identifying characteristic of pearls from Baja California. (See Gem Trade Lab Notes in Spring 1991, p. 42, and Summer 1992, p. 126, for more background information). KH

Natural, with Coating

There has been much speculation over the last few years about the prevalence of artificial coatings applied to cultured pearls to enhance their luster. We have seen few examples of pearl coatings among items submitted to our laboratories. After extensive searching in the marketplace for about two years, we purchased a few necklaces of poor-quality cultured pearls that turned out to be coated, and we identified at least one of the coating substances as a silicone polymer.

The triple-strand natural pearl necklace shown in figure 11 provided a curious example for the East Coast lab. Wear on the pearls, which ranged from 4.30×4.90 mm to 10.89×13.70 mm, indicated that this was an older necklace, so we were rather surprised when magnification revealed some

Figure 11. Most of the natural baroque pearls (4.30×4.90 mm to 10.89×13.70 mm) in this triple strand show a worn, uneven, near-colorless coating.



Figure 10. These approximately 7–9 mm black pearls were cultured in Baja California, in the oyster *Pteria sterna*.

evidence of a thin, transparent, near-colorless coating on most of the pearls. The coating was worn off on the outside center of the pearls and was most evident near the drill holes, where less wear occurs. We infer from the overall condition of the necklace and the slight discoloration of the remaining coating that the coating had been on the pearls for some time.

Most plastics and polymers can be identified by infrared spectroscopy if an adequate spectrum of the material can be obtained. With the client's

permission, we sampled the coating with a piece of "Scotch" brand tape: We attached the tape to a pearl near the drill hole and rapidly pulled it off to take away small pieces of the coating. Using a Nicolet 550 FTIR spectrophotometer, we collected spectra of the tape alone and the tape plus coating material, and subtracted the spectrum of the former. However, the weak signal from the thin pieces of coating was not clearly visible above the noise left after the subtraction. Consequently, we plucked a few bits of coating material from the tape under magnification, and pulverized it with potassium bromide (KBr) to make a pellet. This technique gave a usable spectrum that best matched the Hummel Polymer Library's reference for cellophane. In contrast, although Scotch tape is often referred to as "cellophane" tape, the modern material had a spectrum that matched polypropylene.

It is highly unusual to encounter a strand of coated natural pearls. We can only speculate that the coating may have been applied to protect the pearls from some undesirable condition, such as highly acidic skin.

TM and IR

PHOTO CREDITS

Elizabeth Schrader photographed figures 1, 2, 5, and 11. Maha Tannous provided figures 3 and 8–10. John Koivula photographed figure 4, and Vincent Cracco took figures 6 and 7.

Editors • Mary L. Johnson, John I. Koivula,
Shane F. McClure, and Dino DeGhionno
GIA Gem Trade Laboratory, Carlsbad, California

Contributing Editors
Emmanuel Fritsch, IMN, University of Nantes, France
Henry A. Hänni, SSEF, Basel, Switzerland
Karl Schmetzer, Petershausen, Germany

TUCSON 2000

The kaleidoscope of gems that is Tucson showed many more colors this year than we have seen for some time, and most of the shows were far more successful than in previous years. Although it is impossible to report the full range of items seen by the Gem News editors and their colleagues, following are some of the new, different, and more plentiful gem materials they encountered.

COLORED STONES AND ORGANIC MATERIALS

Amphiboles are not necessarily jade. Jonathan and Meagan Passel of Natural Selection, Austin, Texas, showed GIA Gem Trade Laboratory Senior staff gemologist Cheryl

Wentzell and Gem News editor MLJ an amphibole rock marketed as "Siberian blue nephrite" (also called "Dianite" in Russia). The material ranges from mottled saturated "royal" or "lapis" blue to a mottled desaturated grayish blue (figure 1) similar to "denim" lapis (see, e.g., Fall 1993 Gem News, p. 210). First discovered around 1994, this material has been recovered since 1997 as a byproduct of nephrite jade mining in Sakha (formerly Yakutia), central Siberia. Rough is sold as blocks up to 20 cm across; cabochons typically weigh 15 to 50 ct. About 200–300 kg per year of "gem-quality" material is produced.

An electron microprobe analysis of this material, performed at the University of Texas at Austin and summarized in literature provided by the Passels, stated that the rock is composed of a submicroscopic mixture of quartz,

Figure 1. These two cabochons illustrate the range of color of the amphibole rock marketed as "Siberian blue nephrite." The 27.73 ct oval cabochon on the left measures 30.3 × 16.3 × 6.5 mm; the 20.12 ct shield on the right measures 30.5 × 17.5 × 5.2 mm. Courtesy of Natural Selection; photo by Maha Tannous.



Figure 2. This 59.72 ct tumbled freeform cabochon (31.8 × 18.4 × 12.5 mm) from Nevada is reportedly composed of tremolite/actinolite. Although marketed as "Ghost jade," it lacks the fine-grained, felted structure required to be considered nephrite; hence, it is not a true jade. Photo by Maha Tannous.





Figure 3. This 36.4 × 20.8 × 14.3 mm blue-gray bead consists of the shells from two chitons that have been polished and attached together. Photo by Maha Tannous.

tremolite, and another (blue) amphibole, potassian magnesio-arfvedsonite. The analysis suggests that nearly all the iron is in the ferric state (Fe^{3+}), which is consistent with the fact that the blue color in amphiboles is typically related to Fe^{2+} - Fe^{3+} charge transfer (see, e.g., R. G. Burns, 1993, *Mineralogical Applications of Crystal Field Theory*, 2nd ed., Cambridge University Press, pp. 124–125, 197). Because the blue rock consists mostly of an amphibole that is distinct from tremolite or actinolite, the GIA Gem Trade Laboratory would not consider it nephrite jade.

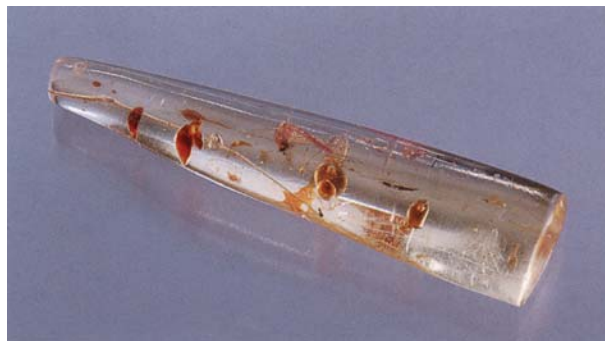
A dark green amphibole rock was being marketed as “Ghost jade” by a company of the same name in Yerington, Nevada. This product was introduced in September 1999 at the Denver, Colorado, mineral show. Product literature stated that the material was composed of fibrous tremolite/actinolite grains, has a hardness that can vary from 5 to 7, and has a density of about 3. The transparency of individual fibrous amphibole grains (figure 2) caused many of the samples to exhibit sheen and, in some cases, what appeared to be a broad “eye.” Company representative Wayne Holland stated that the locality consisted of about seven outcrops in western Nevada, within a 100 mile (about 160 km) radius of Yerington. Again, the GIA Gem Trade Laboratory would not call this material nephrite or jade because, although it reportedly has the appropriate mineral composition, the grains do not form a fine-grained, felted aggregate.

Chitons in jewelry. We have seen many creative uses of animal products in jewelry in past years; this year, at the booth of Blue Caribe Gems, Slidell, Louisiana, we saw “beads” made from the polished shells of chitons (figure 3). These marine mollusks have a series of dorsal plates that articulate like the shell of an armadillo. The shells of two chitons from the Caribbean were polished and glued together, then wrapped with a yellow metal wire to form the approximately 3-cm-long beads. The delicate blue-gray color of the polished chiton shells was reminiscent of pumellyite at first glance.

Unusual copal. Many gemologists are fascinated with inclusions in gems. Because of their excellent preservative nature and degree of transparency, amber and other naturally occurring fossil resins can give scientists a clear and intriguing look at past ecosystems in a microcosm. For decades, this editor (JIK) has closely examined both rough and fashioned samples of fossil resin for interesting and unusual inclusions. At Tucson this year, John Medici of Ostrander, Ohio, had a small collection of polished copal resin specimens from Madagascar. While most of the samples appeared to have rather typical inclusions, such as termites, flies, and ants, one piece immediately stood out because it appeared to contain drops of brownish red liquid that were easily visible without magnification (figure 4). Closer examination of this sample with a 10× loupe revealed that these drops were indeed a somewhat watery liquid of low viscosity, as shown by the presence of free-floating gas bubbles inside some of the largest drops. Since this was the first time such inclusions had been encountered by this editor in a natural resin, the sample was obtained for closer examination.

Several interesting details were revealed with a gemological microscope. As can be seen in figure 5, the appearance of the liquid drops is somewhat reminiscent of blood. It is also interesting to note that the absorption spectrum of the drops as seen through the ocular tube of a gemological microscope (with a small diffraction grating spectroscopy used in place of the eyepiece) was similar to that obtained from a human finger when it is illuminated by a strong fiber-optic light source. This spectrum suggests the presence of iron in the copal fluid inclusions, as does the brownish red color of the liquid itself. Also present with the fluid inclusions were two small flies, which appeared to be a type of midge. A relatively large volume of the reddish liquid was observed in the bodies of these insects (see, e.g., figure 6). Because of the relatively fragile nature of copal, as well as the unusual nature of these

Figure 4. This 35.4-mm-long polished rod-shaped piece of copal resin from Madagascar contains eye-visible droplets of a most unusual brownish red liquid. Photo by Maha Tannous.



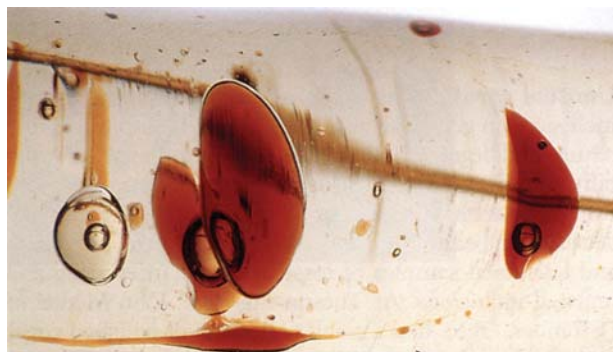


Figure 5. The brownish red fluid droplets trapped in this piece of copal contain mobile gas bubbles. Photomicrograph by John I. Koivula; magnified 10 \times .



Figure 6. This is one of two small midges that were present as inclusions with the red fluid drops in the copal. Notice the small droplets and areas of red liquid trapped within the body of the midge. Photomicrograph by John I. Koivula; magnified 10 \times .

Figure 7. Fine emeralds have been mined recently from the La Pita deposit in Maripi County, Colombia. The emerald crystal occurs with calcite in this 2.5 cm specimen. Courtesy of Graeber/Himes/Jara; photo by Jeff Scovil.



inclusions and their rarity, we performed no other form of testing to identify this liquid. If another sample is located with similar inclusions, then perhaps a more complete analysis can be performed by opening some of the voids to obtain liquid test samples.

Newly commercial emerald deposits in Colombia (La Pita and Polveros). According to long-time emerald dealer Gonzalo Jara of Bogotá, Colombia, significant amounts of emeralds are being produced at two deposits in the vicinity of Muzo and Coscuez in the department of Boyacá. The La Pita deposit is in the county of Maripi, near the Coscuez and Peñas Blancas mines. The Polveros deposit is near the town of Muzo, in the county of Muzo (note that the Muzo mine is actually across the county line, in Quipama County).

The La Pita deposit, which first had significant production in 1998–1999 (after four years of management under exploration and exploitation leases), is being mined by the company Prominas both as an open pit and a single tunnel. Mr. Jara described the emeralds from one pocket at La Pita as being very similar to the Peñas Blancas material—“not as yellow as Coscuez, not as blue as Chivor.” Finished stones range to more than 40 ct. In addition to attractive mineral specimens (figure 7) and facet-quality crystals up to 61 ct, some cat’s-eye emerald has been found at La Pita.

The Polveros deposit has been known for about 10 years, but it only recently began producing commercial quantities (although the production is less than at La Pita). The mine is an open pit. Many of the emerald crystals there are long and thin (prismatic), like pencils.

There also is new production of emeralds from Alto de la Chula, Chivor, which frequently contain quartz inclusions. “Good” and “fine” material has been recovered since August 1999.

Some new examples of drusy hematite. Drusy gem materials have been popular for some years (see, e.g., Summer



Figure 8. Tablets of specular hematite (left) and drusy hematite (right) from Arizona were among the unusual gem materials seen at Tucson this year. The large piece measures $53.4 \times 28.0 \times 4.3$ mm and weighs 60.26 ct; the smaller sample measures $17.1 \times 14.1 \times 3.3$ mm and weighs 10.77 ct. Photo by Maha Tannous.

1998 Gem News, pp. 142–143; Spring 1999 Gem News, p. 54). This year at Tucson, we saw hematite cut as drusy in some different ways. Robert Poley of Sweetwater, Prescott, Arizona, sold tablets of specular hematite from the Bradshaw Mountains in Arizona. Most had a velvety surface—similar to “rainbow hematite” without the play of color—but some had larger crystal faces on the surface (both types are shown in figure 8). Bill Heher of Rare Earth Mining Co., Trumbull, Connecticut, had hematite in a different form—“kidney ore,” fashioned as clouds (figure 9).

Orbicular jasper from Madagascar. Orbicular jasper from this island nation was showcased as a new gem material at Tucson this year. GIA Gem Trade Laboratory staff members Matt Hall and Dr. Troy Blodgett encountered this material at the booth of Paul Obenich, Madagascar Minerals (madminer@dts.mg). The colors and textures of this jasper are quite diverse: Each of the hundreds of polished samples that were observed showed a multitude of colors (including green, blue, pink, and red; see, e.g., figure 10). However, the abundance of spherical nodules (ranging from approximately 1 mm to 1 cm) is the most prominent feature of the jasper; these spheres also occurred in a variety of colors. Jasper is an opaque, cryptocrystalline quartz; however some of these samples, including the one pictured, contained fine-grained quartz crystals in the interstices between the jasper orbicules. The example illustrated resembles thomsonite from Minnesota in color and shape.

According to literature provided by Mr. Obenich, a mineral prospector sold a few samples of orbicular jasper almost 50 years ago; however, the prospector could not recall the location of the outcrop. Only after methodical searching during two expeditions was the jasper found a few years ago in an approximately 50×30 m (170×100



Figure 9. The natural surface of this 43.43 ct piece of “kidney ore” hematite makes an effective representation of a billowing cloud. Courtesy of Rare Earth Mining Co.; photo by Maha Tannous.

foot) area on the northwest coast of Madagascar. The locality reportedly is under water most of the time, so mining can occur only at low tide. About 20 tons of the material has been mined so far; it was available at Tucson as polished slabs, tumbled nodules, eggs, and spheres.

Colorful nephrite. Although many vendors at the Tucson shows had nephrite jade of various qualities, we encountered only one dealer, Go Jolly of Myrtle Creek, Oregon, who had nephrite of the type shown in figure 11. The material, which was reportedly from the Fraser River valley in British Columbia, was eye-catching because of the overall quality of the nephrite itself and the bright green inclusions it contained. With magnification, the nephrite appeared to be free of cracks, which indicates that the inclusions had not unduly strained their host. (In general, eye-visible inclusions in nephrite cause some cracking.)

The inclusions appeared to be translucent light green

Figure 10. Note the pink spheres in this $4.6 \times 3.65 \times 2.25$ cm sample of orbicular jasper from Madagascar. Photo by Maha Tannous.



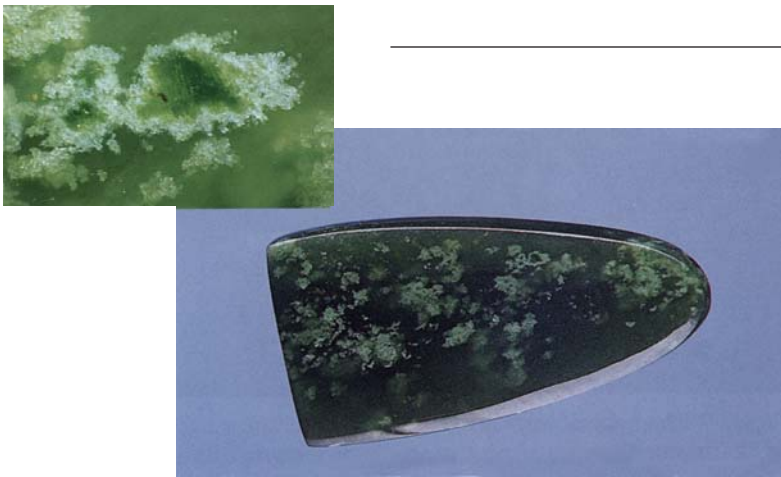


Figure 11. The light green areas in this 9.24 ct cabochon of British Columbia nephrite (23.04 × 11.71 × 3.08 mm) proved to be a combination of nephrite and grossular garnet. Photo by Maha Tannous. The dark green color of the grossular cores in these inclusions in nephrite (inset) results from the presence of chromium. Photomicrograph by John I. Koivula; magnified 15×.

to almost white granular masses. When cut and exposed on the surface during lapidary preparation, some of the inclusions revealed intensely colored, transparent green cores (figure 11, inset). Raman analysis of the inclusions showed that the light green granular areas were composed of a mixture of nephrite and grossular garnet, and the intense green cores were grossular. EDXRF analysis done by GIA research associate Sam Muhlmeister revealed the presence of chromium in the sample, which is apparently the chromophore responsible for the green color in the grossular cores.

This is the first time that we have encountered nephrite with these colorful garnet inclusions. There were about a dozen of these tongue-shaped cabochons on display in the supplier's booth, but we do not know the overall availability of this attractive nephrite.

Tahitian and Australian "keshi" pearls. Byproducts of the pearl culturing process, "keshi" are formed from irritation produced during nucleation of cultured pearls. A Japanese term that refers to a minute particle, *keshi* is also used loosely by the trade to include all sizes of saltwater pearls that have formed around implanted mantle tissue that became separated from the nucleating bead (see A. E. Farn, *Pearls: Natural, Cultured and Imitation*, Butterworth-Heinemann Ltd., Oxford, England, 1986). Typically, the Gem Trade Laboratory would refer to these mantle-tissue-nucleated saltwater pearls as "cultured" (see, e.g., Fall 1991 Gem Trade Lab Notes, p. 175). This year at Tucson we saw several examples of interesting keshi from South Pacific waters.

Maria Matula of Bochert, Sydney, Australia, showed Cheryl Wentzell a significant inventory of keshi, including

two unusually large examples: a 35 × 32 mm "silvery gray" (figure 12) and a 33 × 31 mm "silver-blue." They were recovered in January 2000 from *Pinctada maxima* oysters farmed off the western coast of Australia. These specimens weighed 22.7 and 13.5 grams, respectively.

Gemologist Mona Lee Nesselth of Laurenti and Nesselth, Custom & Estate Jewels in southern California, showed us three strands of baroque Tahitian keshi—two black (figure 13) and one slightly grayish white (figure 14)—that all came from *Pinctada margaritifera* oysters. The keshi in the two black strands, which ranged from 16.4 × 13.5 × 8.8 mm to 8.2 × 7.1 × 5.5 mm, were harvested in the 1999 season. The grayish white keshi, which measured 18.2 × 17.2 × 15.3 mm to 10.4 × 11.1 × 8.1 mm, came from the 1996 harvest. According to Ms. Nesselth, keshi from the second (and later) harvests of the same oysters show more intense colors and have a more metallic luster than those from the first harvest. Ms. Nesselth also showed us a white baroque keshi from Australia, with strong orient reminiscent of a freshwater pearl.

Cheryl Wentzell, Maha Tannous, and MLJ

Pyritized ammonite from Russia, sliced in a new way.

For the past few years, we have seen pyritized Russian ammonites that were sliced longitudinally through the shell, forming a spiral structure. This year, a few Tucson dealers had ammonites that had been sliced another way, cutting through the layers to form a

Figure 12. This large keshi pearl (35 × 32 mm) came from a *Pinctada maxima* harvested off the western coast of Australia. Courtesy of Bochert; photo by Maha Tannous.





Figure 13. These two necklaces of black Tahitian keshi pearls were created by Michelle Laurenti; the largest keshi is 16.4 mm in longest dimension. Courtesy of Laurenti and Nesseth, Custom Estate Jewels; photo by Maha Tannous.



Figure 14. The grayish white keshi pearls in this necklace (largest, 18.2 mm) by Michelle Laurenti formed in Tahitian *Pinctada margaritifera* oysters, which usually produce black cultured pearls. Courtesy of Laurenti and Nesseth, Custom Estate Jewels; photo by Maha Tannous.

pyrite “cartouche.” The large sample in figure 15 came from Demine Vladislav, Moscow, Russia; the ammonite is from the Ryazan area, near Moscow. The outside of this shell also showed some remnants of iridescent carbonate.

An update on ruby and sapphire from Chimwadzulu Hill, Malawi. The existence of gem-quality corundum on Chimwadzulu Hill in southern Malawi was first reported in 1958 (K. Bloomfield, “The Chimwadzulu Hill ultrabasic body,” *Transactions of the Geological Society of South Africa*, Vol. 61). Chimwadzulu Hill is west-northwest of Ntcheu, approximately 5 km from the border with Mozambique. The area mined is on the summit of the hill, at an altitude of about 1,525 m. The eluvial deposits have been worked sporadically since the early 1960s. Early mining efforts recovered mainly sapphire, which was predominantly in blue, green, and yellow hues. Most of the sapphires were not highly saturated, and therefore required heat treatment.

In the 1980s, mining was conducted—with German technical assistance—by a quasi-government organization known as the Malawi Development Corp. Workings were concentrated on the crown of the hill, with some good-quality ruby recovered from one area, but with no discernible continuity or trend in the mineralization. The large quantities of sapphire that entered the market from other locations throughout the world eventually rendered this operation uneconomic, and mining was terminated in 1986. Heavy industry was largely discouraged during the Presidency of Hastings Banda (1964–1994), and no further attempts at organized mining were made in the eight years following mine closure.

In September 1994, Mineral Exploration Pvt. Ltd.

Figure 15. This large (59.1 × 27.8 × 16.7 mm) “cartouche” shape is a Russian pyritized ammonite sliced across the shell. Photo by Maha Tannous.



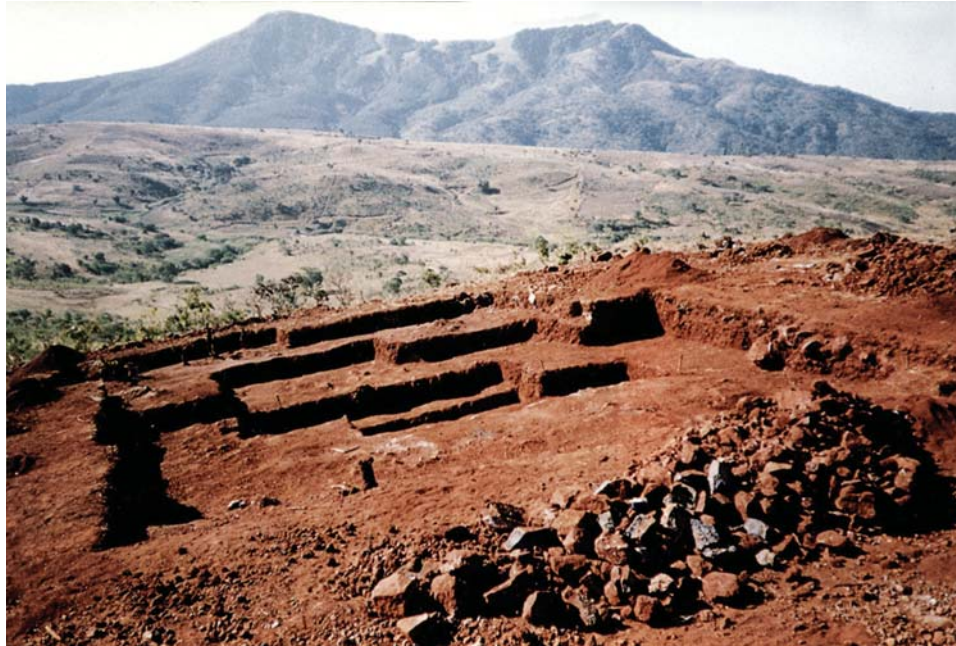


Figure 16. This is a typical ruby production pit on Chimwadzulu Hill in southern Malawi. The view looks north to Donza Mountain. Photo © David Hargreaves.

(Minex) was granted a license to mine on Chimwadzulu Hill and to explore contiguous areas. Willard International, a Panamanian company with head offices in London, is the mine operator and 85% owner of Minex. Geologic exploration and limited mining efforts initiated late in 1995 resulted in the recovery of an estimated 100+ kg of sapphire similar to that described above; rubies were found occasionally, but there was still no identifi-

Figure 17. This 2.27 ct ruby was faceted from Chimwadzulu Hill material. Photo © GIA and Tino Hammid.



able trend to their recovery. However, the subsequent digging of test pits led to the discovery of a significant ruby trend in mid-1997.

Chimwadzulu Hill is composed of an ultramafic body that is hosted by metasedimentary rocks (i.e., gneisses and schists; see the Bloomfield reference cited above, and K. Bloomfield and M. S. Garson, 1965, *The Geology of the Kirk Range—Lisungwe Valley Area*, published by The Government Printer, Zomba, Malawi). The intrusive was subsequently metamorphosed, resulting in the formation of serpentized peridotite and amphibolite. It dips northeast, and has a surface exposure of about 1 km in diameter. Over much of Chimwadzulu Hill, the bedrock has been deeply weathered and altered to an aggregate of deep red, friable, iron-rich, porous clay. In various places, the weathered bedrock is overlain by this residual soil. Corundum is recovered from these soils—particularly where this gem mineral is abundant in the underlying bedrock—and from the weathered bedrock itself.

The systematic test pits revealed that the majority of the chromium-bearing corundum (ruby or orange, pink, or purple sapphire) is localized within areas of weathered bedrock that are usually 20 m or less in lateral extent (figure 16). Approximately 100 of these potential mining targets have been tentatively identified. In limited portions of these “hot spots,” concentrations of chromium-bearing corundum can be very high; one pit 2 × 2 × 2 m yielded 7.6 kg of corundum. Mining of the present site on Chimwadzulu Hill is continuing, as is exploration of other corundum occurrences to the north.

The chromium-bearing corundum forms short columnar to tabular hexagonal crystals or crystal fragments. The basal pinacoids (0001) are very well developed, as are the prism faces (11 $\bar{2}$ 0). On some of the more tabular crystals, the rhombohedral face (10 $\bar{1}$ 1) is prominent. Typical dimensions of complete crystals are 1–3 cm across the basal pinacoid and 0.5–2.0 cm along the c-axis. Although the crystals generally are significantly fractured, the mate-



Figure 18. Here, faceted Malawi rubies ranging from 1.4 to 2.1 have been set in fine jewelry. Photo courtesy of The Silurian Co.

rial between fractures is usually of very high clarity. The color of the chromium-bearing corundum ranges from orange through red, to purplish red, almost reminiscent of rhodolite garnet. In terms of tone, recovered material ranges from pale pink through a very deep red. A few crystals exhibit orange and red banding, or orange and purplish red banding, parallel to the basal pinacoid.

According to David Hargreaves of Willard International, approximately 80 kg of chromium-bearing corundum have been recovered since September 1997. Cutting and marketing of the polished stones is arranged by The Silurian Co. of London. Faceted stones of less than 1 ct are plentiful, and stones of 1–5 ct are not uncommon (figures 17 and 18). A number of very fine gemstones have been cut, the largest of which weighs 16 ct. The clarity of these stones renders heat treatment unnecessary.

John L. Emmett
Crystal Chemistry
Brush Prairie, Washington

Another locality in Paraíba for cuprian elbaite. Every year at the Tucson Gem and Mineral Show, the Friends of Mineralogy hold a symposium. This year, the symposium theme was Brazilian pegmatites. Editor MLJ attended a talk on “Cuprian elbaite from the Bocheiron Zinho Pegmatite, Paraíba, Brazil,” by A. U. Falster, W. B. Simmons, J. W. Nizamoff, and K. L. Webber; Jim Nizamoff presented this talk.

Several pegmatites in Paraíba produce cuprian elbaite

(see, e.g., J. Karfunkel and R. R. Wegner, “Paraíba tourmalines: Distribution, mode of occurrence and geologic environment,” *Canadian Gemmologist*, Vol. 17, No. 4, 1996, pp. 99–106). São José da Batalha is the best known, and the only one to date to produce gem-quality material. The latest entry is Bocheiron Zinho No. 2, which is being mined as an open cut, and is a spodumene/lepidolite/elbaite pegmatite; there is a copper/bismuth-sulfide-rich layer at the footwall.

Most of the elbaite from Bocheiron Zinho shows a blue radial layer between a pink-to-purplish pink core and a thin green rim; sometimes there is a blue core within the pink core. Quantitative chemical analysis revealed copper evenly distributed throughout the tourmaline—in pink and green as well as blue layers—up to 1.5 wt.% Cu_2O (0.25 atoms copper per formula unit). The green layers contain iron, and the pink layers contain manganese. There is up to 25% vacancy in the X site (the sodium site) of this tourmaline, but mineralogically it is still elbaite.

Among the inclusions in these tourmalines are: veins of lepidolite replacing tourmaline, copper metal or copper sulfides (as seen in material from São José da Batalha), and bismuth sulfide. The tourmaline itself does not contain a detectable amount of bismuth. So far, the material at Bocheiron Zinho is not gemmy, but gem-quality crystals may someday be found there.

Tugtupite and other gem materials from Greenland. Several GIA staff members talked to Helge Jessen and Jennifer Patterson of Greenland Resources A/S, Copenhagen, Denmark, who were showing many unusual gem materials from Greenland at the GJX show.

Tugtupite (figure 19) was described by A. Jensen and O. V. Petersen in the Summer 1982 *Gems & Gemology*

Figure 19. The cabochon (about 2.5 cm long) in this pendant is cut from the rare gem mineral tugtupite. Courtesy of Greenland Resources A/S; photo by Maha Tannous.





Figure 20. This pendant (about 2 cm in diameter) contains two half-disks of iridescent orthoamphibole ("Nuummite"). Courtesy of Greenland Resources A/S; photo by Maha Tannous.

("Tugtupite: A gemstone from Greenland," pp. 90–94). Formerly sought only by collectors of rare minerals, this unusual gem is now available commercially as cabochons, occasional faceted stones, and gem rough. Pink to red in color, tugtupite is a silicate of sodium, aluminum, beryllium, and chlorine. It fluoresces orange-to-red to long- and short-wave UV radiation. The mineral is found in hydrothermal veins associated with the Proterozoic (late Precambrian) Ilimaussaq alkaline intrusion, near Narsaq in southern Greenland. According to the

Figure 21. This 441.48 ct zircon was faceted from material recently found in the Ilakaka area of Madagascar. Courtesy of Cynthia Renee Co.; photo by Maha Tannous.



Greenland Resources representatives, the vein that produced the present supply is now exhausted, so the availability of tugtupite is limited until more veins are discovered.

The iridescent orthoamphibole sold under the trade name Nuummite (figure 20), another unusual collectors' stone, was also available—as gem rough, as cabochons, and in jewelry. (For a detailed description of this stone, see P. W. U. Appel and A. Jensen, "A new gem material from Greenland: Iridescent orthoamphibole," Spring 1987 *Gems & Gemology*, pp. 36–42.) Sometimes called "the opal of Greenland," this amphibole is intermediate between anthophyllite and gedrite, and comes from Archean rocks in the Nuuk area of western Greenland. Typical samples were dark green, with iridescent crystal planes.

A third material, sold as "grønlandite," was reported to be compact aventurine quartz from the 3.8 billion-year-old Isua supercrustal rocks in the Nuuk area. It was marketed as the world's oldest gem material. The green color reportedly is caused by inclusions of the chromian mica variety fuchsite. Examples we saw resembled nephrite jade in color, with visual homogeneity. In addition to these materials, we saw ruby in matrix, labradorite, sodalite, pyralispite garnets, and massive yellow prehnite that could easily be mistaken for amber at first glance; all of these were mined in Greenland.

Large faceted zircon. One of the joys of the Tucson shows is seeing gems in unusually large sizes. Staff gemologist Valerie Chabert, from our New York laboratory, noticed a 441.48 ct brown zircon (figure 21) at the booth of Cynthia Renee Co., Fallbrook, California. According to Cynthia Marcusson, the original rough was found in June or July of 1999 at Ilakaka, Madagascar, and weighed about 250 grams. It was subsequently fashioned in Sri Lanka.

Also seen at Tucson. . . Many of the gem materials heralded as new at Tucson this year have been reported in previous issues of *Gems & Gemology*. For the reader's convenience, following are some of these "new" materials seen at Tucson, with previous *Gems & Gemology* references:

- Pink and blue Madagascar sapphires (Summer 1999 Gem News, pp. 149–150)
- Nigerian pink tourmaline and rubellite (Winter 1998 Gem News, pp. 298–299)
- Spessartine, from Brazil, Nigeria, and Zambia in particular (most recently in Spring and Winter 1999 Gem News, pp. 55, 216, and 217, respectively)
- Abundant multicolored sunstone from Oregon (Summer 1997 Gem News, p. 145)
- Widely available Russian demantoid garnets, many showing classic horsetail inclusions (see, e.g., Mattice et al., Fall 1999 *Gems & Gemology*, pp. 151–152)

- Blue opal from Peru and cat's-eye opal (Gem News: Summer 1991, pp. 120–121; Summer 1998, pp. 138–140)

Gaspeite from Australia was widespread and referred to as such; this was a departure from when we first saw this nickel carbonate reported as "Allura" (Summer 1994 Gem News, p. 125–126). Another unusual rare gem material that was far more common this year than previously was deep red eudialyte from Canada (Spring 1999 Gem News, pp. 49–50) and Russia.

TREATMENTS

Moonstone with dichroic backing. GIA Education product manager Wendi Mayerson saw some interesting stones at the booth of Gem Crafters, New York City. These moonstone (orthoclase feldspar) cabochons, sold as "Celestial moonstone," were backed with a very thin coating of a dichroic material. The coating produced moderate color in the stone, as well as a colored chatoyant band or cat's-eye. The five cabochons in figure 22 demonstrate the range of colors that were available; note that the gray cabochon somewhat resembles cat's-eye sillimanite. Natural cat's-eye moonstone of this quality, regardless of its bodycolor, exhibits a chatoyant band that is white. The different colors of the band in each of these stones provide an eye-visible indication of treatment or assembly, which could be easily confirmed by examining the underside of the stone.

According to information provided by the manufacturer, the backings on these samples are rather delicate, and should not be buffed, polished, exposed to abrasive jewelry cleaner, or cleaned using ultrasonic devices.

Figure 22. These five cabochons demonstrate the range of colors available in "Celestial moonstone," that is, moonstone backed with a dichroic film. They range from 5.90–6.10 × 3.85 mm to 7.90–8.00 × 4.05 mm; their total weight is 5.91 ct. Photo by Maha Tannous.



Figure 23. These strands illustrate some of the new colors of dyed freshwater cultured pearls that were seen in Tucson this year. The violetish blue samples are about 4½–5 mm in diameter. Courtesy of Betty Sue King, King's Ransom, Sausalito, California; photo by Maha Tannous.

Instead, special care should be taken to clean the metal before mounting these items, and the stones should be cleaned with water and blotted dry. Hundreds of these cabochons were available at Tucson, in calibrated sizes.

Wendi Mayerson and MLJ

New hues of dyed freshwater cultured pearls. Enormous quantities of freshwater cultured pearls flooded Tucson again this year, and a variety of treated colors were available. New colors included bright yellowish green, "golden" green, and various shades of blue—from light violetish blue (figure 23) through intense "royal" blue. This year, many dealers were calling their strands "heated," although most strands displayed colors that obviously were irradiated or dyed (including pink, green, and blue). As certain dyes may require heat to be activated or set, the term may refer to a heated dye bath; more information is needed about the "heating" process.

Cheryl Wentzell

Heat-treated rubies: Glass or not glass? One of the important issues at Tucson this year was that of the nature of the "fillings" in heat-treated rubies. A major concern was the potential for misidentification of a natural surface-reaching inclusion as foreign material (see, e.g., J. L. Emmett, "Fluxes and the heat treatment of ruby and sapphire," Fall 1999 *Gems & Gemology*, pp. 90–92). Kenneth Scarratt provided the following information.

Since 1984, laboratories and gemologists have been identifying the substances in cavities within ruby and sapphire as "glass" based on visual appearance (surface luster, bubbles, evidence of devitrification, etc.; see, e.g., R. R. Harding and K. Scarratt, "Glass infilling of cavities in natural ruby," October 1984 *Journal of Gemmology*, pp. 293–297; R. E. Kane, "Natural rubies with glass filled cavities," Winter 1984 *Gems & Gemology*, pp. 187–199).



Figure 24. This 86.21 ct white quartz geode (left) from Rio Grande do Sul, Brazil, owes its pearly surface and iridescence to a sputtered coat of silicon. The same coating on white drusy calcite specimens, such as the 18.38 ct piece from Romania on the right, created a sparkling off-white pearly effect. Courtesy of Rare Earth Mining Co.; photo by Maha Tannous.

Sophisticated techniques have not been used routinely, because of the high cost of advanced testing and the fact that (until relatively recently) the quantity of rubies with glass-filled cavities has not been large.

It has become normal practice in Bangkok to use hydrofluoric acid (a strong acid that dissolves silicates

Figure 25. This 43.24 ct hydrothermal synthetic morganite beryl was grown on a seed plate of synthetic emerald; the resulting color combination resembled bicolored tourmaline. Courtesy of Tom Chatham, Chatham Created Gems; photo by Maha Tannous.



easily and which must be handled with great care) to “clean” rubies of any glass remaining on the surface following heat treatment. This is done either by the company that has treated the rubies or later by gem laboratories as an additional service to clients. (The normal technique for the removal of glass in cavities requires that the ruby be immersed in hydrofluoric acid for just a few seconds or minutes.) Within the last few years, this author has experienced several situations where what appeared to be glass within a cavity in ruby could not be removed with hydrofluoric acid. Although these materials had all the visual characteristics of glass fillings, the fact that they could not be removed in the normal manner left their identity open to question.

As a result, over the past several months the AGTA Gemological Testing Center in New York has introduced a policy of recording the Raman spectra of all “glass appearing” substances within cavities in rubies that are submitted for examination. This has been made possible only because of the greatly simplified operation of the latest models of laser Raman microspectrometers compared with earlier versions. In the course of implementing this policy, staff members at the Gemological Testing Center have discovered several fillings that appeared to be glass when examined with magnification but actually were *not* silicate glass. In one instance, a cavity had a level plateau of a transparent substance (slightly undulating and of melted, glass-like appearance) just below the surface of the stone. Raman analysis proved that this substance was in fact corundum with a small area of anatase (a titanium oxide mineral). Both corundum and anatase have sharp peaks at characteristic wavenumbers in their Raman spectra, whereas the glass typically encountered in ruby cavities does not. This example illustrates that care should be taken in identifying what appear to be foreign substances within cavities in ruby.

Kenneth Scarratt
AGTA Gemological Testing Center
New York, NY

Silicon coating of drusy materials. There was a continued abundance of fashioned drusy material at Tucson. In addition to titanium-coated drusy cabochons (see, e.g., Summer 1998 Gem News, pp. 142–143), we saw silicon-coated samples at the booth of Bill Heher, Rare Earth Mining Co. By means of vapor deposition (cathode sputtering), silicon was used to coat white drusy Brazilian agate, which was then repolished. The resulting pearly white specimens displayed strong iridescence (figure 24). Silicon also was used to coat white drusy calcite from Romania, with smaller crystals than the quartz mentioned above, creating sparkling off-white pearly specimens. According to Mr. Heher, only a “pure” white host material produced usable specimens.

Cheryl Wentzell and Sam Muhlmeister

SYNTHETICS AND SIMULANTS

Bicolored synthetic beryl, resembling tourmaline. Tom Chatham of Chatham Created Gems, San Francisco, California, showed us about half a dozen samples of hydrothermal synthetic beryl (see, e.g., figure 25), which his company and Biron of Australia had grown on an experimental basis. For this experiment, they grew synthetic morganite on seed plates of synthetic emerald. When viewed along the seed plate, the color zones formed by the green seed plate and the pink overgrowth were sharp and distinct. Although this material was not a commercial product, it was notable for its interesting appearance, which caused several experienced gemologists to guess at first glance that it was pink-and-green bicolored tourmaline. Of course, no gem-quality synthetic tourmaline has appeared as yet on the market.

MISCELLANEOUS

"Floating diamonds" in jewelry. Graduate Gemologist and jewelry designer Georges Mouzannar, of Joaillerie Georges J. Mouzannar in Kaslik, Lebanon, showed senior staff gemologist Maha Tannous the "floating diamond" line, a collection of 18K white gold jewelry (rings, earrings, and pendants) that features diamonds set in a colorless resin. At first glance, even to an experienced jeweler/gemologist, the diamonds appear to be suspended in mid-air.

The soft resin is cast and hardened by slow, controlled heating in a vacuum to avoid the formation of bubbles. Once hardened, the resin is filed and polished to a high luster. The setting area is etched into the hard resin, and the diamonds are then carefully inserted, with the assistance of a microscope, individually or in arranged

Figure 26. Seven 0.02 ct diamonds have been geometrically set in resin in this 18K white gold ring. Photo by Maha Tannous.

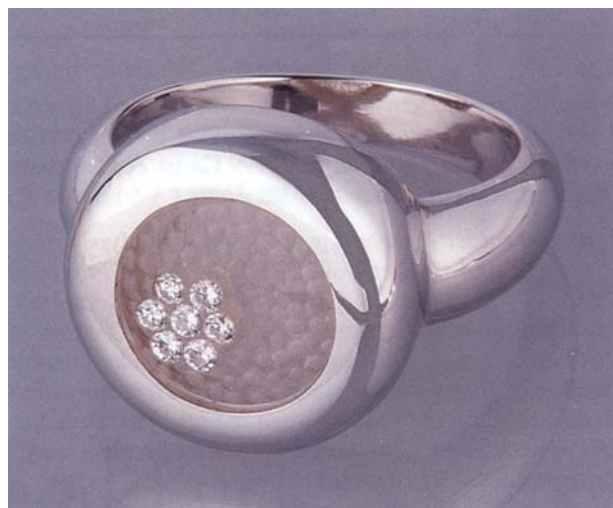


Figure 27. The resin evident in figure 26 is transparent against the skin, which causes the diamonds to appear as if they are floating in air. Photo by Maha Tannous.

geometric groupings (figure 26). The table facet of each diamond is leveled precisely with the surface of the resin so that all of the stones are in the same plane as that surface. The resulting setting is transparent when worn against the skin (figure 27), so the resin-set diamonds appear to be free-floating. Although we know of no systematic durability tests that have been conducted, the line appears to have withstood the hardships of daily wear, including exposure to sunlight and saltwater, since it was introduced in Lebanon well over a year ago.

Maha Tannous

Bismuth egg. Among the most fabulous objets d'art are the Easter eggs created at the turn of the last century for the Romanoff court by Peter Carl Fabergé and his atelier. Since then, gem-set eggs or those carved from ornamental materials continue to be popular. We saw a unique variation on these objects in the room of Gunnar Färber, Swamswegen, Germany, at the Executive Inn in Tucson this year. Crystal grower Udo J. A. Behner of Wadern, Germany, crystallizes bismuth in chicken eggshells (figure 28); the resulting eggs contain miniature scenes of iridescent tarnished skeletal bismuth crystals.

ANNOUNCEMENTS

GIA on the Internet. *Gems & Gemology* is pleased to announce the new design and format of the GIA Web site, www.gia.edu. In addition to its new look and easier navigation, the site features expanded content, including news and events under "Today at GIA." During your visit to the GIA site, be sure to click on *Gems & Gemology*. Our online version now contains a weekly news update, with more features and links on the way.

Faceters' Symposium 2000. Presented by the Faceters' Guild of Southern California, this year's Faceters' Symposium will take place August 4–6 at the Riverside



Figure 28. This 43.0 × 37.4 × 37.0 mm hollow bismuth egg contains a crystalline scene inside. Photo by Maha Tannous.

Convention Center. The Symposium, which is being held in conjunction with the California Federation of Mineralogical Societies Gold & Gem Show, will feature speaker presentations on a number of topics that pertain to faceting. Cutting demonstrations, displays of faceted gemstones as well as faceting equipment, and faceting competitions (Novice through Masters) also will be offered. For more information or to register, contact Glenn Klein at 949-458-5803 (phone), or glennklein@yahoo.com (e-mail).

GANA exhibit in Los Angeles. An exhibition of selected gemstone artworks by members of Gem Artists of North America (GANA) will be on display at the Los Angeles County Museum of Natural History's Hall of Gems and Minerals from May 4–July 30, 2000. Among the works that will be on display is "Bahia," a rutilated quartz crystal from Bahia, Brazil, carved by Glenn Lehrer and Lawrence Stoller. At a height of 1.52 m (5 ft) and a total weight of 273.3 kg (602 lbs), it is the world's largest transparent gem carving. For information on the exhibit, contact the museum at 213-763-3466 (phone), or visit the Web site www.nhm.org/minsci.

Jewelry 2000. The 21st annual Antique & Period Jewelry and Gemstone Conference will take place July 29–August 2 at Bryant College in Smithfield, Rhode Island. Formerly held at the University of Maine at Orono, this conference offers a curriculum of lectures and hands-on seminars conducted by leading gem experts, curators, auction representatives, dealers, appraisers, and designers. "Jump Start," a pre-conference program designed to reinforce basic jewelry skills and concepts, will be held July 27–29. For more details, contact the conference at 212-535-2479

(phone), 212-988-0721 (fax), or visit the Web site www.jonas4jewelry.com.

Tourmaline 2000. This exhibition is ongoing at the German Gemstone Museum in Idar-Oberstein, until August 27, 2000. The exhibit features more than 500 pieces (mostly from private collections in Idar-Oberstein), including crystals, carvings, cabochons, faceted stones, and slabs. Contact Dr. Joachim Zang at 49-6781-33210 (phone), 49-6781-35958 (fax), or Joachim.Zang@T-Online.de (e-mail).

Gemstones at upcoming scientific meetings. These upcoming meetings will feature sections on gemstones:

- Lectures on the geology and mineralogy of the Argyle diamond mine and Australia's opal fields will occur at the *Australia's Greatest Mineral Deposits* conference on June 10–12, 2000, in Broken Hill, New South Wales. The meeting is presented by the Mineralogical Society of New South Wales, 02-9685-9977 (phone), 02-9685-9915 (fax), or p.williams@uws.edu.au (e-mail).
- *Gemological collections in museums and problems of gemology* are among the topics that will be covered at the Mineralogical Museums in the 21st Century meeting in St. Petersburg, Russia, June 26–30, 2000. For more information, call 7-812-328-9481 or e-mail dept@mineral.geol.pu.ru.
- *Australian Gemstones* will be one of the topics at the 15th Australian Geological Convention in Sydney, July 3–7, 2000. A pre-meeting field trip (June 27–July 1) will include a visit to volcanic-associated sapphire deposits. For details, contact the Convention Secretariat at 61-2-9411-4666 (phone) or 61-2-9411-4243 (fax), or visit the web site www.science.uts.edu.au/agc/agchome.html.
- A special session on gems will take place at the 6th International Congress on Applied Mineralogy (ICAM 2000) in Göttingen, Germany, July 13–21, 2000. To learn more, call 49-511-643-2298, fax 49-511-643-3685, e-mail icam2000@bgr.de, or log on to www.bgr.de/icam2000.

ERRATA

1. *Mary Shore of Denver, Colorado*, was omitted from the 1999 Challenge Winners (Summer 1999, p. 135) despite scoring a perfect 100% on the 1999 Gems & Gemology Challenge. Congratulations to Ms. Shore.

2. In a recent letter regarding the Seifert and Hyrs article "Sapphire and Garnet from Kalalani, Tanga Province, Tanzania" (Summer 1999 issue of Gems & Gemology, pp. 108–120), Cedric Simonet and Silvant Okundi of Rockland Kenya Ltd. pointed out that the correct spelling of the word malaia is malaya. They indicated that in Swahili, the word malaya means "prostitute"; it was applied to this gem variety of garnet because it was formerly mistaken for sapphire.

The Dr. Edward J. Gübelin Most Valuable Article Award

The readers have spoken, and your votes for the Dr. Edward J. Gübelin Most Valuable Article Award for *Gems & Gemology* in 1999 shared a common theme: Treatments. From General Electric's new process for removing color from type IIa diamonds to the ongoing concern about the clarity enhancement of emeralds and the fillers used, treatments remained one of the industry's most critical issues in 1999.

First place was awarded to "Observations on GE-Processed Diamonds: A Photographic Record" (Fall 1999), which revealed several interesting features that may be diagnostic of these diamonds. Receiving second place was "On the Identification of Various Emerald Filling Substances" (Summer 1999), an article that evaluated the methods used to distinguish among the many different clarity-enhancement substances. The third-place winner, "Classifying Emerald Clarity Enhancement at the GIA Gem Trade Laboratory" (Winter 1999), presented GIA's new system for classifying the degree of clarity enhancement in a particular emerald.

The authors of these three articles will share cash prizes of \$1,000, \$500, and \$300, respectively. Following are photographs and brief biographies of the winning authors.

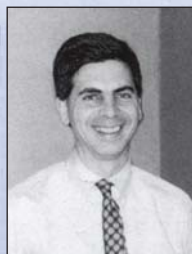
Congratulations also to Ellen Fillingham of Mendon, Michigan, whose ballot was randomly chosen from the many entries to win a leather portfolio and a five-year subscription to *Gems & Gemology*.

First Place

Observations on GE-Processed Diamonds: A Photographic Record

Thomas M. Moses, James E. Shigley, Shane F. McClure, John I. Koivula, and Mark Van Daele

Thomas Moses is vice president of Identification Services, GIA Gem Trade Laboratory in New York. One of the world's foremost gemologists, Mr. Moses is a prolific author and an editor of the Gem Trade Lab Notes section. He attended Bowling Green University in Ohio before entering the jewelry trade more than 20 years ago. **James Shigley** is director of GIA Research in Carlsbad. Dr. Shigley, who received his Ph.D. in geology from Stanford University, has been with GIA since 1982. He has written numerous articles on natural, treated, and synthetic gems. **Shane McClure** is director of West Coast identification services at the GIA Gem Trade



Thomas M. Moses



Mark Van Daele



James E. Shigley, Shane F. McClure, and John I. Koivula



Shane Elen and Mary L. Johnson



Sam Muhlmeister



Maha Tannous

Laboratory in Carlsbad. Mr. McClure has over 20 years of experience in gem identification, has written numerous articles, and is an editor of the Gem Trade Lab Notes and Gem News sections of *Gems & Gemology*. **John Koivula** is chief research gemologist at the GIA Gem Trade Laboratory in Carlsbad, and an editor of the Gem News section. The coauthor (with Dr. Gübelin) of the classic *Photoatlas of Inclusions in Gemstones*, Mr. Koivula holds bachelor's degrees in chemistry and mineralogy from Eastern Washington State University. **Mark Van Daele**, formerly the supervisor of system quality management at the GIA Gem Trade Laboratory in Carlsbad, holds a degree in electromechanical engineering from the Antwerp University of Industrial Engineering. Mr. Van Daele now resides in the United Kingdom, where he is an applications consultant for an international software company.

Second Place

On the Identification of Various Emerald Filling Substances

Mary L. Johnson, Shane Elen, and Sam Muhlmeister

Mary Johnson is manager of Research and Development at the GIA Gem Trade Laboratory in Carlsbad, and an editor of the Gem News section. A frequent contributor to *Gems & Gemology*, she received her Ph.D. in mineralogy and crystallography from Harvard University. **Shane Elen** is analytical equipment supervisor at GIA Research in Carlsbad. He holds an engineering degree from the Camborne School of Mines in Cornwall, UK. With 16 years of experience in the analysis of solid-state materials, he has a strong interest in developing new identification methods for gem materials. **Sam Muhlmeister** is a research associate with the GIA Gem Trade Laboratory in Carlsbad. Born in Germany, he received bachelor's degrees in physics and mathematics from the University of California at Berkeley.

Third Place

Classifying Emerald Clarity Enhancement at the GIA Gem Trade Laboratory

Shane F. McClure, Thomas M. Moses, Maha Tannous, and John I. Koivula

Please see the first-place entry for biographical information on **Shane McClure**, **Thomas Moses**, and **John Koivula**.

Maha Tannous, a senior staff gemologist at the GIA Gem Trade Laboratory in Carlsbad, is an accomplished gem photographer and a frequent contributor to the Gemological Abstracts section. A native of Lebanon, she holds bachelor's degrees in computer science from the University of Texas, Arlington, and in communications/journalism from Southwest Texas State University.

Photos by Joseph Duffy.

GEMS & GEMOLOGY

Challenge



The following 25 questions are based on information from the four 1999 issues of *Gems & Gemology*. Refer to the feature articles and “Notes and New Techniques” in those issues (for the special Fall “Symposium Proceedings” issue, only the Moses et al. GE POL article is included) to find the **single best answer** for each question; then mark your choice on the response card provided between pages 78 and 79 of this issue. (Sorry, no photocopies or facsimiles will be accepted; contact the Subscriptions Department if you wish to purchase additional copies of this issue.) Mail the card so that we receive it no later than Mon-

day, July 10, 2000. Please include your name and address. All entries will be acknowledged after that date with a letter and an answer key.

Score 75% or better, and you will receive a GIA Continuing Education Certificate. If you are a member of GIA Alumni and Associates, you will earn 5 Carat Points toward GIA’s new Alumni Circle of Achievement. (Be sure to include your GIA Alumni membership number on your answer card and submit your Carat card for credit.) Earn a perfect score, and your name will also be featured in the Fall 2000 issue of *Gems & Gemology*. Good luck!

- Since the Zachery treatment was developed in the late 1980s, how much turquoise has been enhanced by this process?
 - Less than one million carats
 - About one million carats
 - Between one and ten million carats
 - More than 10 million carats
- The most diagnostic internal features of Russian hydrothermal synthetic rubies and sapphires are
 - zigzag or mosaic-like growth structures.
 - one- and two-phase spicules.
 - triangular growth hillocks.
 - very fine, short rutile needles.
- The presence of a flash effect in a filled emerald is related to
 - the Cr content of the host emerald.
 - the RI value of the filler.
 - the filler’s fluorescence to long-wave UV.
 - the viscosity of the filler.
- The amethyst coloration in synthetic ametrine develops as a result of
 - the presence of manganese.
 - dumortierite inclusions.
 - exposure to gamma-ray radiation.
 - heating to 350°C after growth.
- The degree of clarity enhancement in an emerald does not correlate directly with value because
 - “eye-clean” stones are always significantly enhanced.
 - “eye-clean” stones are never significantly enhanced.
 - it does not take into account non-surface-reaching inclusions.
 - the appearance of the enhancement changes with the viewing angle.
- The process developed by General Electric to improve the color of GE POL diamonds involves
 - irradiation.
 - irradiation and annealing.
 - bleaching in caustic solutions.
 - high temperature and high pressure.
- Diopside inclusions in Russian demantoid garnet occur as
 - curved fibers.
 - straight, colorless needles.
 - hollow tubes.
 - prisms surrounding chromite.

8. A survey of U.S. patents and European patent applications suggests that the process used to decolorize GE POL diamonds involves healing structural defects by means of
 - A. graphitization.
 - B. plastic deformation.
 - C. nitrogen substitution.
 - D. vacancy migration.
9. A color change from blue-green in daylight to purple in incandescent light is shown by pyrope-spessartine garnets from Bekily, Madagascar, that contain relatively high amounts of
 - A. vanadium.
 - B. cobalt.
 - C. iron.
 - D. manganese.
10. Which of the following distinctive inclusions were reported in some of the GE POL diamonds studied at the GIA Gem Trade Laboratory?
 - A. Graphite
 - B. Curved fibers
 - C. Etch channels
 - D. Hollow hexagonal columns
11. Most Zachery-treated turquoise can be detected by its higher
 - A. refractive index.
 - B. phosphorus content.
 - C. potassium content.
 - D. thermal conductivity.
12. The presence of significant levels of which trace element indicate the natural origin of a colorless sapphire?
 - A. Calcium
 - B. Iron
 - C. Vanadium
 - D. Chromium
13. Which of the following characteristics is *not* useful in separating natural from Russian synthetic ametrine?
 - A. Infrared spectrum
 - B. UV-Vis-NIR spectrum
 - C. Brazil-law twinning in the amethyst portion
 - D. Color zoning
14. The nature of an emerald filling substance is best determined by
 - A. the flash effect.
 - B. infrared spectroscopy.
 - C. Raman microspectrometry.
 - D. a combination of these approaches.
15. Most of the GE POL diamonds examined at GIA were cut in which shape?
 - A. Pear
 - B. Round brilliant
 - C. Marquise
 - D. Oval
16. An emerald classified as "moderate" in GIA's clarity-enhancement classification system has experienced a ____ improvement in face-up appearance due to filling.
 - A. slight
 - B. limited
 - C. noticeable
 - D. obvious
17. In analyzing gemstone inclusions, laser Raman microspectrometry can be used to differentiate between
 - A. minerals with the same crystal structure and chemical composition.
 - B. minerals with similar crystal structures but different chemical compositions.
 - C. surface-reaching inclusions only.
 - D. subsurface inclusions only.
18. All of the following corundum varieties have been produced from the Kalalani area in Tanzania except for
 - A. ruby.
 - B. yellow-brown sapphire.
 - C. reddish orange sapphire.
 - D. dark blue-green sapphire.
19. At the Kalalani area in northeastern Tanzania, gem-quality ruby and sapphire form in
 - A. a granitic gneiss.
 - B. pegmatites.
 - C. marble-hosted deposits.
 - D. basalt-hosted deposits.
20. The GE patents to improve the optical properties of synthetic diamond that followed the initial 1994 European patent application have involved treatment
 - A. at lower temperatures.
 - B. in the diamond stability field.
 - C. in the graphite stability field.
 - D. at diamond-graphite equilibrium.
21. "Palma" is an emerald filler that is most accurately defined as
 - A. a liquid wax.
 - B. an epoxy prepolymer.
 - C. palm oil.
 - D. palm oil plus vegetable dye.
22. At the GIA Gem Trade Laboratory, filled fissures in emeralds are located by
 - A. examination with a microscope using 10× to 25× magnification.
 - B. using darkfield illumination supplemented by fiber-optic lighting.
 - C. careful observation of the stone from all directions.
 - D. all of the above.
23. The primary source for colorless sapphire is
 - A. Madagascar.
 - B. Thailand.
 - C. Tanzania.
 - D. Sri Lanka.
24. Careful observation of Zachery-treated turquoise may reveal
 - A. evidence of filling materials.
 - B. a weak response to a thermal reaction tester.
 - C. a slight fluorescence to short-wave UV radiation.
 - D. blue color concentrations adjacent to fractures.
25. The percentage of the 858 GE POL diamonds studied by GIA that were classified as type IIa was
 - A. 10%.
 - B. 50%.
 - C. 79%.
 - D. 99%.

Book Reviews

Susan B. Johnson & Jana E. Miyahira-Smith, Editors

ROMANCE OF THE GOLCONDA DIAMONDS

By Omar Khalidi, 127 pp., illus., publ. by Grantha Corp., Middleton, NJ, 1999. \$39.95*

This book provides an historical description of the legendary Golconda diamonds, as well as narrative sketches of 22 large (ranging from 9 to 280 ct) diamonds from these deposits. The author, a historian from Hyderabad who has studied early Persian manuscripts related to Golconda, offers a detailed history, along with a number of full-color illustrations taken from these early manuscripts. Contrary to popular belief, the source of these diamonds was not Golconda—the 13th-century fortress located on the outskirts of present-day Hyderabad. Rather it was the gravel deposits near Kurnool (60 miles [96 km] south of Golconda) and in the lower course of the Krishna River (100 miles [160 km] southeast of Golconda). Regrettably, no maps are provided in the book to help the reader visualize the locations of the deposits or the boundaries of the ancient states being discussed. Also, information on the geology of the deposits and the gemology of the diamonds is quite sparse.

Most of the 22 diamonds featured already have been chronicled in Ian Balfour's *Famous Diamonds* (London: Christie, Manson, and Woods, 1997). However, the final chapters in Mr. Khalidi's book present an interesting account of the Nizams of Hyderabad, the last ruling dynasty in that state before it was absorbed into the federal republic of India in 1950. The heirs of the last Nizam ruler, Osman Ali Khan, underwent a lengthy struggle to sell the jewelry of the so-called "richest man on earth" after his death

in 1967. Finally, in 1995, the Indian government purchased the collection, but it still has not been given a prominent showcase.

In summary, *Romance of the Golconda Diamonds* is short on gemology and geography, but sound on history and illustrations. The wide breadth of information on Golconda diamonds in one comprehensive volume is most welcome.

A. J. A. (BRAM) JANSE
Archon Exploration Pty. Ltd.
Carine, Western Australia

RUBY, SAPPHIRE AND EMERALD BUYING GUIDE

By Renee Newman, 164 pp., illus., publ. by International Jewelry Publications, Los Angeles, CA, 2000. US\$19.95*

Can a book capture the romance and beauty of gemstones while offering practical information on how to make the right buying decision? If the gemstones we're referring to are rubies, sapphires, or emeralds, then this book does a terrific job of achieving both.

This buying guide discusses several value factors, with separate chapters on color (i.e., for ruby, sapphire [including fancy-color sapphires], and emerald [including other beryls]), plus combined chapters on shape/cut, carat weight, and clarity/transparency. Each factor is explained using numerous photographs (175 color, 21 black-and-white), charts, and line-drawing illustrations. Also covered in these chapters are grading systems, characteristics of stones by origin, and a discussion of how different kinds of lighting can affect ruby color. The distinctions between ruby and pink sapphire, as well as emerald and green beryl, are mentioned, but unfortu-

nately only two photographs are provided for ruby/pink sapphire and none for emerald/green beryl. Additional chapters cover simulants, synthetics, treatments, care, and cleaning, as well as star ruby and sapphire.

The *Buying Guide* does an excellent job of showing consumers how different grading factors affect beauty and value, but it is unlikely that the average customer could rely solely on this book to detect treatments, simulants, or synthetics. Recognizing this, the author offers tips for choosing a competent appraiser and asking the right questions of the seller. As she did with her previous books (*Diamond Ring Buying Guide*, *Gold Jewelry Buying Guide*, *Gemstone Buying Guide*, and *Pearl Buying Guide*), Ms. Newman has created an extremely helpful reference guide and product knowledge manual. It should be on the shelf of every jeweler whose customers want to know more—often much more—than "How much does it cost?"

DOUGLAS KENNEDY
Gemological Institute of America
Carlsbad, California

ROUGH DIAMONDS: A PRACTICAL GUIDE

By Nizam Peters, 172 pp., illus., publ. by the American Institute of Diamond Cutting, Deerfield Beach, FL, 1997. US\$89.00*

This book appears to be a companion text to the American Institute of Diamond Cutting's course work. It is organized very much like a textbook,

**This book is available for purchase through the GIA Bookstore, 5345 Armada Drive, Carlsbad, CA 92008. Telephone: (800) 421-7250, ext. 4200; outside the U.S. (760) 603-4200. Fax: (760) 603-4266.*

and in fact resembles one except for the oversize format. The material is well organized and very methodical. The text and illustrations are sufficiently clear to educate a novice, at least in the terminology and basic concepts.

The book begins with the very basic shapes commonly found in rough diamonds, and continues with discussions on color, clarity, marking the rough, cutting, and polishing. It covers considerable ground and touches on most of the concepts that rough dealers and manufacturers deal with every day. One drawback is the placement of the pictures. Although the illustrations are excellent, each picture seems to be placed one paragraph out of order, and one must continually turn the page to see the pictures to which the text refers. In addition, although the subject coverage is quite extensive, two areas deserve more attention: finding the grain and determining the probable country of origin of the rough diamonds. The latter information—which frequently can be gleaned from many telltale signs—is often critical to rough dealers and manufacturers. It affects the final value of the finished stone. Generally, rough from Russia and Canada will improve in color when polished, while rough from Sierra Leone, parts of the Ivory Coast, and especially Angola will worsen in color. Country of origin will also affect yields and clarities. Canadian rough, for example, has many small crevices that go deep below the surface. The yield is therefore lower, because the cutter must remove these “gletzes.”

As an instructional accompanying text, *Rough Diamonds* does an excellent job. As a stand-alone reference, it is pretty good, and rather complete. Any gemologist would do well to read this if he or she does not have firsthand contact with the rough diamond trade.

HERTZ HASENFELD
Hasenfeld-Stein, Inc.
New York City

CRYSTAL ENCHANTMENTS: A COMPLETE GUIDE TO STONES AND THEIR MAGICAL PROPERTIES

By D. J. Conway, 343 pp., publ. by
the Crossing Press, Freedom, CA,
1999. US\$18.95

For years, modern society has turned to gems and minerals for the powers of healing, protection, and good fortune they are believed to bring. The recent popularity of “power beads” attests to this cultural phenomenon. In *Crystal Enchantments*, Ms. Conway provides an unusually complete guide to crystals and their “magical uses.” Even if you do not believe in the spiritual principles detailed in this text, there is something for everyone in this book.

The book is divided into three parts. Part I, “The Magical Allure of Stones,” provides an interesting historical view of the use of stones and mineral crystals in jewelry and as talismans. The use and trade of various stones and metals by ancient civilizations (including the Phoenicians, Egyptians, and Greeks) are briefly discussed. The book’s main focus comes in Part II, “Stones and their Powers.” In the second section, approximately 100 materials are listed alphabetically, mainly by species, though several varieties are listed separately (e.g., emerald). Some of the stones are not typical gem materials (e.g., lodestone). Included for each material are the hardness, color(s), sources, facts, history and folklore, and the healing and magical powers that are attributed to it. Part III of the book looks at “Other Uses for Stone Magic.”

Occasionally there are some gemological inaccuracies. For example, fire agate is also referred to as “iris agate” in the text. Generally, though, Ms. Conway does a commendable job of providing accurate mineralogical properties, in conjunction with the extensive spiritual information. Thus, the book is useful for general descriptions and gem information. Although illustrations

of the stones would have been fitting, the book does not suffer for lack of them.

As one who does not use stones and crystals for their magical or spiritual properties, this reviewer still found the text entertaining and informative. A quote from the book comes to mind: “A day when something new is learned is a day not wasted. Even if you should never attempt the magical procedures, you can gain from just learning about and handling stones.” It is an idea that cannot be disputed, and *Crystal Enchantments* is worth a read if only for that very reason.

JANA E. MIYAHIRA-SMITH
Gemological Institute of America
Carlsbad, California

OTHER BOOKS RECEIVED

Diamonds and Precious Stones, by Patrick Voillot, 127 pp., illus., publ. by Harry N. Abrams, New York, 1998, US\$12.95* Intended more for the general enthusiast than the serious gemologist, *Diamonds and Precious Stones* is nonetheless an entertaining read. The beginning of this compact digest is steeped in gem legend and lore, before giving way to a more formal historical treatment of diamond, emerald, ruby, and sapphire. Here Mr. Voillot guides a swift (if at times cursory) tour through the development of gem faceting, the emergence of Antwerp as a cutting center, the discovery of diamonds in South Africa, and the subsequent rise of De Beers. Accounts of famous jewels and profiles of major gem localities are provided. The Documents section at the close of the book is highlighted by excerpts from the chronicles of Marco Polo and Jean-Baptiste Tavernier. *Diamonds and Precious Stones* is richly illustrated throughout, with more than 150 photos, paintings, and illuminated manuscripts.

STUART D. OVERLIN
Gemological Institute of America
Carlsbad, California

Gemological



ABSTRACTS

EDITOR

A. A. Levinson
*University of Calgary, Calgary,
Alberta, Canada*

REVIEW BOARD

Troy Blodgett
GIA Gem Trade Laboratory, Carlsbad

Anne M. Blumer
Bloomington, Illinois

Peter R. Buerki
GIA Research, Carlsbad

Jo Ellen Cole
GIA Museum Services, Carlsbad

R. A. Howie
Royal Holloway, University of London

Mary L. Johnson
GIA Gem Trade Laboratory, Carlsbad

Jeff Lewis
San Diego, California

Wendi M. Mayerson
GIA Gem Trade Laboratory, New York

Jana E. Miyahira-Smith
GIA Education, Carlsbad

Kyaw Soe Moe
GIA Gem Trade Laboratory, Carlsbad

Maha Tannous
GIA Gem Trade Laboratory, Carlsbad

Rolf Tatje
Duisburg University, Germany

Sharon Wakefield
Northwest Gem Lab, Boise, Idaho

June York
GIA Gem Trade Laboratory, Carlsbad

COLORED STONES AND ORGANIC MATERIALS

Amber: Art or artifact, one of the world's most precious discoveries. A. Wilkie, *Elle Décor*, Vol. 10, No. 4, June 1999, pp. 100–102.

Amber is a fossilized tree resin composed of 80% carbon, along with hydrogen, oxygen, and traces of sulfur. Natural colors range from pale yellow to reddish brown. Although amber is found in Asia and the Americas, Europe contains the vast majority of the world's economic deposits, 90% of which occur on the eastern shore of the Baltic Sea.

Amber is one of the earliest materials to be used decoratively. The oldest known European amber artifacts (beads discovered on the British shore of the North Sea) date from 11,000 to 9,000 BC. Archeologists believe that the beads were carried there from the Baltic area by oceanic currents. Amber has also intrigued the art and science communities. Artisans have used amber extensively, ranging from jewelry to the lavishly decorated Amber Room in St. Petersburg (dismantled by the Germans during World War II). Scientists value amber for its ancient organic inclusions: Insects preserved in Lebanese amber provide a window to the past as far back as 125 million years, and Baltic amber is about 40 million years old.

Besides providing a wealth of historical information, this article contains lists of major amber dealers and of museums that have major collections of European amber.

Kenneth A. Patterson

This section is designed to provide as complete a record as practical of the recent literature on gems and gemology. Articles are selected for abstracting solely at the discretion of the section editor and his reviewers, and space limitations may require that we include only those articles that we feel will be of greatest interest to our readership.

Requests for reprints of articles abstracted must be addressed to the author or publisher of the original material.

The reviewer of each article is identified by his or her initials at the end of each abstract. Guest reviewers are identified by their full names. Opinions expressed in an abstract belong to the abstracter and in no way reflect the position of Gems & Gemology or GIA.

© 2000 Gemological Institute of America

Fluid inclusions in emeralds from schist-type deposits. I.

Moroz and Y. Vapnik, *Canadian Gemmologist*, Vol. 20, No. 1, 1999, pp. 8–14.

Fluid inclusions in emeralds from seven schist-type deposits in five countries (Australia, Brazil, Tanzania, Zambia, and Russia) were studied by microthermometry (i.e., using a specially designed heating-freezing stage of a microscope to determine the phases present at various temperatures). Three types of fluid inclusions were found: brine, CO₂, and H₂O-CO₂. Carbonate crystals were common solid phases in these inclusions. The brine-type fluid inclusions are characterized by a low chloride content (i.e., generally <10 wt.% NaCl equivalent). Low-chloride brine inclusions in schist-type emeralds also have been reported from deposits in Austria, South Africa, and Pakistan. Thus, the authors conclude that emeralds containing fluid inclusions consisting of brines with low chloride contents are characteristic of schist-type deposits; this distinguishes them from emeralds formed in other types of deposits, such as those from Colombia and Nigeria, which are oversaturated with NaCl and typically contain halite daughter crystals.

AAL

Mechanism for kosmochlor symplectite and compositional variation zoning in jadeite jade.

L. Qi, S. Zheng, and J. Pei, *Journal of Gems & Gemmology*, Vol. 1, No. 1, 1999, pp. 13–17 [in Chinese with English abstract].

The petrography and geochemistry of kosmochlor (NaCrSi₂O₆, a green pyroxene previously known as *ureyite*) in jadeite from the Tawmaw area of northern Myanmar is reported. The kosmochlor mainly occurs as a symplectite (a “wormy” or irregular intergrowth of different minerals) that replaces or surrounds grains of chromite. Portions of the kosmochlor were metasomatized in a complex multistage process, resulting in a three-component symplectitic zoning of kosmochlor + calcic kosmochlor + uvarovite.

RAH

Market overview of saltwater and freshwater cultured pearls in China.

C. M. Ou-Yang, *Journal of the Gemmological Association of Hong Kong*, Vol. 20, 1997–1998, pp. 8–13.

Although pearl cultivation in China dates back more than 4,000 years, it was not until 1958—when the first experimental pearl farm was built at Hepu (in Guangxi Province)—that serious consideration was given to developing a major national pearl industry. Commercial cultivation began in 1963; from the 1980s onward, both freshwater and saltwater pearl cultivation grew rapidly.

Most saltwater pearl farms are located in the southern provinces of Guangdong, Guangxi, and Hainan. A pearl institute at Zhanjiang (Guangdong) provides professional training for pearl culturing. At Hepu and Beihai (Guangxi, where most of the saltwater pearl cultivation

takes place), approximately 6,000 family-owned farms produce the largest and highest-quality cultured pearls. White cultured pearls are produced at Sanya, in Hainan Province.

Freshwater pearl farms are also located mainly in southern China. The farms—which cultivate both nucleated and non-nucleated cultured pearls—are distributed among ponds, pools, reservoirs, cisterns, and lakes.

Most pearls produced in China are sent to Hong Kong for processing and then distributed internationally. About 90% undergo some or all of the following processes: drilling, bleaching, whitening, and polishing. Readers will also find interesting information about pearl cultivation practices, production, and value factors.

Paige Tullos

Oxygen isotopes and emerald trade routes since antiquity.

G. Giuliani, M. Chaussidon, H. J. Schubnel, D. H. Piat, C. Rollion-Bard, C. France-Lanord, D. Giard, D. de Narvaez, and B. Rondeau, *Science*, Vol. 287, No. 5453, January 28, 2000, pp. 631–633.

The oxygen-isotopic composition of emerald is influenced by the nature of the hydrothermal fluids from which it crystallizes, the composition and intensity of interaction with the surrounding host rock, and the temperature of its crystallization. Due to locality-specific differences in these factors, precise measurements of oxygen isotopes can be used to indicate emerald provenance. Using an ion microprobe, the authors analyzed nine historic emeralds—ranging from the Gallo-Roman epoch [although not delineated in the article, we believe this period dates from approximately 100 to 500 AD—*Ed.*] to the 18th century—to (1) determine their provenance, and (2) examine accepted theories about ancient gemstone trading routes.

The data obtained from a Gallo-Roman period earring from Ain, France, suggest a Pakistani provenance (Swat Valley), contrary to the previously accepted Roman sources in Austria and Egypt. A 51.5 ct emerald in the Holy Crown of France (13th century), does have an Austrian provenance. Two emeralds that were originally described by Abbé Hauy (the founder of mineralogy) in 1806 were also analyzed: one is from Austria (the Habachtal mines), while the other is Egyptian. Four emeralds from the treasury of the Nizam of Hyderabad in India were cut in the 18th century AD; these are historically called “old mine” emeralds. One probably came from Afghanistan, but three others apparently came from Colombia: The Peña Blanca [also referred to as Peñas Blancas (“white rocks”)], Coscuez, and Tequendama mines are cited as their exact sources. Such findings refute the belief that these particular stones were from ancient forgotten mines in southeast Asia, and suggest that Spanish trade of South American emeralds in the 16th and 17th centuries was worldwide in scope. A 1.51 ct rough emerald from the 1622 AD shipwreck of the Spanish galleon *Nuestra Señora de*

Atocha off the coast of Florida is from Colombia, specifically, the Tequendama mine in the Muzo district. [Abstracter's note: The conclusions reached in this study are based on the assumption that isotopic values found in emeralds from a given locality are restricted to narrow ranges, which apparently do not overlap between the localities considered important by the authors. According to earlier research cited in this article, most of the specific mines were represented by only 2–3 samples.] *JL*

Study on clinopyroxene minerals of jadeite jade. T. Zou, X. Yu, F. Xia, and W. Chen, *Journal of Gems & Gemmology*, Vol. 1, No. 1, 1999, pp. 27–32 [in Chinese with English abstract].

In addition to the mineral jadeite ($\text{NaAlSi}_2\text{O}_6$), other pyroxenes that may occur in jadeite jade include chromian jadeite, diopsidic jadeite, kosmochloric jadeite, omphacite, kosmochloric omphacite, diopsidic kosmochlor, jadeitic kosmochlor, diopside, clinoenstatite, diopsidic clinoenstatite, aegirine-augite, and aegirine. Chemical analyses on samples collected in Myanmar, as well as selected analyses from the literature, are tabulated and classified. The authors stipulate that only jade with >50 mol.% of the jadeite component should be called *jadeite jade*; the other types of clinopyroxene-bearing jade should be termed *aegirine jade*, *omphacite jade*, etc. *RAH*

Myanmar steps up production. P. Sutton, *Jewellery New Asia*, No. 176, April 1999, pp. 76–78, 80–81, 83.

The government of Myanmar has issued licenses permitting five companies—some with ties to experienced Japanese, Australian, and Thai interests—to establish new pearl farms. These facilities, with the assistance of the state-owned Myanma Pearl Enterprise, should increase both the quantity and quality of pearls from Myanmar in the coming years. The farming region is located in the Mergui Archipelago in the Andaman Sea (extreme southern Myanmar), which has a historic reputation for yielding superb South Sea pearls. The region is a “security area”: There is no tourism or logging, and access is limited. While the pearl farms will suffer from muddy water during the monsoon season, as well as from a limited infrastructure, the area also has the advantage of pollution-free waters.

Current pearl cultivation in the area is from *Pinctada maxima* mollusks. Although today most of the mollusks are gathered from the wild, some of the companies are committed to establishing hatcheries to ensure a regular and abundant supply. Major operations are expected to be developed by Japanese-owned Tasaki and Australian-owned Myanmar Atlantic. Tasaki has a license to farm up to 200,000 mollusks annually. The company is investing heavily in infrastructure, including water and power plants, shell cleaning and inspection facilities, and a hatchery. Myanmar Atlantic has a license to farm 50,000 mollusks a year and is applying to raise this to 300,000.

With the new equipment, technology, and experience being incorporated into the various operations, significant increases in cultured pearl production could come as early as 2002. *JEM-S*

Türkis [Turquoise]. *extraLapis*, No. 16, 1999, 96 pp. [in German]

This issue, like its predecessors in the *extraLapis* series, is devoted to a specific mineral or region—in this case, turquoise. It contains several maps and sketches and, as usual, is lavishly illustrated. The 11 chapters have been prepared by six contributors (W. Lieber, G. Liu, E. Gübelin, C. Meister, A. Ahmed, and S. Weiss), as well as the editorial staff of *Lapis*.

The first three chapters present a comprehensive description of the mineralogical characteristics of turquoise, including its position in the turquoise group (which also includes planerite, aheylite, faustite, and chalcociderite), historic data, and color. The text points out that “green turquoise” is likely to be planerite (a complete solid solution exists between turquoise and planerite), but its traditional and well-understood designation as “turquoise” should not be altered. Next follows a geologic description of turquoise formation, which requires aluminum, copper, and phosphate. In most cases, turquoise deposits are associated with porphyry copper ores in arid regions. This section of the issue concludes with an extensive listing of significant turquoise deposits worldwide. In addition to the commercially important gem turquoise deposits, the list also includes many lesser known localities, which are of special interest for mineral collectors because they typically yield crystalline material.

The main part of the issue (comprising seven chapters) is dedicated to descriptions of the world's most important turquoise deposits, both past and present. These are the deposits of the American Southwest, China and Tibet, Iran, and Egypt (Sinai). The discussion of the American deposits is supplemented by photographs showing different styles of Indian turquoise jewelry (Pueblo, Navajo, Hopi, and Zuni). There are two parts to the section on Iranian turquoise. The first was written by E. Gübelin before the Islamic Revolution 20 years ago, and describes the ancient deposits and the mines that were producing up to that time. The second is an update from 1998 (by C. Meister) that reflects the present situation. He reports that, with the arrival of the mullahs, turquoise production dropped considerably but never ceased entirely. Most of the gems produced recently, however, are being sold within Iran or to Islamic countries, and the finest qualities now fetch about US\$125 per gram in Mashad. The section concludes with a description of the deposits in Cornwall, England. Here, turquoise and other minerals of the turquoise group are a byproduct of tin and tungsten mining; they occur as crystallized crusts, forming beautiful collector specimens. Veins with massive, cuttable turquoise occasionally have been found, but never in commercial quantities.

The last chapter provides a short but comprehensive review of turquoise colors, treatments, imitations and simulants, CIBJO regulations, quality considerations, and values. RT

DIAMONDS

'Aquarium' set to revolutionise diamond security. *Mining Journal, London*, Vol. 332, No. 8522, March 12, 1999, p. 176.

De Beers has developed a "fully-automated diamond recovery plant and sorthouse complex" for installation at the Jwaneng mine in Botswana. The system eliminates the final hand-sorting of rough diamonds, which will greatly reduce theft. It is expected to come online in June 2000 at an estimated cost of US\$77 million. The name *Aquarium* comes from the acronyms of its two components: CARP (completely automated recovery plant) and FISH (fully integrated sorting house). CARP is equipped with magnetic rollers, concentrators, and an improved X-ray sorting machine. FISH consists of several automated processes that clean, sort, size, weigh, and package the diamonds. Detailed information such as sizes and amounts recovered will be available within 24 hours of processing at the Aquarium complex. Using this system, De Beers plans to process the old recovery dumps.

MLJ

Characterization of a notable historic gem diamond showing the alexandrite effect. T. Lu, Y. Liu, J. Shigley, T. Moses, and I. M. Reinitz, *Journal of Crystal Growth*, Vol. 193, 1998, pp. 577–584.

The French merchant Jean-Baptiste Tavernier brought back many notable diamonds from his travels to India in the 16th century, some of which he described as having a greasy appearance in daylight. One of these is the Tavernier diamond, a 56.07 ct old-style pear-shaped brilliant. It exhibits the alexandrite effect: a color change from light brown in incandescent light to light pink in daylight. This study examined the optical and spectroscopic features of this diamond to provide a better understanding of this phenomenon.

Examination with magnification and crossed polarizers revealed anomalous birefringence (strain) patterns and high-order interference colors. Both features are common and diagnostic in natural diamonds. Higher magnification revealed brown graining, a result of slip on crystallographic planes. UV fluorescence imaging showed an irregular distribution of intensity, with nitrogen-bearing lattice defects cited as the cause of fluorescence. Spectral transmission tests showed a peak at 420 nm with daylight-equivalent illumination, a feature that was not seen with incandescent light. The authors conclude that slip planes contribute to the brown color in incandescent light, while the nitrogen-bearing defects (and resulting intense blue fluorescence) cause the pink color seen in daylight. JL

The effect of structure development in electron-irradiated type Ia diamond. T. D. Ositinskaya and V. N. Tkach, *Journal of Materials Science*, Vol. 34, No. 12, 1999, pp. 2891–2897.

For this study of the development of structural defects in diamonds, a type Ia natural diamond crystal was irradiated in a linear accelerator with 3.5 MeV electrons. Prior to irradiation, electron paramagnetic resonance (EPR), positron annihilation (ACAR), infrared, and visible spectra were recorded. Then the crystal was exposed to increasing doses of radiation: 5×10^{16} , 2×10^{17} , 4×10^{17} , and 2×10^{18} e/cm². For the final dose, the crystal was cooled with liquid nitrogen (80–90 K). After each exposure, the authors investigated the crystal structure using several methods, including EPR, ACAR, and visible spectroscopy.

Initially, the crystal was "colorless" and transparent. The crystal remained transparent through the first three doses, while the color changed from "sky" blue to blue-green. After the final exposure (at low temperature), the specimen became opaque and a structural change developed that was visible to the unaided eye.

Cathodoluminescence (CL) imaging of zones with a visibly defective structure revealed a series of overlapping, hexagonal planes. CL spectra of these zones suggested that the major building material for the growth of these planar defects is most likely mobile interstitial carbon that binds with nitrogen. However, additional investigations are required to provide a comprehensive explanation for the origin and growth of the planar defects in this specimen. SW

How to steal a diamond. M. Hart, *Atlantic Monthly*, Vol. 283, No. 3, March 1999, pp. 28, 30, 32, 34.

Regardless of the precautions taken, theft from diamond mines (euphemistically called "leakage") is relentless and perhaps inevitable. Diamond theft is particularly prevalent in those parts of Africa where diamonds occur as secondary deposits—on the beaches of South Africa and Namibia, or in the alluvial deposits of Angola and Zaire. In such situations, diamonds are spread over a large surface area, and mining methods require considerable human contact with the stones. The result is a relatively high degree of theft compared to the mining of kimberlite pipes (primary deposits), where the area of kimberlite exposure on the surface is limited and most of the mining process is mechanized. Ingenious methods of theft at the South African and Namibian beach areas have been recorded, such as attaching diamonds to homing pigeons, and using crossbows to shoot hollow arrows filled with diamonds over perimeter fences. Criminal syndicates appear to be involved in at least some of these thefts.

The extent of diamond leakage varies from mine to mine and can only be estimated. Alexor, the South African state-owned mine on the Atlantic Ocean south of the Orange River, estimates that as much as 30% of its production is stolen (about US\$15 million worth annually). Namdeb, the beach and offshore joint venture of the

Namibian government and De Beers, also loses as much as 30% of its production to theft, which amounts to about \$160 million annually. In recent years, De Beers spent an estimated \$15 million per week (\$780 million on an annualized basis) "mopping up" illegal diamond production in Angola to maintain stability in the market. With total world production of rough diamonds valued at about \$7 billion, it is evident that the theft of rough diamonds from producing mines (and illegal mining) is very significant in terms of both value and caratage. AAL

A simple model to describe the anisotropy of diamond polishing. F. M. van Bouwelen and W. J. P. van Enkevort, *Diamond and Related Materials*, Vol. 8, March 1999, pp. 840–844.

Diamond polishers know that diamond acts softer (that is, material is removed more rapidly) in some directions than others. Until recently, this anisotropy of polishing hardness was believed to be related to the differences of indentation hardness along the different directions. The proposed mechanism was that polishing caused microcleavages along the {111} planes, but close examination of polished diamond surfaces with a scanning electron microscope shows smoothness of these surfaces down to a few nanometers in depth. Microcleavages were found only when attempts were made to polish along a {111} plane directly. Furthermore, the material removed during polishing was analyzed and found to be amorphous, mostly sp²-bonded carbon (graphite type) rather than microscopic chips of diamond.

Polishing applies force to the surface of a diamond, and this force deforms the sp³ bonds between the carbon atoms on the surface. Calculations of this deformation show that along the soft polishing directions, the bond deformation is highly localized, causing the carbon-carbon bonds to transform to the weaker sp² type. This allows the carbon atoms to be scraped off the surface more easily. Along the hard directions, however, the deformation is spread out and the bonds do not weaken.

The directional dependence of this weakening, and the resulting ease of polishing, are described in terms of periodic bond chain (PBC) vectors. A PBC-related model is used to explain why it is easier to polish an oblique plane away from the principal planes than toward them.

Ilene Reinitz

GEM LOCALITIES

Guatemala jadeitites and albitites were formed by deuterium-rich serpentinizing fluids deep within a subduction zone. C. A. Johnson and G. E. Harlow, *Geology*, Vol. 27, No. 7, July 1999, pp. 629–632.

The oxygen and hydrogen isotope geochemistry of jadeitite and associated albitite rocks from the Motagua Valley in Guatemala were studied to elucidate the role of metasomatic fluids in their formation. Albitite consists almost exclusively of the plagioclase mineral albite.

Jadeitite is made up predominantly of jadeite pyroxene; minor amounts of albite, white mica, and some other minerals also may be present. These types of rocks commonly form deep in the earth at subduction zones, where metamorphic reactions occur under high pressures.

Data from Guatemalan jadeite suggest that the H₂O-rich fluids that facilitated the metamorphism contained 1 to 8 wt.% NaCl, and had high hydrogen isotope ratios similar to those of seawater. Fluid inclusion and isotopic similarities between the Motagua Valley rocks and a type of calcium-rich metasomatic rock called rodingite suggest that the fluids present in both cases were nearly identical. Since rodingites can form in low-pressure environments (i.e., in subduction settings or near mid-oceanic spreading ridges), the surmised source of the metasomatic fluids in the jadeitites and albitites is seawater. The seawater was included with the rocks as they were subducted from the ocean floor to the depths (29 ± 11 km) at which metamorphism took place. JL

Le jade-jadeite du Guatemala—Archeologie d'une redécouverte [Jadeite jade: Archaeology of a rediscovery]. F. Gendron, *Revue de Gemmologie*, No. 136, February 1999, pp. 36–43 [in French].

Jadeite jade was revered by Aztec (Mexico) and numerous Central American civilizations. However, until relatively recently, the origin of that jadeite remained a mystery. At one time it was believed that the material originated in China, but the major mineralogical differences between jadeite and nephrite (the only jade that is native to China) made that theory untenable. Although a number of articles between 1910 and 1946 mentioned "jade" discoveries in several Mexican locales, that "jade" has since been identified as nephrite and "smaragdite" (a green actinolite pseudomorph after pyroxene).

In 1954, Dr. William Foshag, an American geologist, published a compilation of Central American regions with metamorphic environments favorable for the occurrence of jadeite. Included in this list was the Motagua River valley in southeastern Guatemala. Foshag concluded that this area was the source of some, and possibly all, of the Central American jadeite. He studied archeological samples of Central American jadeite and classified them into seven types, based on their gemological properties.

Several expeditions were formed to explore the Motagua River valley before the location was rediscovered in 1973. The presence of the deposit contributed to the development of lapidary arts in the town of Antigua, where jadeite jewelry with a European flair, as well as reproductions of archeological pieces, are fabricated by local lapidaries. MT

Möng Hsu ruby revisited—Some further data. U. T. Hlaing, *Australian Gemmologist*, Vol. 20, No. 7, 1999, pp. 289–292.

New data are presented in the form of a geologic cross section at Loi Hsawnshtoa, a dominant peak in the Möng

Hsu area and one of the primary (*in situ*) sources of ruby. The mineralization is hosted by a specific dolomitic marble horizon rich in Mg, Fe, and Al, with associated minerals that include tourmaline, pyrite, quartz, tremolite, andalusite, pargasite, and micas. Studies of the primary mineral assemblages indicate that the rubies formed under medium-grade metamorphic conditions (i.e., amphibolite facies) at temperatures of 450°–600°C and pressures of 2–6 kbar. Small pegmatites were emplaced within the ruby-bearing formation, and larger igneous bodies—possibly related to the formation of ruby—exist at depth.

Chemical analyses with a proton microprobe of 23 ruby samples (7 faceted and 16 rough stones) from at least four different locations within the Möng Hsu mining area yield the following mean values (in ppm, with range in parentheses): Ti = 730 (61–2,097); V = 211 (30–657); Cr = 5,932 (120–20,596); Fe = 33 (0–163); Ga = 66 (24–114); and K = 19 (0–70). The Cr and Ti values of Möng Hsu rubies are higher than those of Mogok rubies; Ga concentrations are comparable.

This article also reports the first two crystals of sapphire, as distinguished from the blue (sapphire) cores of rubies, from Möng Hsu (precise locality unknown).

KSM

Sapphire fever. *Life*, March 2000, pp. 28–30, 33.

In this pictorial, photographer Louise Gubb captures the drama of the sapphire boom that has drawn an estimated 100,000 prospectors to Ilakaka, Madagascar. The miners dig by hand, under difficult and dangerous conditions, and sell the sapphires to middlemen (some of them heavily armed), who in turn sell the gems to foreign buyers. According to American buyer Tom Cushman, "There are robberies and shootings just about every night." The sapphire market, meanwhile, continues to thrive.

Stuart D. Overlin

INSTRUMENTS AND TECHNIQUES

Light years ahead. D. A. Yonick, *Basel Magazine*, No. 7, October 1999, pp. 47–48, 50–51.

Color is an important factor in determining the value of a gemstone—even subtle differences can make a major difference in the stone's appearance. Because lighting can significantly affect gemstone color, many in the gem industry want to set international lighting standards for colored stones that are similar to those used in many other industries (e.g., paint, textile, plastic, ink, and paper). North daylight is the acknowledged standard for the gem trade, but this is impractical to use because its quality differs with geographic location and time of day. As the day progresses, for example, the color composition of daylight moves from the yellow into the blue range. Clearly, daylight simulation with an internationally accepted lamp is needed. Lamp manufacturers and the CIE (International Commission on Illumination) use two para-

eters, *color temperature* and *color rendering*, to compare the quality of artificial light from a lamp with that of natural daylight.

Color appearance varies with the operating temperature of the lamp, hence, "color temperature." Increasing temperature reduces yellow and enhances blue. The CIE uses certain standards for color temperature, which are measured in Kelvin (K): 5500K ("D55") and 6500K ("D65"). The best color temperature for diamond is D65 (the "blue-white" range), whereas D55 is best for colored stones (the "neutral white" range). Color rendering compares the light source to be evaluated against an arbitrary reference of 16 primary and supplementary colors, yielding a "color rendering index" (CRI); the maximum CRI that a light source can receive is 100.

Although most gem experts agree that color temperature and CRI should be the basis for an international light source, they cannot agree on the relative importance of each parameter. This issue is complicated by the impact of different viewing environments (e.g., for grading or display). Two light sources of the same color temperature could have high but not identical CRI ratings, yet drastically different daylight simulation quality.

Currently the industry uses a wide array of light sources to buy and sell gems, including daylight fluorescent simulators, warm incandescent spotlights, and filtered tungsten halogen sources. The CIE, in its *Assessment of Daylight Simulators: Publication 51*, indicates that the best technology for simulating daylight uses filtered tungsten halogen lamps. Given the many independently minded individuals in the gem trade, consensus is "light years" away.

KSM

Modern mineral identification techniques: Part I—WDS and EDS. T. Nikischer, *Mineralogical Record*, Vol. 30, No. 4, 1999, pp. 297–300.

Once fairly reliable, classical indicators such as physical and optical properties are often insufficient today to determine a specimen's identity. This is due, in part, to the ever-decreasing size of specimens that need to be identified. As a result, advanced testing is becoming more common for mineral identification.

Although both structure and chemistry can be studied with X-rays, this article focuses on how X-ray microanalysis methods can be used to determine the qualitative or quantitative chemical composition of a specimen. Two such methods, energy-dispersive spectroscopy (EDS) and wavelength-dispersive spectroscopy (WDS), are becoming quite popular, since they are both nondestructive and can analyze a small area of a specimen with a focused electron beam. The article describes the many specimen/beam interactions that provide the basis for this type of microanalysis. It compares and contrasts EDS and WDS, explaining their strengths and weaknesses, and concludes that they compliment one another. Instruments are available that have both capabilities—a desirable feature, since it is becoming increasingly common to

use two or more confirming techniques to determine a specimen's identity with certainty. WMM

JEWELRY RETAILING

Going global. M. Z. Epstein, *American Jewelry Manufacturer*, Vol. 44, No. 3, March 1999, pp. 74–79.

All successful strategies for doing business overseas incorporate three key elements: research, partnerships, and patience. This article expands on these three fundamentals, and offers 10 specific recommendations: (1) understand the market, (2) open distribution channels, (3) establish a long-term strategy, (4) use a skilled translator, (5) develop an Internet presence, (6) identify key vendors, (7) price competitively, (8) carve a niche and defend it, (9) seek legal advice when necessary, and (10) tap into export assistance programs.

Many successful U.S. firms are quoted in the article, presenting both helpful suggestions and pitfalls to avoid. Names, telephone numbers, Web sites, and e-mail addresses are given for many companies and government agencies that can help a company market its product overseas. AMB

How I lost that sale. W. G. Shuster, *Jewelers Circular Keystone*, Vol. 170, No. 10, October 1999, pp. 114–116.

According to a recent *JCK* poll, speaking before thinking has caused more than half of U.S. jewelers to lose sales at one time or another. These costly blunders fall mainly into three general categories: tasteless jokes, thoughtless remarks, and telling a customer what he or she needs. Examples of inappropriate remarks that have caused retailers to lose sales include:

- Assuming that jewelry is being purchased for a spouse
- Mistaking girlfriends for mothers
- Focusing on the wrong individual when a couple comes in to shop
- Assuming that a customer is pregnant
- Telling a customer that the piece of jewelry is not worth repairing when, in fact, the piece has high emotional value to the customer
- Advising a customer what he/she can afford
- Making derogatory remarks about competitors
- Forcing a decision before the customer is ready

A little tact, thoughtfulness, and common sense can go a long way in avoiding such blunders. MT

Quality: Biggest influence in consumer's choice. *Jewellery News Asia*, No. 180, August 1999, p. 45.

According to three surveys conducted by *USA Today* in the first half of 1999, quality is the most important consideration for consumers when purchasing jewelry and watches. Value and price are close behind. The least important factors are the store name and location, which is interesting in view of today's emphasis on jewelry store name branding.

The survey also determined where consumers are most likely to purchase their jewelry. The jewelry store ranked first, with almost 70% of the respondents selecting this option. Department stores and discount (or outlet) stores ranked second and third, respectively. Although 43.3% of those surveyed believe that shopping on-line is a great idea, only 10% selected this as their primary shopping venue. AMB

Won't you e-my valentine? J. B. Weinbach, *Wall Street Journal*, January 21, 2000, p. W6.

Valentine's Day is one of the truly romantic jewelry-giving opportunities of the year. This article featured an exercise in a rather untraditional method of shopping for the gift—on the Internet. Online purchases were selected from six electronic retailers: Ashford, Adornis, Mondera, Bestselections, Jewelry, and Luxuryfinder (all “.com's"). Side-by-side comparisons analyzed the service, quality, and packaging, as well as on-line gift-giving advice and pricing (in this case, for earrings ranging from \$500 to \$1,000). Perhaps the most interesting test was the assessment of these earrings by a panel of discriminating professional women.

Overall, Ashford.com was recommended for superb gift-giving advice, as well as for packaging, return policy, and service. Luxuryfinder was a disappointment, as it had few earrings (other than costume jewelry) priced under \$1,000. According to Luxuryfinder's president, the company's inventory was being replenished after the Christmas Holiday. Adornis ranked high for its overnight service, customer-friendly return policy, gift-giving suggestions, and packaging.

For gentlemen in search of “Tiffany-quality service and merchandise without Tiffany-size crowds,” electronic retailers may seem the perfect answer. However, as one panelist warned, “It's a turnoff. I'd rather know that someone went to the store.” Perhaps romance is still alive in the electronic age, after all.

Angelique Crown

MISCELLANEOUS

Gem futures: Trends in colored stones, diamonds, and pearls. D. A. Yonick, *American Jewelry Manufacturer*, Vol. 44, No. 6, June 1999, pp. 44–49.

The new millennium will bring exciting changes in the gem and jewelry industry. To explore developing trends, Ms. Yonick solicited the opinions of several experts from diverse segments of the industry.

- Gordon Austin (mining specialist): The colored stone industry faces the challenge of decreasing availability of high-quality gemstones. Easily accessible surface deposits are approaching depletion. Increasingly, future production will come from underground mining that will require major investments in technology, including sophisticated mining equipment and processing plants. Such investments will involve consortiums of

investors as well as small companies; some large marketers, manufacturers, and cutters may invest in mining projects to procure the needed raw materials.

- Steve Avery (gem cutter): Manufacturers and designers will distinguish themselves from the competition with innovative cuts, as well as with a higher quality of cutting. The copying of creative designs by mass producers is problematic.
- James Peach (president, U.S. Pearl Co.): The importance of Chinese and South Seas pearl producers is increasing at the expense of the Japanese, who have lost their century-long virtual monopoly on cultured pearls. Nevertheless, even if the Japanese Akoya pearl industry does not revive, Japan will likely remain an important distributor and investor in pearl production worldwide, including in the South Seas countries with whom it is presently competing.
- Antoinette Matlins (author): There will be increased demand for colored stones—particularly sapphire, ruby, and emerald—that are accompanied by laboratory reports stating that the stones are natural and untreated. Awareness of the distinction between enhanced and unenhanced gems by the gem-buying public will increase. Those stones that are not typically treated (e.g., tsavorite, and red and pink spinel) will be in high demand.
- Martin Rapaport (diamond publisher, wholesaler, and economist): The diamond market will evolve into a “low end” and a “high end,” with little in between. China and India will become major consumers of low-end diamonds over the next five-to-eight years. Mass marketers in the U.S. and elsewhere (including the Internet) will also contribute significantly to a phenomenal growth in inexpensive diamond jewelry. At the other extreme, high-end diamond jewelry will be in great demand by Baby Boomers interested in quality and value as they reach their peak spending years. Certification will become increasingly important, as enhancements (e.g., GE POL) will be a major concern.

Lila Taylor

Refocusing De Beers. C. Gordon, *Basel Magazine*, No. 1, April 1999, pp. 53–54, 56.

The recent corporate separation of De Beers from Anglo American allows the former to focus on its primary concern—the diamond industry. De Beers is becoming a more streamlined organization. Although some entities within De Beers are being dissolved, the CSO will remain the dominant unit, as well as the conduit for a high percentage of the world’s diamonds. It is hoped that this repackaging will give the company a more “coherent visual identity,” and better unite production and marketing.

External forces may have helped trigger these internal changes. In South Africa, unexplored mineral rights may become nationalized, and an anti-monopoly law is under consideration. Increased competition from other produc-

ers is another outside stimulus. As a result, De Beers is trying to become the “joint venture partner of choice” by offering its expertise and proprietary technology in mining development as an incentive to potential partners.

Specific responses to the external stimuli include the activities of DebTech, the research and development arm of De Beers, which has engineered such innovative projects as CARP (Completely Automated Recovery Plant) and FISH (Fully Integrated Sort House). Such automation in mining and processing helps solve the dual problems of security and labor shortages. New technology that involves the recrushing of small ore materials (<25 mm) will improve diamond recovery at several De Beers mines. Details are given regarding the implementation of these new technologies and the mines in which they will be used. Examples are also cited where De Beers is upgrading its mines by introducing International Standards (ISO) in areas such as environmental management, quality management, and health and safety. Throughout all of the changes, one thing remains the same: De Beers’s determination to retain control over prices, production, and the market.

WMM

Training to win. M. Z. Epstein, *American Jewelry Manufacturer*, Vol. 44, No. 7, July 1999, pp. 51–59.

U.S. jewelry companies need to stay competitive with overseas firms by reducing employee turnover and making their workforces more productive. Giving employees the skills they need to leave is often the best way to keep them. This article suggests seven ways to tackle turnover and increase productivity with training.

1. Establish an internal training program using human resources, videos, or partnerships with colleges.
2. Seek government-sponsored programs. Manufacturers’ Partnership is a network of 70 nonprofit centers charged with helping U.S. manufacturers compete. Several state Departments of Labor also offer programs.
3. Use the Internet/Intranet to offer training. One source is the Computer Consultants Association, which can be reached at 800-774-4222.
4. Embrace technology. Keep employees apprised of the latest manufacturing technology using symposiums and training programs at trade shows. Training and modern equipment go hand in hand.
5. Add to existing skills. Many schools offer short programs that can help workers hone their skills.
6. Offer tuition reimbursement. This helps keep the good employees, and it also improves their skill levels. This may be tax deductible for the company.
7. Encourage employee communication by having employees offer helpful criticism to one other, and alternating who gives advice.

Overall, those companies that invest the most in workplace learning have higher net sales and revenues per employee. This is a lesson manufacturers can’t afford to ignore.

Lynn Waters